

R_b and R_c ?

Contributions to the Moriond Workshop on R_b and R_c
XXXI Rencontres de Moriond
QCD and High Energy Hadronic Interactions
March 1996

Alain Blondel¹⁾, Andrew O. Bazarko²⁾, Jeffrey A. Snyder³⁾, Fernando Martínez-Vidal⁴⁾,
Giovanni Calderini⁵⁾, Jérôme Baudot²⁾, Helenka Przysieszniak⁶⁾²⁾, Pippa S. Wells²⁾,
James G. Branson⁷⁾, Piotr H. Chankowski⁸⁾, Pierre Chiapetta⁹⁾

Abstract

As of March 1996, the measurements of R_b and R_c were in serious discrepancy with the Standard Model expectations. The programme committee of Moriond QCD organized an extensive discussion session on the subject. The experimental facts were described critically by specialists of these measurements, and possible interpretations by new physics were presented. The written contributions to the Moriond proceedings are collated in the following.

¹⁾ Ecole Polytechnique, Palaiseau, France.

²⁾ CERN, Geneva, Switzerland

³⁾ Yale University, New Haven, USA

⁴⁾ University of Valencia, Spain

⁵⁾ Scuola Normale Superiore, Pisa, Italy

⁶⁾ University of Alberta, Canada

⁷⁾ University of California, San Diego, USA

⁸⁾ Institute of Theoretical Physics, Warsaw University, Poland

⁹⁾ Centre de Physique Théorique, Marseille, France

Contributions to the R_b, R_c workshop

- 1 **Introduction: R_b, R_c and QCD** (Alain Blondel)
- 2 **R_b measurements using lifetime tags at LEP** (Andrew Bazarko)
- 3 **A high purity measurement of R_b at SLD** (Jeffrey Snyder)
- 4 **Measurement of R_b using leptons, event shape and multivariate tags at LEP**
(Fernando Martínez-Vidal)
- 5 **Is our knowledge of the charm sector correct?** (Giovanni Calderini)
- 6 **R_c measurements at LEP** (Jerôme Baudot)
- 7 **Gluon splitting into heavy quarks** (Helenka Przysiezniak)
- 8 **Are the LEP and SLD heavy flavour data averaged correctly?** (Pippa Wells)
- 9 **Effects of QCD in R_b and R_c** (James Branson)
- 10 **R_b in the MSSM: how big can it be?** (Piotr Chankowski)
- 11 **Hadrophilic Z' : an explanation of LEP1, SLC and CDF anomalies?**
(Pierre Chiappetta)
- 12 **Summary: R_b, R_c and QCD** (Alain Blondel)

Introduction: R_b , R_c and QCD

Alain BLONDEL

L.P.N.H.E. Ecole Polytechnique, IN²P³-CNRS, 91128 Palaiseau France; and CERN, PPE division



Precision measurements using the b quark, i.e. the isopartner of the heaviest fermion top, probe new physics that could have escaped the more precise tests using light fermions and leptons in particular. At present, the measured decay rate of the Z boson in b quarks is 3 standard deviations away from the Standard Model (SM) value. Is this the long-sought new physics? Or could this be an experimental artefact? After a brief introduction of the important observables in this game, I recall the accuracy (10^{-3}) with which the Standard Model (SM) works for the light fermions (section 2) In comparison, the 2% (resp. 7%) discrepancy in R_b (resp. R_c) seems enormous (section 3). Of course, given the difficulty of the measurement, one should first ask how it could be wrong, (section 4), before trying to find how new physics could explain it (section 5). Although this topic is at first sight the concern of electroweak aficionados, I will explain in section 6 how it is linked, via the total hadronic width, to the determination of the strong coupling constant α_s , and therefore constitutes an adequate topic of discussion for a forum of hadronic interaction experts.

1 Definitions

The observables R_b , R_c , and R_ℓ are defined as ratios of partial decay widths of the Z boson:

$$R_b = \frac{\Gamma_{Z \rightarrow b\bar{b}}}{\Gamma_{Z \rightarrow \text{hadrons}}} ; \quad R_c = \frac{\Gamma_{Z \rightarrow c\bar{c}}}{\Gamma_{Z \rightarrow \text{hadrons}}} ; \quad R_\ell = \frac{\Gamma_{Z \rightarrow \text{hadrons}}}{\Gamma_{Z \rightarrow \ell^+ \ell^-}}. \quad (1)$$

They are obtained from the corresponding event ratios at the Z pole, after a small correction for photon exchange.

2 The Standard Model Works

The situation of precision electroweak measurements was reviewed by Malgeri [1, 2] at Moriond Electroweak 1996. The weak mixing angle $\sin^2 \theta_w^{\text{eff}}$ is now measured from forward-backward and polarization asymmetries at the Z pole with a relative precision of 1.210^{-3} , the leptonic width of the Z 1.610^{-3} , the W mass 210^{-3} , all in perfect agreement with the SM predictions. As is well known, the agreement of these measurements with the SM would not be achieved if electroweak radiative corrections were not taken into account. Moreover, a good fit is obtained only for a given range of the top quark mass, remarkably enough, consistent for the various observables, and with the latest determination of the top quark mass [3]. The high quality of the agreement between the most precise observations can be seen on figure 1.

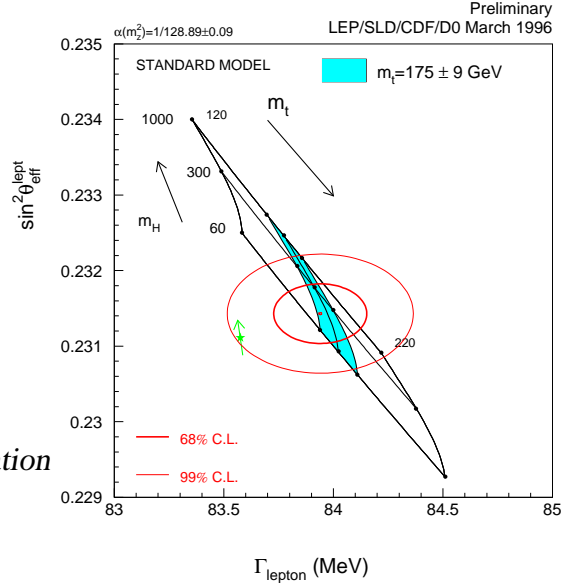
Figure 1:

Contours of constant χ^2 for $\sin^2 \theta_w^{\text{eff}}$ versus Γ_ℓ . The SM predictions as a function of M_t and M_H are shown.

The star indicates the predictions of the SM, if the only electroweak correction applied is the running of $\alpha(M_Z^2)$.

The arrow indicated on the star shows the influence of the $\alpha(M_Z^2)$ error on the predictions.

The agreement with the latest determination of the top quark mass is striking.



3 R_b does not

The first precise measurements of R_b came in early 1993, when analysis of data taken with vertex detectors at LEP became available. Since summer 1993, the situation has

evolved slowly, with a discrepancy of the combined average of the LEP experiments growing slowly from about two standard deviations to more than three. This slow evolution can be explained by the fact that results were systematically limited from the very beginning. Progress can only come from improved techniques and understanding.

In addition measurements of R_c have developed a discrepancy at the level of 2 standard deviations, so that the present results are [2]:

$$R_b = 0.2211 \pm 0.0016 \quad \text{SM Value : } 0.2155 \quad \text{discrepancy : } 3.5\sigma \quad (2)$$

$$R_c = 0.1598 \pm 0.0069 \quad \text{SM Value : } 0.172 \quad \text{discrepancy : } 1.8\sigma \quad (3)$$

with a negative correlation of -0.30. The correlation stems from the fact that charm events are the main background to the $Z \rightarrow b\bar{b}$ signal.

One very popular scenario for discrepancies from the Standard Model in R_b and R_c is the possibility of new effects in the $Z \rightarrow b\bar{b}$ partial width, $\Gamma_b = \Gamma_b^{\text{SM}} + \delta\Gamma_b$. If one takes this scenario, the relative change of R_b due to this new effect is large, while that of R_c , or R_ℓ is small:

$$\frac{\delta R_b}{R_b} = \frac{\delta\Gamma_b}{\Gamma_b} \times 1 - R_b; \quad \frac{\delta R_c}{R_c} = -\frac{\delta\Gamma_b}{\Gamma_b} \times R_b; \quad \frac{\delta R_\ell}{R_\ell} = +\frac{\delta\Gamma_b}{\Gamma_b} \times R_b \quad (4)$$

Taking this constraint into account is essentially equivalent to forcing R_c to its Standard Model Value of 0.172. This also shifts the best value of R_b via the correlation:

$$R_b, (R_c \text{ fixed to SM}) = 0.2202 \pm 0.0016 \quad (5)$$

Which is 2.9 standard deviations from the SM expectation.

The precision in the Standard Model prediction is very good. Dominant sources of uncertainty are [4]: i) the top quark mass error itself, $M_t = 175 \pm 9$ GeV leads to $\Delta R_b = 0.0003$; ii) the uncertainty in the b quark mass corrections, 0.5 MeV error on M_b gives $\Delta R_b = 0.0002$; iii) the QCD corrections essentially cancel in R_b , residual ones are estimated to give an error smaller than $\Delta R_b = 0.0001$. An error in the calculation can be ruled out as source of the observed discrepancy.

4 Experimental Procedure

The art of experimenters is to design efficient and self-calibrating b -tags. This is developed in detail in the following articles [5, 7]. There are three main sources of information to design a tag: i) the presence of large transverse momentum leptons (lepton tag); ii) the presence of tracks that miss significantly the primary vertex, indicating the presence of a heavy object with large multiplicity decaying with a long lifetime (lifetime tag); iii) consistency of the event shape with the presence of a heavy boosted object (event shape tag); The lifetime tag is by far the most efficient, SLD has recently achieved up to 37% efficiency with a purity of 97% [6].

By now, all experiments use an internal calibration of the tag by the double tagging technique: since b quarks are produced in pairs, one can take events where one b is tagged and count which fraction of these have the second b tagged to extract the tagging efficiency

(ϵ_b). If N_t is the number of events with one tag and N_{tt} the number of events with two tags, then one gets two equations:

$$\frac{N_t}{2N_{had}} = \epsilon_b R_b; \quad \frac{N_{tt}}{N_{had}} = \epsilon_b^2 R_b. \quad (6)$$

which can be solved for ϵ_b and R_b . This avoids the need to calculate ϵ_b from a model, that would have to describe very well vertexing and other delicacies but also fragmentation and decays of b -hadrons, inducing considerable uncertainty. In practice, things are not so simple. Equations 6 are only valid in absence of backgrounds and assume explicitly that in a $Z \rightarrow b\bar{b}$ event, the probabilities to tag the two b s are independent statistically. They have to be modified for these effects:

$$\frac{N_t}{2N_{had}} = \epsilon_b R_b + \epsilon_c R_c + \epsilon_{uds} R_{uds}; \quad \frac{N_{tt}}{N_{had}} = C_b \epsilon_b^2 R_b + \epsilon_c^2 R_c + \epsilon_{uds}^2 R_{uds}, \quad (7)$$

where $C_b \simeq 1 - \rho$, ρ being the correlation of tagging efficiency between the two hemispheres in a $Z \rightarrow b\bar{b}$ event, while $\epsilon_c, \epsilon_{uds}$ are the efficiency of the tag for charm and u, d, s events respectively.

Both hemisphere correlations and background tag efficiencies are obtained from Monte-Carlo. This is where systematic errors originate, and they dominate the measurement errors. **The key issues are: hemisphere correlations and charm background.** . These are explained in great detail by A. Bazarko [5], J. Snyder [6], F. Martinez-Vidal [7], for the various methods of b -tagging, J. Baudot [8] and G. Calderini [9] for the measurement of R_c and the understanding of charm background, J. Branson [10] for the influence of hadronization and QCD on the hemisphere correlations. A collective mistake of 2% in the hemisphere correlations could explain the observed anomaly...

Finally, since several methods are used by different experimental group, comes the very delicate task of combining them to produce one number. This is particularly difficult here, since systematic errors dominate. This question is addressed by P. Wells [11].

5 Physics interpretations

Any scenario that explains the observed discrepancy in terms of new physics must i) produce large effects on at least R_b and possibly R_c , ii) preserve all existing precision tests of the Standard Model, both in Z decays and in other experiments such as W -mass, neutrino-scattering, and also b -hadron decays. This is not easy. Here are three examples:

1)An apparent increase in Γ_b could be due to additional production of $b\bar{b}$ pairs by gluons (**gluon splitting**) in the hadronization process. Experimental cross-checks can be made, as summarized by H. Przysieszniak [12]. This of course would not explain a low value of R_c .

2)Radiative corrections to the $Z \rightarrow b\bar{b}$ vertex could be induced by new particles that couple to the b quark. Although, *a priori*, such effects have a natural tendency to decrease R_b , models with enough parameter space, such as Supersymmetry, can be arranged to increase it. Complete fits to the Minimal Supersymmetric Model are described by P. Chankowski [13].

3)A brute force explanation could be that the couplings of the physical Z boson are not those of the Standard Model. Mixing with a Z' would do it, provided couplings of the Z' to leptons are suppressed, in order to respect the leptonic measurements. These Z' are called hadrophilic or leptophobic. Such a scenario is presented by Chiapetta [14].

α_s measurements which does not include that from R_ℓ . Thanks to new evaluations of α_s from hadronic τ decays and lattice QCD calculations of the Quarkonium spectra, the World average value of α_s is now rather precise: 0.118 ± 0.003 . (Although the 10 measurements used give a χ^2 of 9, the error has been conservatively increased. It would be 0.0017 if the errors given on each individual measurement were taken at face value).

The agreement between $\alpha_s = 0.123 \pm 0.004$ obtained from the hadronic width, and 0.118 ± 0.003 from the world average can be translated in a possible deviation in R_b using equation 9:

$$\delta\alpha_s = 0.005 \pm 0.005 \quad \Rightarrow \quad \delta R_b = 0.0012 \pm 0.0013 \quad \Rightarrow \quad R_b = 0.2167 \pm 0.0013 \quad (10)$$

One realizes that R_ℓ provides a more powerful test, although less direct, of the following question: is there an anomaly in the $Z \rightarrow b\bar{b}$ partial width? Although the possible anomaly is of the same sign as that indicated by the measurement of R_b itself, it is much smaller, and not significant. The direct measurement of R_b and this indirect one differ by 1.7 standard deviations. This is well seen on figure 2 where the measurements of $\sin^2 \theta_w^{\text{eff}}$, R_b and R_ℓ are compared in the $\sin^2 \theta_w^{\text{eff}}, R_b$ plane.

References

- [1] For LEP and SLD data, see: L. Malgeri, in XXXI Rencontres de Moriond, weak Interactions and Unified Theories, ed. Tran Than Van, to appear in the Proceedings. For the W mass: K. Streets, (Do coll.) and D. Benjamin (CDF coll.), in XXXI Rencontres de Moriond, weak Interactions and Unified Theories, ed. Tran Than Van, to appear in the Proceedings.
- [2] The LEP Collaborations, CERN-PPE 95-172. Update for the 1996 winter conferences, LEPEWWG 96-01. Contains a very complete list of experimental references on precision measurements at LEP, Fermilab and SLC.
- [3] CDF Coll. G. Tartarelli, (CDF/PUB/TOP/PUBLIC/3664) in XXXI Rencontres de Moriond, weak Interactions and Unified Theories, ed. Tran Than Van, to appear in the Proceedings.
D0 Coll. R. Hall, *ibid*.
- [4] Reports of the working group on precision calculations at the Z resonance, CERN yellow report CERN 95-03 (1995).
- [5] A. Bazarko, these proceedings.
- [6] J. Snyder, these proceedings.
- [7] F. Martinez-Vidal, these proceedings.
- [8] J. Baudot, these proceedings.
- [9] G. Calderini, these proceedings.
- [10] J. Branson, these proceedings.
- [11] P. Wells, these proceedings.
- [12] H. Przysieszniak, these proceedings.
- [13] P. Chankowski, these proceedings.
- [14] P. Chiapetta, these proceedings.
- [15] L. Montanet et al., Physical Review D50, 1173 (1994)
and 1995 off-year partial update for the 1996 edition available on the PDG WWW pages (URL: <http://pdg.lbl.gov/>).

R_b MEASUREMENTS USING LIFETIME TAGS AT LEP

Andrew O. Bazarko
CERN, CH-1211 Geneva 23

ABSTRACT

$R_b = \Gamma_{Z^0 \rightarrow b\bar{b}} / \Gamma_{Z^0 \rightarrow \text{hadrons}}$ measurements by ALEPH, DELPHI, and OPAL using lifetime tags are reviewed. These measurements currently dominate the world average value of R_b .

1. Introduction

The current average of LEP and SLD measurements of R_b , the ratio of the Z^0 partial width into b quarks and its total hadronic partial width, finds¹ $R_b = 0.2202 \pm 0.0016$ when R_c is fixed to its Standard Model value of 0.172. This is almost 3σ from the Standard Model prediction, $R_b^{\text{SM}} = 0.2155 \pm 0.0004$. Of the many observables measured precisely at the Z^0 resonance, R_b is found to differ most significantly with the Standard Model.

R_b has the feature that most Electroweak and QCD radiative corrections cancel in the ratio, leaving R_b sensitive to radiative corrections that couple preferentially to b quarks, like the large CKM coupling to top quarks. For example, R_b is expected to differ from R_d by approximately 2% for $m_t = 175 \text{ GeV}/c^2$.

R_b is obtained by measuring the ratio of $b\bar{b}$ and hadronic cross sections at the Z^0 pole. The experimental problem is to tag a subsample of $b\bar{b}$ events with known efficiency and purity. $Z^0 \rightarrow b\bar{b}$ events are different enough from other Z^0 decays that high purity tagging is possible. Of the tagging methods used, lifetime tags offer the best performance and measurements using them dominate the current world average. This article covers the R_b measurements using lifetime tags performed by ALEPH,² DELPHI,³ and OPAL.⁴ Other LEP R_b measurements, particularly DELPHI's multivariate analysis, which includes lifetime information, are described by Martinez-Vidal.⁵ Finally, SLD has designed a high purity tag, which, in addition to lifetime information, uses the invariant mass of the tracks emerging from a reconstructed secondary vertex; new results with this tag are presented by Snyder.⁶

2. Lifetime b tagging

Events are divided into hemispheres by the plane perpendicular to the thrust axis, or in the case of ALEPH by the plane perpendicular to the highest momentum jet. With the “double tag method” both event hemispheres have a chance to be tagged. Two quantities, the numbers of tagged hemispheres N_s and double-tagged events N_d , are measured, allowing two unknowns, R_b and ϵ_b , to be determined:

$$\begin{aligned} N_s &= 2N(R_b\epsilon_b + R_c\epsilon_c + R_{uds}\epsilon_{uds}) \\ N_d &= N[R_b\epsilon_b^2(1 + \rho) + R_c\epsilon_c^2 + R_{uds}\epsilon_{uds}^2] \end{aligned} \quad (1)$$

where N is the number of hadronic events and ϵ_b , ϵ_c , ϵ_{uds} , are the hemisphere tagging efficiencies for the respective quark flavors. A correlation parameter ρ is introduced, because the efficiency to tag both hemispheres can differ from the square of the single tag efficiency, $\epsilon_b^d = \epsilon_b^2(1 + \rho)$. Compared with *event* tagging, the double tag method avoids the large systematic uncertainty due to ϵ_b in favor of a smaller systematic uncertainty due to ρ and an overall statistical precision limited by the number of double-tagged events N_d .

2.1. Primary vertex reconstruction

At LEP the region of beam overlap or beamspot is about $120 \mu\text{m}$ in the horizontal direction, $10 \mu\text{m}$ in the vertical, and 1 cm along the beams. The Z^0 decay point — the primary vertex — must be reconstructed for each event by augmenting the beamspot constraint with information from the tracks in the event.

To do this, DELPHI and OPAL begin by fitting a primary vertex using the beamspot and all tracks compatible with it. The track with the largest $\Delta\chi^2$ contribution to the overall χ^2 is examined. If its $\Delta\chi^2$ exceeds a designated threshold the track is dropped and the fit is repeated. This process continues until no track contributes a $\Delta\chi^2$ above the threshold.

ALEPH associates every track with a jet and projects each track into the plane perpendicular to its jet. This procedure removes most of the effect of lifetime for tracks originating

from the decay of long-lived particles. A primary vertex is fitted with the projected tracks and the beamspot. In following iterations, tracks consistent with the fitted primary vertex also contribute their longitudinal components to the fit. A track is deemed consistent with the primary vertex if its point of closest approach to its jet along the direction of the jet is behind the primary vertex.

Using such algorithms, it is possible to reconstruct the Z^0 decay point at LEP with a resolution of about $60 \mu\text{m}$ in both the horizontal and beam directions.

2.2. Impact parameter significance

ALEPH and DELPHI employ lifetime tags based on track impact parameter significance. The impact parameter is the distance of closest approach in space between a track and the primary vertex, and it is signed positive (negative) if the point of closest approach between the track and its associated jet is in front of (behind) the primary vertex. The impact parameter significance \mathcal{S} is the ratio of the signed impact parameter and its error.

Tracks originating from the decay of long-lived particles will tend to have positive impact parameter significances, whereas tracks originating from the primary vertex will have significances of random sign, due to limited resolution. The distribution of track impact parameter significances is shown in Figure 1. The negative \mathcal{S} distribution therefore provides a measure of the tag's resolution function R . The probability \mathcal{P}_T that a track originates from the primary vertex is obtained from the integral over R . Probabilities from tracks with positive \mathcal{S} in a hemisphere are combined to form a hemisphere probability \mathcal{P}_H , which is the tagging variable.

2.3. Decay length significance

OPAL's lifetime tag is based on the distance between the primary vertex and a reconstructed secondary vertex. Using an iterative procedure similar to the one described for primary vertex finding, a secondary vertex is fitted for each jet if at least four associated charged tracks contribute $\Delta\chi^2 < 4$ to the fit. The vertex decay length L is the distance from the primary to the secondary vertex along the total momentum vector of the tracks assigned to the secondary vertex. It is signed positive (negative) if the secondary vertex is in front of (behind) the primary along the same momentum vector. Like the negative \mathcal{S} distribution, the negative L/σ_L distribution provides a control sample with which to measure resolution effects. The distribution of decay length significances is shown in Figure 2.

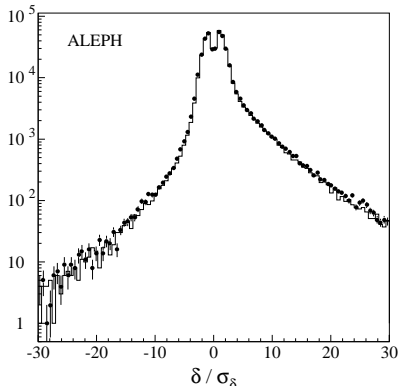


Figure 1: Track impact parameter significance distribution for data (points) and simulation (histogram) from ALEPH.

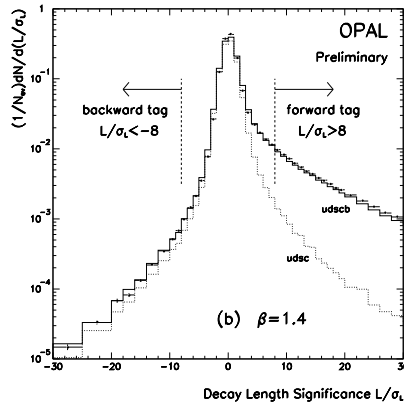


Figure 2: Decay length significance distribution for data (points) and simulation (histograms) from OPAL.

3. Summary of results

The R_b results from LEP using lifetime tags are presented in Figure 3. They are essentially the same as those available at the time of the 1995 summer conferences, when DELPHI and OPAL presented preliminary updates of published results. The only development is that DELPHI has finalized its updates and submitted them for publication.

- ALEPH’s R_b measurement uses an impact parameter significance tag.
- DELPHI makes three separate R_b measurements, all of which include lifetime information and two of which rely explicitly on an impact parameter significance tag. The first R_b measurement is procedurally the same as ALEPH’s. The second measurement is from a mixed tag analysis, where a lepton tag is also used. In this case, a sample of lifetime-tagged hemispheres is selected. Double-tagged events are those from the sample with a lepton tag in the opposite hemisphere. The purity of the lepton tag is estimated from fits to lepton distributions. Because the double-tagged events are chosen this way, this measurement is statistically independent from the first measurement. DELPHI’s third R_b measurement is from a multivariate analysis, in which lifetime and event shape variables are combined to provide tagging criteria; see Martinez-Vidal.⁵
- OPAL requires either a decay length significance tag *or* a lepton tag. Tagging events in this way provides increased statistics from lifetime-lepton double-tagged events that is similar to the combination of DELPHI’s lifetime and mixed tag measurements.

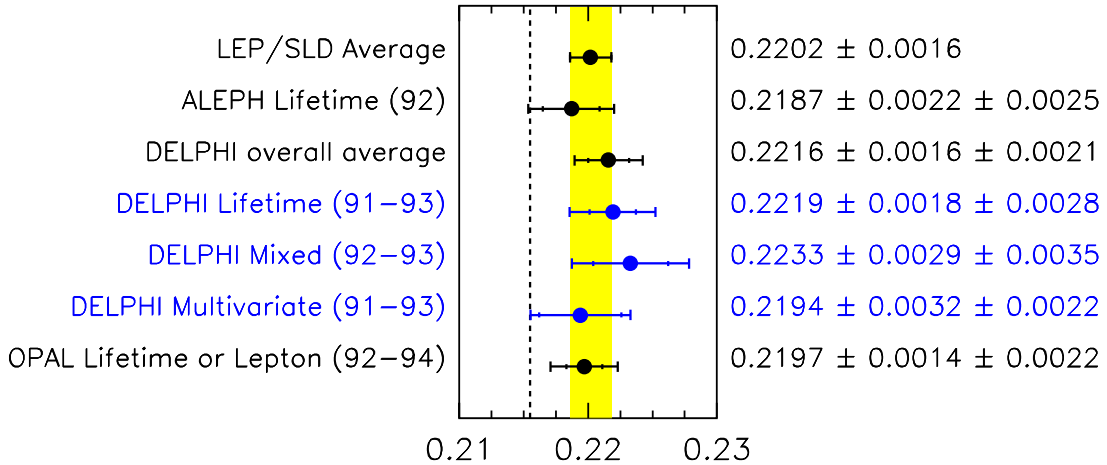


Figure 3: R_b measurements performed by the LEP experiments using lifetime tags, with R_c fixed to its Standard Model value of 0.172. The smaller error bars indicate the statistical uncertainty and the overall error bars indicate statistical and systematic uncertainties added in quadrature. Data samples included are given in years. The three individual measurements contributing to DELPHI’s overall measurement are also shown. The LEP/SLD average, from Ref. [1], includes an estimate of correlated uncertainties between experiments.

4. Sources of systematic uncertainty

The dominant uncertainties in lifetime tags are due to charm background and hemisphere correlations. The impact of these uncertainties on R_b is given by:

$$\frac{\Delta R_b}{R_b} \approx -1.5 \frac{\Delta \epsilon_c}{\epsilon_b} \quad \text{and} \quad \frac{\Delta R_b}{R_b} = \Delta \rho \quad (2)$$

That is, the uncertainty in ρ translates directly into a relative error in R_b , whereas the impact of the uncertainty in ϵ_c is relative to the b tagging efficiency. A performance summary of lifetime tags (for OPAL, of the combined lifetime-lepton tag) is given in the following table.

	ϵ_b	ϵ_c	ϵ_{uds}	ρ
ALEPH	26	1.18 ± 0.15	0.088 ± 0.010	-5.7 ± 0.8
DELPHI	21	1.67 ± 0.15	0.260 ± 0.013	-4.8 ± 0.6
OPAL	23	1.36 ± 0.13	0.103 ± 0.016	0.59 ± 0.32

4.1. Charm contamination

Uncertainties in estimating ϵ_c are listed below. These uncertainties are reviewed by Calderini.¹⁰

- Charmed hadron production fractions. Because the D^+ lifetime is long, the relative production rate of D^0 and D^+ is important. In the past, the only available measurements of the relative D^0 , D^+ , D_s^- , and Λ_c rates were from CLEO⁷ and ARGUS⁸ at $\sqrt{s} = 10.55$ GeV. Measurements at LEP have verified that these relative rates apply at $\sqrt{s} = 91$ GeV. This source of uncertainty contributes about 0.0009 to the error on R_b .
- Charmed hadron decay multiplicities. Higher decay multiplicities cause tags more readily, making uncertainties in topological branching ratios an important source of error. D meson decay multiplicities were measured by Mark III,⁹ including tracks from $K^0 \rightarrow \pi\pi$ decay. At LEP K^0 's are sufficiently boosted to be excluded from secondary vertex or impact parameter tags, so an additional uncertainty arises from this difference. The uncertainty due to decay multiplicities contributes about 0.0009 to the error on R_b .
- Charmed hadron lifetime and fragmentation uncertainties each contribute about 0.0004 to the error on R_b .

4.2. Hemisphere correlations

Several sources can introduce correlations in the tagging efficiencies between the hemispheres. Three general sources of correlation are identified:

- Geometrical correlations. Events tend to be back-to-back, and tracks from both hemispheres tend to occupy similar regions of the detector's acceptance, introducing a positive correlation.
- Event shape correlations. Gluon radiation correlates the momenta of the b and \bar{b} quarks, taking energy away from both and increasing the effect of multiple scattering. Both hemispheres are then less likely to tag, which introduces a positive correlation. Hard gluon radiation can force both b's into the same hemisphere, thereby producing a negative correlation. Uncertainties arising from such QCD effects are discussed by Branson.¹¹
- Correlations due to the shared primary vertex. Effects that tend to inflate or shrink the primary vertex uncertainty cause correlations, both positive and negative. For example, a hemisphere with a particularly long b hadron decay length tends to offer fewer tracks for the primary vertex reconstruction, making its uncertainty greater. While the hemisphere with the long decay length results in a tag, tagging the opposite hemisphere is less likely, leading to a negative correlation.

Correlations are estimated using Monte Carlo simulation. The Monte Carlo simulation's ability to reliably calculate a source of correlation is checked against data by studying the tagging efficiency as a function of an observable that reflects the correlating effect. For example, using the orientation of the thrust axis to study geometrical effects, or the thrust value to study the effects of gluon radiation. To the extent that the hemisphere correlations are due to gross detector or algorithm effects the simulations are believed to be reliable. In practice, correlation uncertainties are also limited by the Monte Carlo simulation statistics available to set them. In the LEP/SLD average, the uncertainties due to hemisphere correlations are assumed to be uncorrelated between experiments.

4.3. Light quark contamination

Uncertainties in ϵ_{uds} are due to resolution fluctuations and to uncertainties associated with long-lived particles produced in fragmentation, predominantly K_s^0 and hyperons. Heavy quarks produced in gluon splitting are constrained by recent measurements by DELPHI and OPAL, which are in good agreement with theoretical predictions; these are reviewed by Przysieszniak-Frey.¹²

The overall systematic uncertainties are given in Figure 3. The combination of DELPHI's lifetime and mixed tag measurements provides a systematic uncertainty of 0.0026.

5. Conclusions and Outlook

The R_b measurements from LEP are systematics limited. Caution must therefore be used when trying to assign a confidence level to the two and three sigma uncertainties. Because more statistics alone won't help, new techniques must be developed to improve future measurements. One new technique presented by SLD at this meeting is the use of the reconstructed mass of secondary vertices as a tagging variable.

As new techniques are applied, uncertainties will be scrutinized. Charmed hadron production and decay uncertainties are well understood and are straightforward to propagate. Account is taken of how these uncertainties are correlated between experiments. On the other hand, uncertainties due to the hemisphere correlations are less straightforward to estimate, and it is much more difficult to account for any correlated uncertainties between experiments.

The era of LEP running at the Z^0 pole came to a close in 1995. With three to four million Z^0 events per LEP experiment, there is hope that better R_b measurements are still possible. Future measurements, from LEP and SLD, might answer the question of whether R_b is incompatible with its Standard Model expectation.

I thank my colleagues in the LEP collaborations, particularly the members of the Heavy Flavour Electroweak Working Group, and my ALEPH collaborators.

References

1. The LEP Electroweak Working Group and the SLD Heavy Flavor Group. "A Combination of Preliminary LEP and SLD Electroweak Measurements and Constraints on the Standard Model." LEPEWWG/96-01. Internal note prepared from contributions to the 1996 winter conferences. Pippa Wells, these proceedings.
2. D. Buskulic *et al.* (ALEPH). Physics Letters B 313 (1993) 535.
3. P. Abreu *et al.* (DELPHI). CERN-PPE/96-15. Submitted to Z. Phys. C.
4. R. Akers *et al.* (OPAL). Z. Phys. C 65 (1995) 17. "An Update of the Measurement of $\Gamma_{b\bar{b}}/\Gamma_{had}$ using a Double Tagging Method." Contributed paper to EPS-HEP-95, Brussels, eps0278.
5. Fernando Martinez-Vidal, these proceedings.
6. Jeffery Snyder, these proceedings.
7. D. Bortoletto *et al.*, (CLEO). Phys. Rev. D 37 (1988) 1719.
8. H. Albrecht *et al.*, (ARGUS). Z. Phys. C 52 (1991) 353.
9. D. Coffman *et al.*, (MARK III). Phys. Lett. B 263 (1991) 135.
10. Giovanni Calderini, these proceedings.
11. James Branson, these proceedings.
12. Helena Przysieszniak-Frey, these proceedings.

A High Purity Measurement of R_b at SLD

Jeffrey A. Snyder

Physics Dept., Yale University, New Haven, CT 06511, U.S.A.

Representing the SLD Collaboration

ABSTRACT

Precision measurement of R_b can provide important information about the Standard Model and beyond. SLD has developed a new method for measuring R_b with very high purity. This measurement has the lowest systematic error reported to date and future measurements using this method will likely have the lowest total uncertainty.

This paper will be divided into the five sections: introduction, hardware, topological vertexing tag method, results and conclusions. The introduction will discuss the importance of R_b and the problems with other measurement techniques. The hardware section will give a brief description of the SLC/SLD system concentrating on its advantages over LEP. An outlook towards the future of SLD R_b measurements will be included in the conclusions.

1 Introduction

The quantity R_b is defined as:

$$R_b \equiv \frac{\Gamma(Z^0 \rightarrow b\bar{b})}{\Gamma(Z^0 \rightarrow \text{hadrons})} \quad (1)$$

Most of the standard model corrections to the partial widths are common to all quarks and thus cancel in the ratio. Only the b vertex corrections (δ_b^{vert}) are significant in R_b ; in essence, R_b isolates the b vertex corrections. The largest standard model contribution to δ_b^{vert} come from loops containing top quarks and is hence sensitive to m_{top} . Many type of new physics have similar contributions: for example, chargino/stop loops in supersymmetry or charged Higgs/top loops in the Higgs doublet model. These effects are typically 1%, so a very precise measurement of R_b along with a precise measurement of the top mass can rule out certain types of new physics.¹⁾

2 Hardware

The SLAC Large Detector (SLD) is a large general-purpose detector optimized to work at the Z^0 resonance.²⁾ For this analysis the most important components are the central drift chamber (CDC) and the vertex detector (VXD2). The CDC is a jet-cell drift chamber with 80 planes of wires arranged in 10 superlayers of 8 wires each. The hit resolution is approximately $100\mu\text{m}$ in the $r\phi$ direction. Using charge division, some z information is obtained, but the resolution is poor. The VXD2 is a unique design which uses charge-coupled devices (CCDs) to obtain true 3-d hits rather than using microstrips or crossed strips which can lead to hit confusion. There are over 100 million pixels in this device — arranged in two logical layers. The hit resolution is about $5\mu\text{m}$ in all three dimensions.³⁾

The SLAC Linear Collider (SLC) is a novel type of collider. Both electrons and positrons are accelerated down the same linac, but at the end they are sent into different arcs. At the end of the collider arcs the two bunches are travelling directly at one another with their center of mass at rest. The bunches collide at the center of SLD and any remnants are directed toward beam dumps. The beam spot size was (on average) $2.5\mu\text{m} \times 0.6\mu\text{m}$ during the 1994 run. The pulse-to-pulse jitter in the interaction point is significantly smaller than this size.

This small and stable beam spot allows us to use the *average* interaction point ($\langle\text{IP}\rangle$) position over several Z^0 decays to determine the transverse location of a given Z^0 decay. This method avoids the misidentification of the primary vertex that would arise if only that decay's tracks were used for the interaction point determination. It also reduces the tagging correlations due to poor IP measurements, and it makes it easier to understand and simulate the impact parameter resolutions. The uncertainty in the xy - $\langle\text{IP}\rangle$ position is $7\mu\text{m}$ for most events. The z position of the interaction point must be determined on an event-by-event basis, but we can use the xy position in this determination. The uncertainty in the z position of the IP is estimated to be $38\mu\text{m}$.

3 Topological Vertexing Tag Method

The general method for measuring R_b involves several basic steps. First one must obtain a pure $Z^0 \rightarrow q\bar{q}$ sample. The standard method is to require a large number of charged tracks and large visible energy in the event. Next one must form a tag variable. This variable must be able to remove most non- b decays while still efficiently tagging b decays. By doing so it also

removes charm and light quark modeling systematics, including correlation with R_c . There are several characteristics of B hadrons that are useful for tagging: the B–lifetime is long ($\sim 1.51\text{ps}$), the B–mass is large ($\sim 5\text{GeV}/c^2$) and the semi–leptonic decay spectrum is hard.

Single (or event) tag methods use the number of events and the number of tagged events to calculate R_b . In order to do this they rely on Monte Carlo estimates of the tagging efficiencies for each quark ($\epsilon_i \equiv N_{\text{tagged}}^i/N_{\text{true}}^i$). In double (or hemisphere) tag methods the most critical efficiency, ϵ_b , is measured from the data (ϵ_b^{data}) while the other efficiencies are estimated from Monte Carlo. The b –purity of the tag is often denoted as $\Pi_b \equiv N_{\text{tagged}}^b/N_{\text{tagged}}^{\text{all}}$.

3.1 Disadvantage of Lifetime Tagging Methods

All lifetime–based tagging methods share a common disadvantage: The purity is limited due to the long lifetime of primary charm events. Simply because of the exponential nature of lifetimes, it is difficult to improve the purity of a given tag without significant efficiency loss. The measurements done at the LEP experiments are already systematically limited by residual charm.⁴⁾ In addition, SLD’s measurement is not more precise despite our better resolution and precision (IP) advantage.

3.2 Topological Vertexing

Vertices are found by forming a 3–d vertex probability from the overlap of individual track probability functions.⁵⁾ We define D as the distance from the primary vertex (PV) to the decay vertex, L is the distance along this axis from the PV to the point of closest approach (POCA) for this track, and T is the transverse distance between the track’s POCA and the vertex axis. Tracks satisfying $L/D > 0.3$ & $T < 1\text{mm}$ are attached to the most distant vertex from the primary vertex. The invariant mass of the tracks forming the vertex can then be used as a tagging variable.

Since there is usually neutral energy missing we attempt to determine this and add it back to the invariant mass. If all the momentum were associated with the vertex, then the direction of the vertex axis would agree with the direction of the vertex momentum. If it does not, then we add back the missing p_t to align the two vectors. Because of tracking errors, there are many cases where the apparent missing p_t is very large. We eliminate most of these by minimizing the p_t to be consistent with both the vertex and (IP) errors and by limiting the total mass ($\mathcal{M} = \sqrt{M_{\text{raw}}^2 + |p_t^v|^2 + |p_t^v|}$) to be less than twice the raw mass. In many cases the missing p_t is consistent with zero and no mass is added to the vertex.

3.3 Event Selection

In order to separate fully–recorded hadronic events from all others (partially measured hadronic events, leptonic Z^0 events and non– Z^0 events) we require several characteristics of each event: For $Z^0 \rightarrow \ell^+ \ell^-$ rejection, the event must have at least 7 good tracks in CDC and more than 18 GeV in charged tracks. Our fiducial acceptance is $|\cos(\theta_{\text{thrust}})| < 0.71$. To verify that the detector is in operating condition, we require at least 3 tracks with at least 2 vertex detector hits and at least 1 track starting at $r_{r\phi} < 39\text{cm}$. To reduce gluon splitting events we require the number of reconstructed jets to be either two or three.

Similarly, we select quality tracks based on many criteria: For the drift chamber (CDC) segment of the track we require $|\delta_Z| < 1.5\text{cm}$, $|\delta_{r\phi}| < 1.0\text{cm}$, $\chi^2/\text{d.o.f.} < 5$, $p_t > 0.4\text{GeV}/c$, $r_0 < 40\text{cm}$, ≥ 40 CDC hits, and $|\cos \theta| < 0.80$. For the combined track (CDC+VXD) we require $\sigma_{r\phi} < 250\mu\text{m}$, $\chi^2/\text{d.o.f.} < 5$, and $|\delta_{xy}| < 3\text{mm}$.

3.4 Determining R_b from Double Hemisphere b -Tags

From data one measures the single hemisphere tag fraction and the double tag event fraction:

$$F_S = \epsilon_b R_b + \epsilon_c R_c + \epsilon_{uds}(1 - R_b - R_c) \quad (2)$$

$$F_D = \epsilon_b^{\text{double}} R_b + \epsilon_c^{\text{double}} R_c + \epsilon_{uds}^{\text{double}}(1 - R_b - R_c) \quad (3)$$

where: ϵ_i is the hemisphere tagging efficiency and $\epsilon_i^{\text{double}}$ is the double hemisphere tagging efficiency. The two hemispheres in an event might be *correlated*. We define the correlation coefficient, λ , such that:

$$\epsilon^{\text{double}} = \epsilon^2 + (\epsilon - \epsilon^2)\lambda \quad \Rightarrow \quad \lambda = \frac{\epsilon^{\text{double}} - \epsilon^2}{\epsilon - \epsilon^2} \quad (4)$$

$$\Rightarrow \quad F_D = [\epsilon_b^2 + (\epsilon_b - \epsilon_b^2)\lambda_b] R_b + \epsilon_c^2 R_c + \epsilon_{uds}^2(1 - R_b - R_c) \quad (5)$$

where it is assumed that λ_c and λ_{uds} are negligible.

We can solve for ϵ_b and R_b :

$$\epsilon_b^{\text{data}} = \frac{F_D - R_c \epsilon_c (\epsilon_c - \epsilon_{uds}) - F_S \epsilon_{uds} - \lambda_b R_b (\epsilon_b^{\text{data}} - [\epsilon_b^{\text{data}}]^2)}{F_S - R_c (\epsilon_c - \epsilon_{uds}) - \epsilon_{uds}} \quad (6)$$

$$R_b = \frac{(F_S - R_c (\epsilon_c - \epsilon_{uds}) - \epsilon_{uds})^2}{F_D - R_c (\epsilon_c - \epsilon_{uds})^2 + \epsilon_{uds}^2 - 2F_S \epsilon_{uds} - \lambda_b R_b (\epsilon_b^{\text{data}} - [\epsilon_b^{\text{data}}]^2)} \quad (7)$$

These coupled equations can then be solved by initially setting ϵ_b^{data} and R_b to zero and *iterating* until both quantities converge. Note that λ_b , ϵ_c and ϵ_{uds} come from the Monte Carlo simulation while R_c comes from other measurements or the standard model value.

4 Results

Using the 1993—1995 data we find 71210 events which pass the selection criteria as hadronic events. The efficiencies and b -purity are shown in figure 1 For a mass cut of 2.0 GeV/ c^2 we measure:

$$R_b = 0.2176 \quad \text{and} \quad \epsilon_b^{\text{data}} = 36.9 \pm 0.6\% \quad (8)$$

assuming an $R_c = 0.171$. From the Monte Carlo we expect: $\epsilon_b = 35.9\%$, $\epsilon_c = 1.06\%$, $\epsilon_{uds} = 0.07\%$, and $\lambda_b = 0.47\%$ which implies $\Pi_b = 97.2\%$. The statistical error, $\sigma_{R_b}(\text{stat.}) = 0.0033$.

The systematics are shown in figure 2. The largest physics systematic contribution comes from the b -correlation estimate. The many charm systematics also combine to give a large contribution. The double-tagging essentially eliminates the b -quark systematics. The detector systematics are dominated by the uncertainties in the impact resolution z component.

The result is therefore:

$$R_b = 0.2176 \pm 0.0033_{(\text{stat})} \pm 0.0017_{(\text{sys})} \pm 0.0008_{(R_c)} \quad (9)$$

5 Conclusions

SLD has successfully used a topological vertex tagging method to measure R_b . By utilizing the high mass of B mesons a very high purity can be obtained while retaining high efficiency. This mass tag method relies on the small $\langle \text{IP} \rangle$ provided by the SLC and the precise resolution

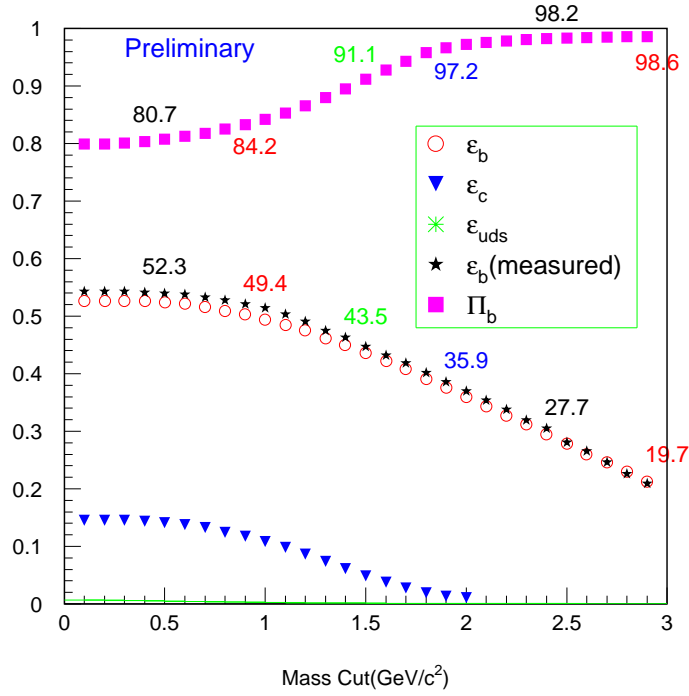


Figure 1: Performance of the mass tag as a function of mass cut.

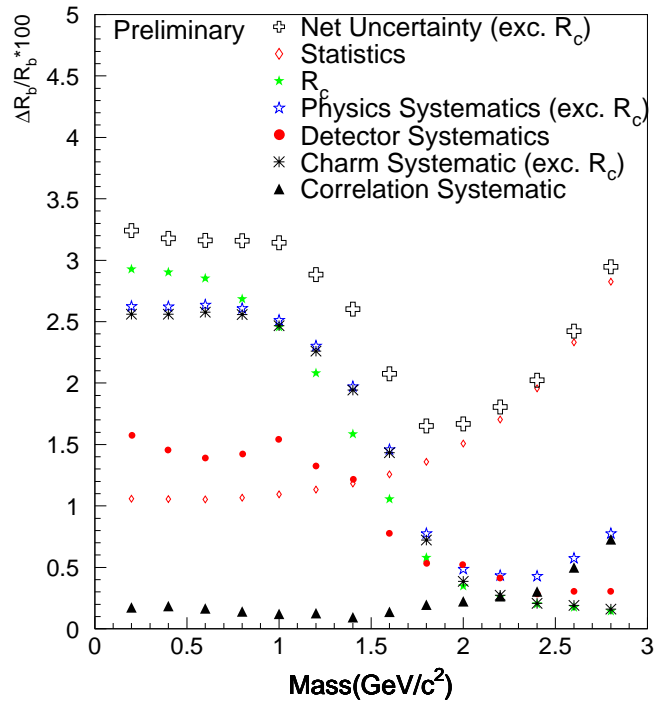


Figure 2: Net uncertainty as a function of mass cut.

of SLD's vertex detector. Other experiments may have some difficulty in using this exact method.

SLD is scheduled to run for another three years to accumulate half a million more Z^0 decays. This additional data will allow the use of harder cuts to further eliminate primary charm backgrounds. We have also installed an improved vertex detector which should enhance our b -tagging efficiency. This will assist in reducing systematics:

- ϵ_c term: $dR_b \simeq \left(\frac{-2R_c}{\epsilon_b}\right)d\epsilon_c$
- R_c term: $dR_b \simeq \left(\frac{-2\epsilon_c}{\epsilon_b}\right)dR_c$
- λ_b term: $dR_b \simeq \left(\frac{R_b}{\epsilon_b}\right)d\lambda_b$

We also expect that further study of the correlation systematics will allow us to reduce that uncertainty.

REFERENCES

- [1] See *e.g.*: "Heavy Flavours," J.H. Kühn and P.M. Zerwas *et al.* in *Z Physics at LEP 1*, G. Altarelli, R. Kleiss and C. Verzegnassi, eds., CERN Yellow Book 89-08, vol. 1 (1989) 267. "High Energy Tests of the Electroweak Standard Model," M. Swartz, presented at the XVIth Inter. Symp. on Lepton-Photon Interactions, Ithaca, NY, August 1993. "Estimation of Oblique Electroweak Corrections," M.E. Peskin and T. Takeuchi, *Phys. Rev.* **D46** (1992) 381.
- [2] "The SLD Design Report," SLAC-Report-273, 1984 (unpublished).
- [3] "Design and Performance of the SLD Vertex Detector, a 120 MPixel Tracking System," G.D. Agnew *et al.*, Proc. of the XXVIth Inter. Conf. on High Energy Physics, Dallas, TX, August 1992, p. 1862.
- [4] A. Bazarko, these proceedings.
- [5] "ZVTOP — A Topological Vertex Finding Algorithm for Hadronic Jets," D. Jackson, to be submitted to *Nucl. Inst. Meth.*

MEASUREMENT OF $R_b = \Gamma_{b\bar{b}}/\Gamma_{had}$ USING LEPTONS, EVENT SHAPE AND MULTIVARIATE TAGS AT LEP

F. Martínez-Vidal

IFIC, Centro Mixto Univ. of Valencia – CSIC,
Avda. Dr. Moliner 50, E-46100 Burjassot (Valencia), Spain

Abstract

The partial decay width of the Z to $b\bar{b}$ quark pairs has been precisely measured by the LEP collaborations using methods based on lifetime tags. In this paper, alternative measurements using lepton, event shape and multivariate tags are presented and the combined results are compared with the lifetime tagging measurements. The accuracy of lifetime measurements is actually dominated by systematics. Any improvement in precision requires better external knowledge of the charm and light quark physics affecting R_b . However, analyses combining leptons, event shape and lifetime information have not the same limitations in systematic errors and the statistics of analyzed events is still partial. Therefore including the high global LEP statistics, such alternative analyses are promising and interesting improvements in precision on R_b can be reached.

1 Introduction

In the Standard Model, the decay $Z \rightarrow b\bar{b}$ differs from other hadronic Z decays because of the existence of final state electroweak interactions involving the top quark. The effect of these vertex corrections can be isolated in the $R_b = \Gamma_{b\bar{b}}/\Gamma_{\text{had}}$ ratio, independently of other theoretical uncertainties due to the strong coupling constant, Higgs mass, higher order corrections in the Z propagator (oblique corrections) and in the vertex due to light quark loops, which basically cancel in the ratio. Thus, the value of R_b can be used to infer the top mass through these vertex corrections in the Minimal Standard Model ¹⁾. As the top quark discovery has recently been reported by the CDF and D0 collaborations and its mass measured ²⁾, the theoretical prediction of R_b is very precise. Therefore it is extremely important to study experimentally the top quark mass effect, since it provides a privileged tool to reveal virtual effects of new physics ³⁾. However, it requires a high precision measurement better than 0.5%. The latest R_b LEP average value is 0.75% precise and disagrees about 3 standard deviations from the Standard Model prediction ⁴⁾.

The precise R_b measurement is experimentally difficult mainly because quarks can not be observed as such. One can consider that the task of b-tagging is twofold. On one hand, one is interested in having as pure and efficient as possible b quark subsamples. On the other hand, one is interested in having a classifier for which the efficiencies are well known. So far, the most precise results are obtained from double lifetime tag analyses, as described in detail by A. O. Bazarko ⁵⁾. In this kind of analyses the b-tagging performances are powerful (typically of 35% efficiency for 90% purity) and the efficiency is measured directly from data obtaining a good statistical accuracy combined with a reduced systematic error. However, contaminations of non-b flavours and hemisphere correlations (including vertex-vertex and lepton-vertex from mixed tags) are estimated from simulation. Hemisphere correlations are small (in the range from 0 to 2%, depending on the value of the cut). The corresponding systematic errors are also small and basically dominated by statistical effects inside each experiment. So, it seems that they are well under control ¹⁾. However, backgrounds are relatively large, specially from charm events. The consequence is that R_b is quite sensitive to Monte Carlo inputs from the charm sector whose values, coming mainly from low energy data, have still large uncertainties and rather unstable central values with time ⁷⁾. Moreover, as the inputs are common, the systematic uncertainties are correlated between individual experiments and they are difficult to reduce when combining them. Finally, another important problem of these analyses is the large correlation with the R_c parameter (about -35%) which means that the final R_b value depends strongly on the assumed value of R_c .

Therefore, to resolve the question of whether the R_b deviation is real, it is strongly required to wait more reliable and fine measurements of low energy data and to use alternative analyses measuring R_b as independently as possible from all previously mentioned sources of systematics. They may be affected by other kind of systematics, but in the combination with other results the total error can be reduced. This paper reviews such alternative LEP analyses. First, in section 2 we shall describe how R_b is extracted from lepton tagging. Section 3 reviews the event shape analyses from ALEPH and L3 and section 4 describes the DELPHI multivariate analysis, which combines event shape and lifetime information to tag b quarks. Finally, in section 5 we present the conclusions. All results presented in this review have been published and references are given in the corresponding sections.

2 R_b from global lepton fits

Lepton tagging relies on heavy quark semileptonic decays. Due to the hard fragmentation of heavy quarks and their high mass, the b semileptonic decay will produce leptons with a high momentum (p) and a high momentum transverse (p_{\perp}) to the jet axis (which is used as an estimator of the heavy quark direction). As it is shown in figure 1, the lepton momentum distributions for b and c quarks are rather similar, but the transverse momentum distribution from c decays is softer than that from b quark decays, allowing a separation between $b\bar{b}$ and $c\bar{c}$ events. The upper limit of b-tagging efficiency

¹May be the only effect not so well understood is the gluon radiation ⁶⁾.

is twice the b semileptonic decay ratio (about 10% for e and μ separately). Momentum cuts and identification efficiencies for inclusive leptons and muons lowers the limit to below 10% for about 90% purity.

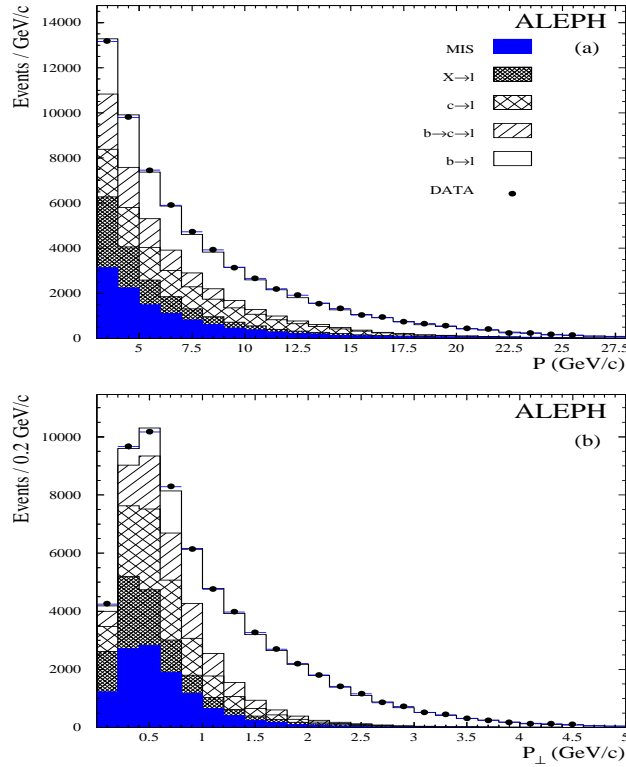


Figure 1: (a) Momentum and (b) momentum transverse to the jet axis for identified leptons (e and μ in hadronic Z decays). All lepton candidate sources taken from simulation are indicated.

The number of prompt leptons in a sample of hadronic events is determined by the products $R_b \text{ Br}(b \rightarrow \ell)$, $R_b \text{ Br}(b \rightarrow c \rightarrow \ell)$ and $R_c \text{ Br}(c \rightarrow \ell)$. The individual factors in the products can be isolated by a simultaneous consideration of the (p, p_{\perp}) spectrum of single and dilepton events. Such maximum likelihood fits are performed by all four LEP collaborations. By extending the fit to include the $\cos\theta$ variation of the number of single and dilepton events, A_{FB}^b , A_{FB}^c can in principle be measured. As the momentum spectrum of the leptons is strongly affected by the heavy quark fragmentation, the parameters $\langle x_E(c) \rangle$ and $\langle x_E(b) \rangle$ can be extracted from these fits within the framework of a particular fragmentation model. Finally, the average b mixing parameter $\bar{\chi}$ can also be obtained. The choice of exactly which of these nine heavy flavour parameters have to be measured and which need to be taken from external sources is a balance between statistics and systematics. Only ALEPH performs a global fit with all nine quantities. DELPHI fixes $\langle x_E(c) \rangle$, A_{FB}^b and A_{FB}^c from external measurements and OPAL fixes additionally R_c . From the (p, p_{\perp}) spectrum, L3 measures R_b and $\text{Br}(b \rightarrow \ell)$.

The results obtained by the four LEP collaborations are published in reference ⁸⁾ and summarized in table 1. Uncorrelated errors between experiments arise from knowledge of lepton identification efficiencies and the contamination by instrumental backgrounds. Correlated errors come from semileptonic decay model, semileptonic branching ratios and b and c fragmentation model. Parameters which are fitted do not contribute with systematic uncertainties. The small number of dilepton events limits the statistical error. However, the results have a different systematics from the lifetime measurements and therefore help to reduce the systematic error in overall LEP averages.

3 Event shape analyses from ALEPH and L3

The high mass and hard fragmentation of the b quark can be exploited by another separation technique, with no restriction to any particular decay mode. Little energy is lost by gluon radiation in the

Experiment	ALEPH	DELPHI	L3	OPAL	Combined LEP
Data Sample	90-91	91-92	90-91	90-91	
Tagging	lepton	lepton	lepton	lepton	lepton
R_b	0.2162	0.2145	0.2187	0.2250	0.2189
Statistical	0.0062	0.0089	0.0081	0.0110	0.0028
Uncorrelated	0.0028	0.0063	0.0047	0.0035	0.0025
Correlated	0.0042	0.0023	0.0034	0.0057	0.0012
Total Systematic	0.0050	0.0067	0.0058	0.0066	0.0028
$a(R_c)$			-0.023	-0.013	-0.007

Table 1: Results of R_b from global lepton fits. Three errors are quoted: the first is statistical, the second from uncorrelated systematics and the third from common systematics. All results are obtained fixing $R_c = 0.171$ according to the Standard Model prediction. The $a(R_c)$ factor denotes the explicit dependence of the result on the assumed value of R_c , in the format $a(R_c) \frac{R_c - 0.171}{R_c}$.

hadronization process of b quarks. Thus, the resulting B hadron (and subsequently, its decay products) carries out a large fraction of the primary quark energy, typically about 70%. In contrast, in light quark events most particles are produced in gluon fragmentation producing a rather soft and broad energy spectrum of particles. Similarly to the case of the semileptonic decays, the b quark mass affects the jet characteristics. By one hand, the b decay products have a relatively large transverse momentum with respect to the b quark direction, resulting in broader jets (higher jet sphericity) compared to light quark events. By other hand, the jet boost is also smaller for b quark jets. The practical problem is that none of the above properties alone is sufficient to tag b events with high purity and good efficiency. With a multidimensional analysis or neural network, the correlation between these properties can properly be accounted for and better tagging performances achieved. However, the final performances of the networks show good efficiencies but do not reach high b purities.

L3 has developed an event shape tagging based on a non conventional one layer neural network (NN) using a total of 11 variables (5 for each of the two most energetic jets of the events plus 1 global one) combined with orthonormal transformations of the input variables ⁹⁾. The variables only use calorimetric measurements to make the result as independent as possible of the semileptonic branching ratio and the Monte Carlo description of the data is tested with a high p_{\perp} (>1 GeV) muon to the opposite jet. For instance, figure 2(a) shows the distribution for all data compared to the muon-tagged events for the jet sphericity. L3 quotes 35% efficiency for 60% purity for global event, but the efficiency is less than 10% at 80% purity.

With this tagging, R_b is measured from a fit to the data distribution of the NN output by varying the b and non-b contribution from simulation, as can be seen in figure 2(b) (Single Tag Method). The obtained result is shown in table 2. The systematic error is dominated by uncertainties in the fragmentation, which reflect uncertainties in tagging efficiency for the single tag method.

To overcome this problem of dependence on fragmentation, ALEPH uses a double tag hemisphere method combining two event shape discriminators with a high p_{\perp} lepton tag ¹⁰⁾ (similar to the lifetime-mixed method ⁵⁾). In this case, the efficiencies of the discriminators are measured with the lepton tag, whose purity is evaluated for each bin of transverse momentum from the global lepton fit (section 2). The first event shape discriminator is based on a conventional feed-forward 4 layers NN with nine variables for each hemisphere. In the second discriminator, a likelihood built combination of two variables is used: a *moment of inertia* and a *lateral mass*. Both discriminators have very similar performances (75% efficiency for 35% purity for hemisphere tagging). So results from the two methods can be combined taking into account correlations. The quoted value is shown in table 2. The systematic error is dominated in this case by uncertainties in the determination of the lepton purity and on the Monte Carlo statistics in the estimate of hemisphere correlations (event shape-lepton correlations). Fragmentation effects are almost negligible at the level of statistical precision of the analysis: for example, the largest effect identified is from b fragmentation where the systematic is one half the statistical error.

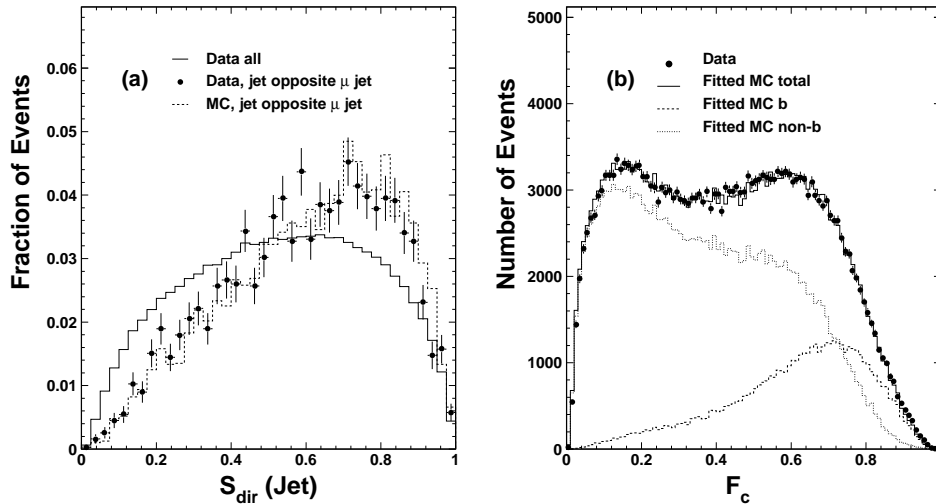


Figure 2: (a) Jet sphericity distribution for all jets compared to the muon-tagged sample in the L3 neural network. (b) Fit of the network response to the data. Also shown is the response for b and non-b events separately.

Experiment	ALEPH	L3	Combined LEP
Data Sample	90-91	91	
Tagging	shape	shape	shape
R_b	0.2279	0.2220	0.2249
Statistical	0.0054	0.0030	0.0034
Uncorrelated	0.0036	0.0053	0.0035
Correlated	0.0032	0.0036	0.0034
Total Systematic	0.0048	0.0064	0.0049
$a(R_c)$	-0.004	-0.021	-0.013

Table 2: Results of R_b from event shape analyses at LEP. Uncertainties from fragmentation are taken as correlated systematics.

4 The DELPHI multivariate analysis

In the double lifetime tag analyses, hemispheres are tagged as b and non-b. This leads to two equations with six unknowns: R_b , R_c , three flavour tagging efficiencies (uds, c and b) and the b hemisphere tag correlation. To obtain R_b and the b efficiency from data, R_c has to be fixed to the Standard Model value or external measurements. The background efficiencies and the correlation have to be taken from simulation. If the number of equations for physical observables were larger than the number of unknowns, the latter could be extracted directly from the data, and the simulation would be required only to estimate systematic errors and the influence of hemisphere correlations, reducing the dependence on simulation to a very small level. That is the principle of DELPHI multivariate analysis ¹¹⁾. Also and contrary to all other analyses, a primary vertex is computed on each side to reduce as much as possible the correlation between opposite hemispheres.

To provide the physical observables, a classical multivariate analysis technique based on flavour likelihood estimators (\mathcal{L}_{uds} , \mathcal{L}_c and \mathcal{L}_b) is used ¹²⁾. The total number of variables is thirteen and they combine lifetime and event shape information. According to a classification criteria (which is called *winning margin* Δ and which is defined as the difference between the maximum and the second flavour likelihood), each hemisphere is classified between six exclusive tagging categories ordered by increasing b purity (uds-tight, uds-loose, charm, b-loose, b-medium and b-tight). There are 21 different observables (combinations of two hemispheres tags) and 17 independent unknowns: R_b , R_c and 15 uds, c and b tagging efficiencies. The direct fit of this double tag matrix is degenerated. The

degeneracy in the b sector can be removed if two or more estimates of the six b efficiencies are found and injected in the fit of the double tag matrix ¹²⁾. These estimates are obtained from the fraction of hemispheres tagged in one of the previously defined categories, while the opposite hemisphere is tagged as b with a given value of winning margin. The property of these category fractions is that their asymptotic values provide an estimate of the corresponding b efficiencies. In practice, a global least square fit is performed to the double tag matrix and to the six winning margin distributions. The only assumption of the analysis is a parameterization of the background for the distributions and a reasonable b purity in the region of hard cuts. Figure 3 shows these distributions together with their fits. Effects of remaining backgrounds are small and are included in the systematic uncertainties. In this way all tagging efficiencies and backgrounds are finally derived from the data and the simulation is only required to estimate systematic errors on the assumptions of the method and the influence of hemisphere correlations. Moreover, it can be shown that R_c has no explicit influence on R_b and only remains a residual R_c dependence due to backgrounds.

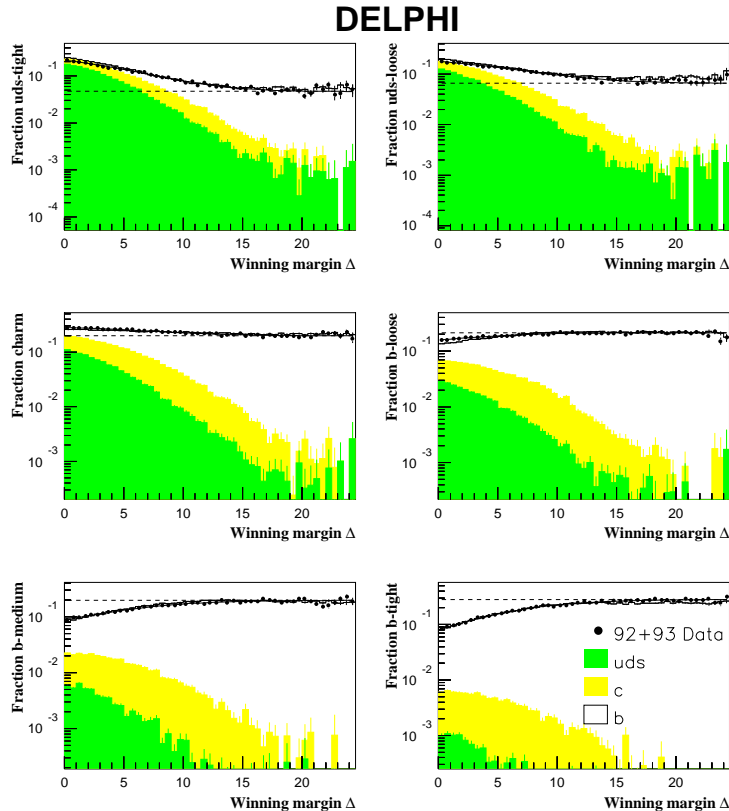


Figure 3: Distributions of the fraction of events tagged as b in one hemisphere with a given value of winning margin, that are classified in one of the defined categories in the other hemisphere. The dashed lines show the b efficiencies fitted from the data. The distributions for simulation are also shown, together with the contributions of uds , c and b quarks. To show the small backgrounds in the region of hard cuts, the vertical scale on each plot goes down to one per mil of the efficiency.

The quoted result using the 1991 to 1993 data set is shown in table 3 ¹¹⁾. The total error is dominated by statistics. The systematic error is also largely dominated by Monte Carlo statistics (0.0020) with two main contributions: hemisphere correlations (the number of correlation coefficients is rather large) and analysis method, which includes the assumption of asymptotic purity and the background parameterization for the winning margin distributions. The correlated errors with the lifetime measurements, i.e. charm and light quark systematics and gluon radiation, which dominate there the total error, are in this case almost negligible (0.0008). Fragmentation effects are also negligible.

5 Conclusions

The results of lifetime, leptons, event shape and multivariate tags (event shape+lifetime) from LEP, and their most recent average are summarized and compared in table 3.

Tagging	lifetime	leptons	shape	DELPHI multivariate	Combined LEP
R_b	0.2201	0.2189	0.2249	0.2194	0.2203
Statistical	0.0010	0.0028	0.0034	0.0032	0.0009
Uncorrelated	0.0009	0.0025	0.0035	0.0020	0.0008
Correlated	0.0016	0.0012	0.0034	0.0008	0.0011
Total Systematic	0.0019	0.0028	0.0049	0.0022	0.0014
$a(R_c)$	-0.017	-0.007	-0.013	-0.005	

Table 3: Summary of all R_b measurements at LEP considering each method separately. All results are obtained fixing $R_c = 0.171$ according to the Standard Model prediction.

From this table several conclusions can be extracted. First, lifetime measurements give the best statistical accuracy but they are seriously limited by systematics which are correlated between experiments. This systematics can not be reduced without significant improvements in the external inputs for charm and light quark physics affecting the measurement of R_b ⁷⁾. Second, lepton and event shape measurements are more statistically limited but help in the average because they are almost uncorrelated with the lifetime measurements. Third, the DELPHI multivariate analysis has low systematics (which can be reduced because it comes mainly from simulation statistics) compared to the lifetime analyses. The systematics is different and therefore uncorrelated. The statistical precision is poorer, but appears to be almost uncorrelated. The dependence with R_c about four times smaller.

After correction taking into account photon exchange, the LEP average is $R_b^0 = 0.2206 \pm 0.0009(\text{stat}) \pm 0.0014(\text{syst})$, where R_c is fixed to the Standard Model prediction of 0.171 and its correlation is -35%. The current precision is 0.75% and the central value is about three standard deviations higher than the Standard Model prediction of $R_b^0 = 0.2155 \pm 0.0005$ computed with the ZFITTER program ¹³⁾ for top quark mass $m_t = 180 \pm 12 \text{ GeV}/c^2$ ²⁾. Errors from lifetime measurements will become difficult to go any further without better external inputs for charm and light quark physics affecting R_b ⁷⁾. Alternative high statistics analyses combining event shape and lifetime information (as the DELPHI multivariate) are promising and interesting improvements in precision can be reached.

Acknowledgements

I would like to thank to the Organization of the XXIIIst Rencontres de Moriond for the warmful and fruitful atmosphere of the Conference. My very special thanks to Christian de la Vaissière by its decisive work with me, its continous encouragement and help in the preparation this review. Thanks to K. Moenig by providing me with the average results presented here and T. Baroncelli for his useful comments when preparing my talk.

References

1. A.A. Akhundov, D.Yu. Bardin, T. Riemann, Nucl. Phys. **B276** (1986) 1.
J. Bernabeu, A. Pich, A. Santamaria, Phys. Lett. **B200** (1988) 569.
J. Bernabeu, A. Pich, A. Santamaria, Nucl. Phys. **B363** (1991) 326.
A. Denner, W. Hollik, B. Lampe, Z. Phys. **C60** (1993) 193.
2. F. Abe *et al.* (CDF Collaboration), FERMILAB-PUB-95/022-E.
S. Abachi *et al.* (D0 Collaboration), FERMILAB-PUB-95/028-E.
3. A. Djouadi *et al.*, Nucl. Phys. **B349** (1991) 48.
R. Sekhar Chivukula, BUHEP-94-22, hep-ph/9409233.

- P. Chiappetta, these proceedings.
P. Chankowski, these proceedings.
4. The LEP Collaborations ALEPH, DELPHI, L3, OPAL and The Electroweak Working Group, CERN-PPE/95-172, 24 November 1995.
P.S. Wells, these proceedings.
 5. A.O. Bazarko, these proceedings.
 6. J.G. Branson, these proceedings.
 7. G. Calderini, these proceedings.
 8. D. Buskulic *et al.* (ALEPH Collaboration), *Z. Phys.* **C62** (1994) 179.
P. Abreu *et al.* (DELPHI Collaboration), *Z. Phys.* **C66** (1995) 323.
L3 Collaboration, *L3 results on R_b and $Br(b \rightarrow \ell)$ for the Glasgow Conference*, L3 Note 1625.
R. Akers *et al.* (OPAL Collaboration), *Z. Phys.* **C60** (1993) 199.
 9. O. Adriani *et al.* (L3 Collaboration), *Phys. Lett.* **B307** (1993) 237.
 10. D. Buskulic *et al.* (ALEPH Collaboration), *Phys. Lett.* **B313** (1993) 549.
 11. P. Abreu *et al.* (DELPHI Collaboration), *Z. Phys.* **C65** (1995) 555.
P. Abreu *et al.*, CERN-PPE/96-15, 30 January 1996. To be appear in *Z. Phys. C*.
 12. P. Billoir *et al.* NIM A 360 (1995) 532-558.
 13. D. Bardin *et al.*, CERN-TH 6443/92.

Is our Knowledge of the Charm Sector Correct?

Giovanni Calderini
Scuola Normale Superiore and INFN, Pisa, Italy

On behalf of the ALEPH, DELPHI, L3 and OPAL Collaborations

Abstract

A lot of techniques are used to measure $R_b = \frac{\Gamma(Z \rightarrow b\bar{b})}{\Gamma(Z \rightarrow q\bar{q})}$ and they involve different sources of systematic errors. Nevertheless, charm sector knowledge is one of the largest limitations to R_b accuracy apart from the particular method used.

Some of the most important techniques to extract R_b are examined, and for each of them the largest sources of uncertainties coming from the charm sector are reviewed. New recent results from the charm physics are reported, and their incidence on R_b systematics is discussed.

1 Introduction

Several methods have been recently used to measure $R_b = \frac{\Gamma(Z \rightarrow b\bar{b})}{\Gamma(Z \rightarrow q\bar{q})}$, and some of them have also been combined. Each technique involves different sources of systematic errors, but the uncertainty due to the charm sector knowledge is one of the critical ones for all the different methods. A few measurements by several experiments are taken into consideration, and for each one the relevant systematic uncertainties from the charm sector are examined. The improvements expected due to recent results from charm physics are also discussed.

2 Different Methods to Extract R_b

The selection of $b\bar{b}$ events can be obtained using several tags, which are based on the different properties of heavy flavour events with respect to the light quark ones and to the discrepancies that $b\bar{b}$ events present from the residual $c\bar{c}$ decays. The competitiveness of these tags has changed with time, owing to the constant development of detectors. For this reason, the techniques applied a few years ago have been generally replaced by new ones, which are more appropriate to exploit the improved detector performances.

2.1 Lifetime Tag

This is at present the most efficient tag to select $b\bar{b}$ events. It has become possible due to the excellent tracking performance of new vertex silicon detectors.

A probability P_H that all the tracks in the event come from the primary vertex is built. A cut on this variable allows a selection of $b\bar{b}$ events with a low $c\bar{c}$ background (Fig. 1). This

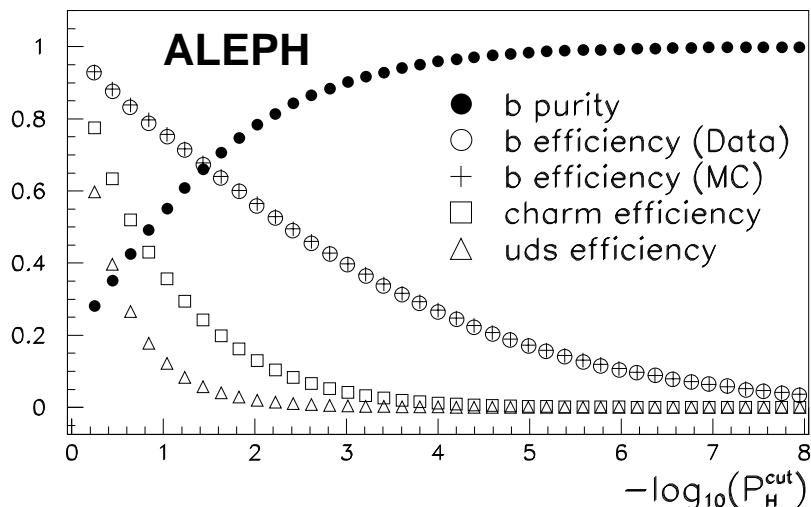


Figure 1: Performance of cut in P_H for $b\bar{b}$ event section

technique is sometimes replaced by looking for secondary vertices far from the interaction point. From a comparison between the number of events in which both hemispheres are tagged and the number of the single tagged events, the efficiency of b -tag can be extracted directly from data; for this reason the method is basically insensitive to all the systematics from b sector.

This kind of analysis has been studied by several experiments [1, 2, 3, 4] and many sources of systematic uncertainties have been quoted by each of them (Tab. 1). As a matter of fact,

	ALEPH [1]	DELPHI [2]	OPAL [3]	SLD [4]
c prod. fractions	0.0009	0.0016	0.0009	0.0013
c decay mult.	0.0006	0.0010	0.0010	0.0018
c lifetimes	0.0005	0.0006	0.0004	0.0003
c fragmentation	0.0001	0.0005	0.0008	0.0012
gluon splitting	0.0003	0.0003	0.0005	0.0004
uds background	0.0002	0.0006	0.0003	0.0001
Total Syst.	0.0014	0.0023	0.0017	0.0025

Table 1: Sources of systematic errors on R_b related to the charm physics for lifetime-tag analyses by different experiments

the largest ones for this kind of tag are the c production and the decay multiplicity for charmed hadrons.

2.1.1 Charm production rates

At present, the LEP working group takes the input values for c -production rates from low energy experiments. An implicit assumption underlies this procedure, the charm production must be the same at low energies as at LEP. The validity of this hypothesis will be discussed in the following. The values used from CLEO [5] and ARGUS [6] are quoted in Tab. 2.

More recently, LEP experiments too have provided measurements of rates for charm production. The general strategy for these analyses is to isolate a sample of events containing a candidate D . A two-component fit is performed to the D momentum distribution in order to extract simultaneously ($b \rightarrow D$) and ($c \rightarrow D$) contributions (Fig. 2).

Values for charm production provided by LEP experiments with this type of method are collected and summarized in Tab. 2.

Error source	Value and Range (Low. Energy)	New values from LEP
D^0 fraction in $c\bar{c}$ events	0.557 ± 0.053	0.583 ± 0.035 PRELIM.
D^+ fraction in	0.248 ± 0.037	0.233 ± 0.024 PRELIM.
D_s fraction	0.12 ± 0.05	0.097 ± 0.022 PRELIM.
Λ_c fraction	0.08 ± 0.05	0.076 ± 0.033 PRELIM.

Table 2: Rates for charmed meson production in $c\bar{c}$ events from low-energy experiments used as input for R_b measurement, compared with the recent LEP results

There is a very good agreement between LEP numbers and low-energy ones and this is a confirmation of our initial assumption. The charm production is substantially the same at LEP and low energy experiments, where seems to be no significative suppression for the heaviest charm states. A second comment for the LEP values is that the present accuracies seem to be very good and fully competitive with the CLEO/ARGUS results. For this reason, in the next future, a good gain could be reached in R_b measurement using as input for charm production values an average of low energy and LEP results.

In a simultaneous fit anyway the two components ($b \rightarrow D$) and ($c \rightarrow D$) are anti-correlated. For this reason an important check of this measurements can be provided by a recent ALEPH

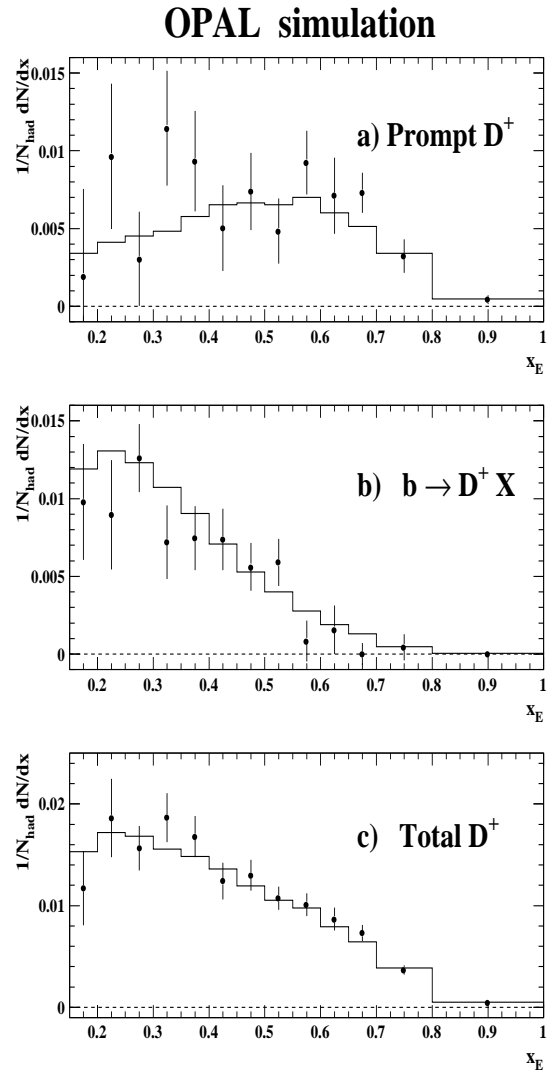
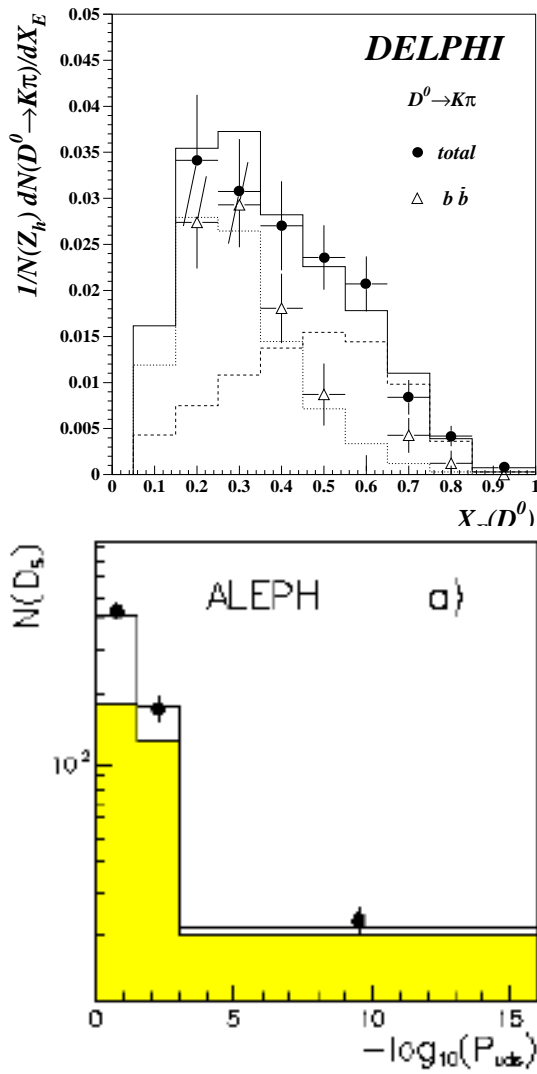


Figure 2: Examples of fit to distributions of D candidates to extract ($b \rightarrow D$) and ($c \rightarrow D$) contributions

analysis. It is possible to restrict to a very pure $b\bar{b}$ sample of events in order to be insensitive to D production from charm. The D invariant mass distribution is fitted to compute the D production rate in $b\bar{b}$ events. This technique requires a careful study of background sources, since they are often resonant in the D mass region. This ALEPH measurement, with the addition of simple assumptions on $J\psi$ and Ξ_c production allows also a new estimation for n_c (Tab. 3).

Experiment	Measure in %	Er. stat.	Err. BR	Er. sys.
ALEPH (PRELIM.)	$f(b \rightarrow D^0 X) = 57.3$	2.4	2.0	1.8
ALEPH (PRELIM.)	$f(b \rightarrow D^+ X) = 21.3$	1.3	1.4	1.2
ALEPH (PRELIM.)	$f(b \rightarrow D_s X) = 18.8$	2.2	2.2	1.4
ALEPH (PRELIM.)	$f(b \rightarrow \Lambda_c X) = 12.0$	3.5	1.6	0.8
ALEPH + CLEO	$f(b \rightarrow \Xi_c X) = 7.2$	-	-	3.2
CLEO	$f(b \rightarrow charm.) = 1.8(\times 2)$	0.3	-	$\pm_{0.}^{1.0}$
Total	$n_c = 1.202$	0.049	0.036	$\pm_{0.043}^{0.042}$

Table 3: D production rate in $b\bar{b}$ events from ALEPH, leading to a preliminary n_c estimation

In conclusion, the present knowledge of charm production rates seems generally satisfying. There are several papers published by different experiments, which allow averages and cross-checks. A further improvement will be achieved when LEP measurements will be officially added to the input values in R_b analyses.

2.1.2 Charged Multiplicity

Apart from charm production, the second large source of systematic errors on R_b coming from the charm sector, is the decay multiplicity. At present there is only one measurement (MARK III) [7] of the average number of tracks coming from the D^\pm , D^0 and D_s decays. The uncertainty in R_b due to charm decay multiplicity is computed as the sum in quadrature of the separate uncertainties from different D mesons, weighted by their relative contributions. The average D decay multiplicity quoted by MARK III is

$$n_{ch} = 2.56 \pm 0.06$$

Unluckily this is the only measurement available for n_{ch} . Moreover its worth as an input in R_b analyses is affected by the additional problem that it is missing of Λ_c contribution. There's also a problem of definition, since in most of R_b analyses the charged pions from K_s are not taken into the track counting, while in MARK III analysis they are considered in extracting the D decay multiplicity. For this reason, an additional uncertainty is quoted by the R_b LEP working group, on the basis of the known fraction of K_s production in D decays [8]

$$BR(D \rightarrow K_s X) = (46 \pm 6)\%$$

A general remark can be done. While in the case of charm production rate, the scenario seems satisfying, for charge multiplicity the bibliography is not so rich. There is jut one measurement available and substantially the information which we obtain from this requires some attention, due to the use of different definitions with respect to most R_b analyses. LEP seems to be somehow missing for this kind of study.

2.2 Lepton Tag

This tag was the first in time to be developed. It is essentially based on cuts on momentum and transverse momentum of leptons with respect to the jet axis to which they belong. The high mass of the heavy quarks and their hard fragmentation functions lead to the leptons having a hard momentum spectrum and a large momentum component transverse to the heavy hadron direction. The transverse momentum is typically smaller for c decays than for b decays, allowing the two to be separated on a statistical basis. At present, this tag is much less performant than the lifetime tag and for this reason it is often used in combination with the latter. For this b -tagging technique, the main source of systematic error due to charm sector is the $BR(c \rightarrow l)$. This quantity has not yet been measured at LEP, partly because the leptons originating from $c \rightarrow l$ decays have a substantial overlap in their momentum distribution with lepton candidates from other sources. Measurements of $BR(c \rightarrow l)$ have been made in the continuum below the $\Upsilon(4s)$ at ARGUS [9], where no b pairs are produced. There are also measurements made at PEP and PETRA [10]. The average result for this branching ratio is:

$$BR(c \rightarrow l) = (9.8 \pm 0.5)\%$$

Anyway this type of tag is becoming less and less competitive with respect to the lifetime tag, so that the impact of this systematics on the R_b accuracy is much more reduced.

2.3 Conclusions

It appears that for R_b purposes, our knowledge of the charm sector is acceptable, but there is still some weak spot due essentially to measurements done by a single experiment. Apart from this we should note that LEP numbers in the charm sector get more and more competitive and a good gain is foreseen when this results will be official included into the averages used for R_b .

References

- [1] D. Buskulic *et al.*, ALEPH Collaboration, Phys. Lett. **B313** (1993) 237.
- [2] P. Abreu *et al.*, DELPHI Collaboration, "Measurement of the partial decay width $R_b = \frac{\Gamma(Z \rightarrow b\bar{b})}{\Gamma(Z \rightarrow q\bar{q})}$ with the DELPHI detector at LEP", CERN-PPE/96-015.
- [3] R. Akers *et al.*, OPAL Collaboration, Z. Phys. **C65** (1995) 17.
- [4] SLD Collaboration, "Measurement of R_b at SLD", Talk presented by Erez Etzion at Moriond QCD, 1996.
- [5] D. Bortoletto *et al.*, CLEO Collaboration, Phys. Rev. **D37** (1988) 1719.
- [6] H. Albrecht *et al.*, ARGUS Collaboration, Z. Phys. **C52** (1991) 353.
- [7] D. Coffman *et al.*, MARK III Collaboration, Phys. Lett. **B263** (1991) 135.
- [8] Particle Data Group, Phys. Rev. **D45** (1992).
- [9] H. Albrecht *et al.*, ARGUS Collaboration, Phys. Lett. **B278** (1992) 202.
- [10] T. Pal *et al.*, DELCO Collaboration, Phys. Rev. **D33** (1986) 2708;
W. Bartel *et al.*, JADE Collaboration, Z. Phys. **C33** (1987) 339;
R. A. Ong *et al.*, MARK II Collaboration, Phys. Rev. Lett. **60** (1988) 2587.

R_c MEASUREMENTS AT LEP

Jérôme BAUDOT

CERN, CH-1211 Geneva 23, Switzerland

representing the LEP collaborations

ABSTRACT

The partial width $R_c = \frac{\Gamma(Z \rightarrow c\bar{c})}{\Gamma(Z \rightarrow q\bar{q})}$ is a basic observable in Z physics. Within the Standard Model its value is accurately predicted and other experimental measurements at LEP involve its knowledge. The DELPHI and OPAL collaborations have presented several R_c measurements. All methods are based on charmed hadron reconstruction and b/c separation. The LEP average, computed by the LEP Electroweak Heavy Flavor Working Group, is presented to be 0.1596 ± 0.0074 . This is 1.8 standard deviation below the Standard Model expectation.

1. INTRODUCTION

R_c is defined as the partial width $\frac{\Gamma(Z \rightarrow c\bar{c})}{\Gamma(Z \rightarrow q\bar{q})}$. Contrary to R_b , its prediction in the Standard Model does not involve large radiative correction. In particular the R_c value is not very sensitive to the top quark or Higgs boson mass. Making a precise R_c measurement is therefore both a good test of Standard Model and an usefull input for other related heavy flavour measurements, like R_b . It improves the knowledge of the charm sector at LEP.

All recent R_c measurements at LEP are based on the determination of cross section of charmed hadrons in $c\bar{c}$ events. Older measurements using leptons have been already published¹⁾ and will not be reviewed here. First single charmed hadron rate determination is presented. Then techniques to separate primary c quark hadronization and b hadron weak decays to charm are discussed. In order to reduce the amount of external inputs, double charm tagging methods are also used to measure $P(c \rightarrow D^{*+}) \times Br(D^{*+} \rightarrow D^0\pi^+)$ and R_c . They are described in the fourth section. Finally comparison of systematic errors and combination of results are given.

2. SINGLE TAG

At LEP, charm is dominantly produced through the weak decay $Z \rightarrow c\bar{c}$, followed by the hadronisation $P(c \rightarrow \text{charmed hadron})$ and the decay of the charmed hadron. The rate for the production of single charmed hadrons is composed of the following terms:

$$\text{single rate} = R_c \times P(c \rightarrow \text{charmed hadron}) \times Br(\text{charmed hadron} \rightarrow \text{final state}). \quad (1)$$

To derive R_c from the measurement, the reconstruction efficiency of the charmed hadron into the final state needs to be known. This is the main part of the internal systematic uncertainty (see table 1). The techniques used to determine the relative proportion of charmed hadrons originating from primary c quark hadronisation and bottom hadrons decay are reviewed in section 3.

2.1. D^{*+} rate

The most easily detectable charmed hadron is the D^{*+} in the decay $D^{*+} \rightarrow D^0\pi^+$, because of the low Q value of the reaction. LEP collaborations^{2,3,5)} have collected a few thousand of such decays. Extracting R_c from this measurement however is limited by the dependance on external parameters, in particular the hadronisation fraction $P(c \rightarrow D^{*+}) \times Br(D^{*+} \rightarrow D^0\pi^+) \times Br(D^0 \rightarrow K^-\pi^+)$. Until Moriond 95, only low energy experiments were providing a value for this input. Now $P(c \rightarrow D^{*+}) \times Br(D^{*+} \rightarrow D^0\pi^+)$ is measured at LEP with double charm tag (see section 4.1). This input contributes around 5% to the systematic uncertainty, which is almost at the level of statistical and internal systematic errors (see table 1).

2.2. Charm counting

Every charmed hadron produced at LEP will eventually decay into one of the ground-state charmed hadrons (G_c) $D^0, D^+, D_s^+, \Lambda_c^+, \Xi_c^+, \Xi_c^0$ or Ω_c^+ . Measuring their production rate (1) therefore provides another method^{6,7)} to determine R_c through equation 2 :

$$\sum_{G_c} P(c \rightarrow G_c) = 1 \quad \text{and then} \quad R_c = \sum_{G_c} \text{single rate}(G_c) = \sum_{G_c} R_c \times P(c \rightarrow G_c). \quad (2)$$

Note also that all the charmed groundstate hadrons have not been reconstructed. The Ξ_c^+, Ξ_c^0 and Ω_c^+ rates are estimated from the Λ_c^+ rate, so that the total rate of charm baryon in c quark hadronisation is 1.14 ± 0.05 the Λ_c^+ rate⁶⁾ (this only contributes to 0.4% to the systematic error).

Contrary to the single D^{*+} rate method, the individual fraction $P(c \rightarrow \text{charmed hadron})$ does not need to be known here. Only the branching ratios $Br(\text{charmed hadron} \rightarrow \text{final state})$ is taken from external sources. But due to a higher background, statistical and systematic errors are greater (see table 1).

3. b/c SEPARATION TECHNIQUES

To distinguish between $Z \rightarrow c \rightarrow \text{charmed hadron}$ and $Z \rightarrow b \rightarrow \text{bottom hadron} \rightarrow \text{charmed hadron}$, information from either the reconstructed hadron or the event shape can be used.

3.1. Charm hadron variables

The exclusive reconstruction of a charmed hadron provides precise information on momentum and decay length (or flight time). When produced in bottom decays charmed hadrons have a lower average momenta (see figure 1b) and a higher decay length (see figure 1a) than in charm decay. Those differences allow a statistical separation³⁻⁷). The main systematic comes

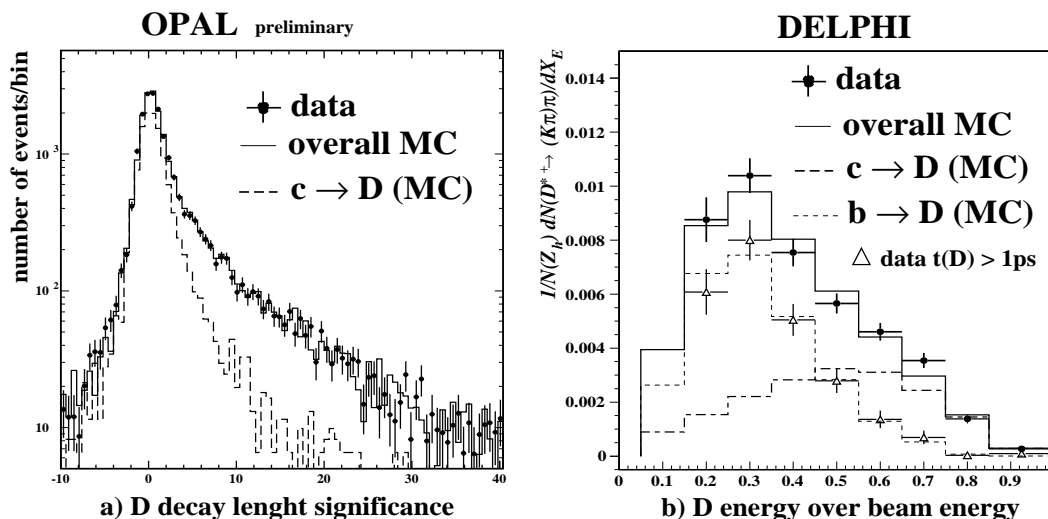


Figure 1: Distribution of discriminant variables between b and c events when a D meson is exclusively reconstructed.

from uncertainties in the simulation, with dominant errors due to the fragmentation parameters and lifetimes (see table 1).

3.2. Event and jet variables

Other variables related to the jet or the event shape can also be used to separate $b\bar{b}$ and $c\bar{c}$ events. DELPHI uses an anti- B cut on a variable computed from the impact parameter significance of tracks in the event. This cut allows to reach a 80% charm purity in the mixed tag method⁹) (see subsection 4.1 and figure 2b). This B -tagging benefits from the accurate study done for R_b measurements. OPAL^{3,4,6}) trains a neural network with jet and event shape variables to achieve a statistical separation of the two sources of charm hadrons (see figure 2a).

4. DOUBLE TAG

Single tag (1) measurements are sensitive to the product $R_c \times P(c \rightarrow \text{charmed hadron})$. If one charmed hadron is tagged in each hemisphere of the event, then it provides an additional

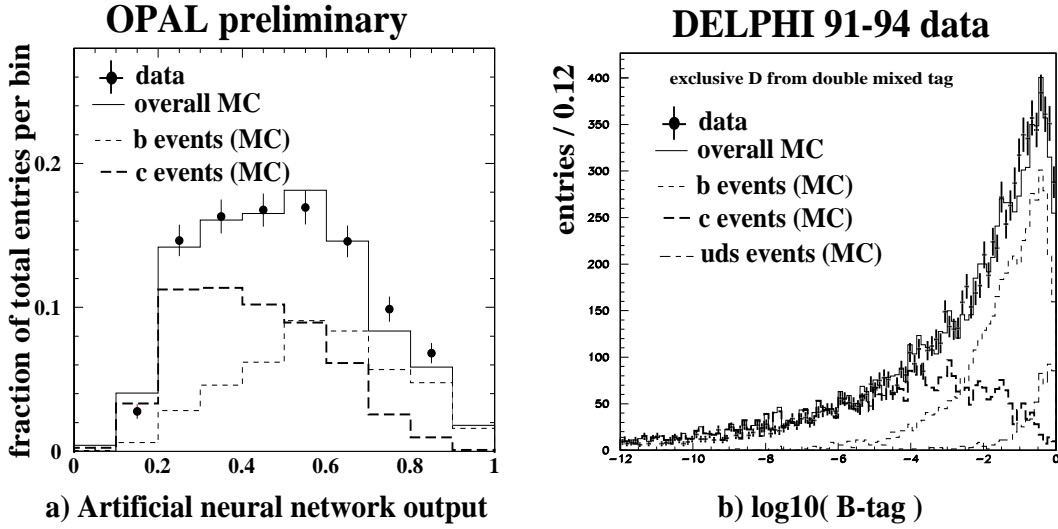


Figure 2: Distribution of discriminant variables based on event or jet shapes and lifetime tag.

information:

$$\text{double rate} = R_c \times (P(c \rightarrow \text{charm hadron}))^2. \quad (3)$$

Thus both R_c and $P(c \rightarrow \text{charm hadron})$ can be estimated with respectively the ratio :

$$R_c \propto \frac{(\text{single rate})^2}{\text{double rate}}, \quad (4)$$

$$P(c \rightarrow \text{charm hadron}) \propto \frac{\text{double rate}}{\text{single rate}}. \quad (5)$$

However a double tag requires a lot of statistics that the exclusive reconstruction alone can not provide. The particular kinematics of the decay $D^{*+} \rightarrow D^0 \pi^+$ offers a solution. The pion, noted π_* , is produced with a very small transverse momentum ($40 \text{ MeV}/c^2$) with respect to the D^{*+} direction. This provides a unique feature to tag D^{*+} decay through an excess of events in the p_t^2 distribution of tracks in the jet.

4.1. Mixed inclusive / exclusive tag

Charm is tagged in one hemisphere by the exclusive reconstruction of $D^{*+} \rightarrow D^0 \pi^+$ decays followed by four or five different channels for D^0 decays to increase the available statistics. In the other hemisphere, the π_* is used to tag charm. Both the OPAL⁴⁾ and DELPHI⁹⁾ collaboration measure $P(c \rightarrow D^{*+}) \times Br(D^{*+} \rightarrow D^0 \pi^+)$ with this double tagging method. Note that this method does not require the knowledge of the efficiency for D^0 decay reconstruction, since it cancels in the ratio (5). The crucial point here is the estimation of the π_* signal. The p_t^2 distribution of all π_* candidate is shown in figure 3. The background shape can be controlled using exclusive candidates outside the D^{*+} mass region or wrong charge correlations between D^{*+} and π_* , but it is the main source of internal systematic error.

Results for $P(c \rightarrow D^{*+}) \times Br(D^{*+} \rightarrow D^0 \pi^+)$ are presented in figure 4. The LEP average is compatible with the low energy data¹⁰⁾, thus the average has been used to extract R_c from single D^{*+} rate.

4.2. Double inclusive tag

A completely double inclusive tag is presented by the DELPHI⁸⁾ collaboration, where charm is tagged with the simultaneous detection of π_* in both hemispheres. As shown in (4, 5)

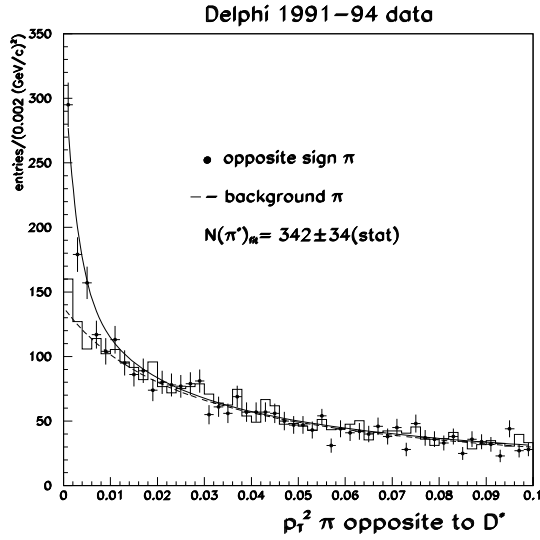


Figure 3: Distribution of the transverse momentum w.r.t the jet for π_* candidates. The background shape is fixed, and the solid line is the overall fit.

it provides both new independent measurements for R_c and $P(c \rightarrow D^{*+}) \times Br(D^{*+} \rightarrow D^0 \pi^+)$.

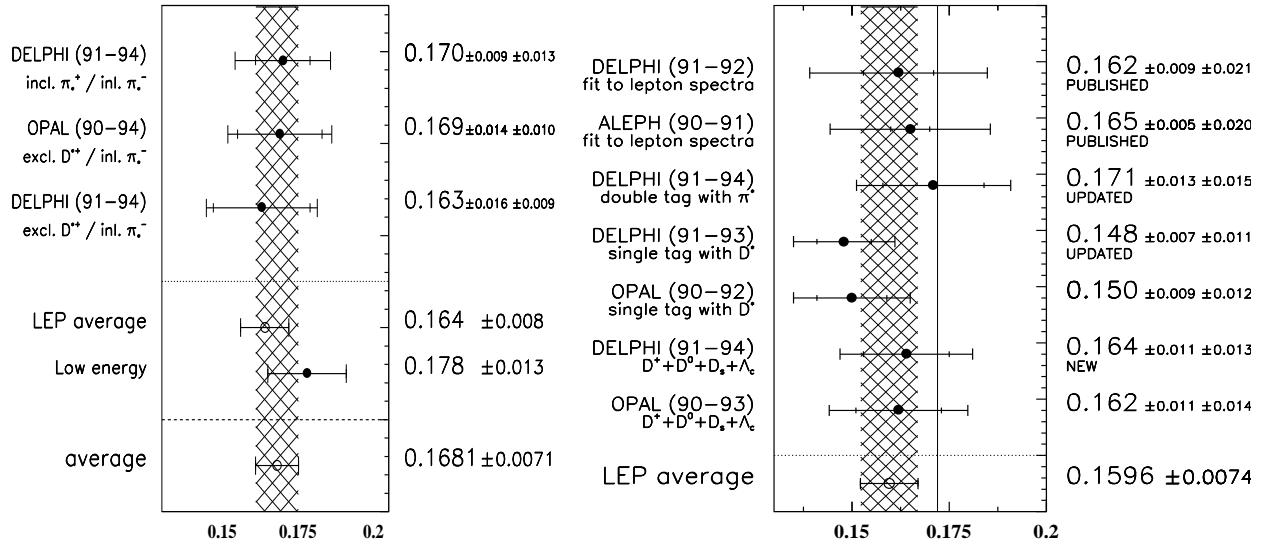
The π_* candidates are selected in the range $p_t^2 < 0.01$ $(\text{GeV}/c)^2$ in order to suppress background and bottom decays contamination. The signal contribution is estimated with a fit to four different p_t^2 distributions for single and double tagged events such that shapes for background and signal can be fixed entirely with data. This technique contributes to 4% to the internal systematic error. Then the bottom decays contribution is subtracted using $P(b \rightarrow D^{*+})$ measurement from single tag method, which is the only input, and contributes 3% to the uncertainty (see table 1).

Table 1: Comparison of uncertainties from different R_c measurements

methods	Charm counting $D^0 + D^+ + D_s^+ + \Lambda_c^+$	Single tag exclusive D^*	Double tag inclusive π_*
statistics	$\sim 7\%$	$\sim 6\%$	$\sim 8\%$
internal systematics	$\sim 5\%$	2 – 6%	$\sim 7\%$
fragmentation	$\sim 5\%$	$\sim 4\%$	$\sim 4\%$
b, c hadrons lifetimes	$\sim 3\%$	$\sim 2\%$	-
$g \rightarrow c\bar{c}$	$\sim 1\%$	$\sim 1\%$	-
branching ratio (PDG 95)	$\sim 3\%$	$\sim 3\%$	-
$P(c \rightarrow D^*)B(D^* \rightarrow D^0 \pi)$	-	$\sim 4\%$	-
internal $b \rightarrow D^*$	-	-	$\sim 3\%$
Total precision	11%	11%	12%

5. COMBINATION OF MEASUREMENTS AND CONCLUSION

The results are presented in figure 4. Whereas the lepton analysis¹⁾ have been published, most other measurements are preliminary. They all rely on the same input parameters, e.g. branching ratios for groundstates or fragmentation parameters, and the systematic errors have been computed in the same way (see table 1). The average¹⁰⁾ of the LEP Electroweak Heavy



(a) $P(c \rightarrow D^{*+}) \times Br(D^{*+} \rightarrow D^0 \pi^+)$

(b) R_c individual measurements and the average computed with all heavy flavour constraints

Figure 4: Measurements obtained by LEP collaborations using charm mesons reconstruction. The solid vertical line stands for the Standard Model expectation

Flavor Working Group has been done consistently with the procedure described in this proceeding¹¹⁾ including all correlations between different measurements. R_c measurement at LEP is $0.1596 \pm 0.0038(\text{stat}) \pm 0.0064(\text{syst})$, 1.8 standard deviation below the Standard Model expectation of 0.1725.

Acknowledgement

This review has been made possible thanks to numerous contacts with collaborators of both DELPHI and OPAL and thanks to the work of the LEP Electroweak Heavy Flavor Working Group. I would like to thank personally P. Antilogus, T. Behnke, D. Bloch, M. Hildreh, K. Moenig, F. Pierre and P.S. Wells.

References

1. ALEPH coll., D. Buskulic *et al.*, Phys. Lett. **B313** (1993) 535 and DELPHI coll., P. Abreu *et al.*, Z.Phys. **C65** (1995) 569
2. ALEPH coll., D. Buskulic *et al.*, Z.Phys. **C62** (1994) 1
3. OPAL coll., R. Akers *et al.*, Z.Phys. **C67** (1995) 57
4. OPAL coll., contributed paper to the EPS-HEP conference, Brussels 1995, eps0289, OPAL physics note PN175
5. DELPHI coll., contributed paper to the EPS-HEP conference, Brussels, eps0557, DELPHI note 95-101
6. OPAL coll. CERN-PPE/96-51
7. DELPHI coll., DELPHI note 96-30 PHYS 604
8. DELPHI coll., DELPHI note 96-33 PHYS 606
9. DELPHI coll., DELPHI note 96-34 PHYS 607
10. LEP Electroweak Heavy Flavor Working Group, LEPEWWG/96-01
11. P.S. Wells, this proceeding

Gluon Splitting into Heavy Quarks In e^+e^- Annihilations

H. Przysiezniak

U.of Alberta and CERN, PPE Division, 1211 Geneva 23

Abstract

Measurements of the multiplicity of heavy quark pairs from gluon splitting in e^+e^- annihilations at LEP are presented. A counting technique, based on the b-tagging of jets in 4-jet topologies, has been used by DELPHI to measure $\bar{n}_{g \rightarrow b\bar{b}}$. The mean multiplicity of gluons splitting into $b\bar{b}$ was measured to be

$$\bar{n}_{g \rightarrow b\bar{b}} = (0.22 \pm 0.13) \times 10^{-2}.$$

The multiplicity of gluons splitting into $c\bar{c}$ $\bar{n}_{g \rightarrow c\bar{c}}$ has been measured by OPAL in two separate analyses. In the first, the production of $D^{*\pm}$ mesons at very low x_{D^*} is studied and indications for $c\bar{c}$ production from gluon splitting is found. The mean multiplicity of this process in multihadronic Z^0 decays is measured to be $\bar{n}_{g \rightarrow c\bar{c}} = (4.4 \pm 1.4 \pm 1.5) \times 10^{-2}$. In the second, a 3-jet event topology is selected and charmed hadrons are tagged in the lowest energy jet using leptons. From this, a value of $\bar{n}_{g \rightarrow c\bar{c}} = (2.26 \pm 0.28 \pm 0.45) \times 10^{-2}$ is determined. Averaging the two measurements yields the final value of

$$\bar{n}_{g \rightarrow c\bar{c}} = (2.38 \pm 0.48) \times 10^{-2}.$$

Both the $\bar{n}_{g \rightarrow b\bar{b}}$ and $\bar{n}_{g \rightarrow c\bar{c}}$ measurements are consistent with theoretical expectations.

Presented at the XXXIst Rencontres de Moriond,
QCD and High Energy Hadronic Interactions, 23–30 March, 1996.

1 Introduction

Heavy quarks can be produced in e^+e^- annihilation via two processes: $e^+e^- \rightarrow Q\bar{Q}$, the direct production, and $e^+e^- \rightarrow q\bar{q}g$, where the gluon produces two heavy quarks, $g \rightarrow c\bar{c}$ or $g \rightarrow b\bar{b}$. The process of gluons splitting into heavy quarks can be reliably calculated in perturbative QCD theory, since it is an infrared finite quantity. However, in calculations at jet energy scales well above the quark mass, as produced in the process $e^+e^- \rightarrow Z^0 \rightarrow q\bar{q}g$, large logarithmic terms arise at all orders of the perturbative expansion, spoiling its convergence. Theoretical predictions differ significantly from one another (see Table 1). A measurement of these quantities would allow an important comparison with QCD calculations. Since the Standard Model prediction for $\Gamma_{b\bar{b}}/\Gamma_{\text{had}}$ differs by almost three standard deviations from the experimental value ¹⁾, knowledge of $\bar{n}_{g \rightarrow c\bar{c}}$ and $\bar{n}_{g \rightarrow b\bar{b}}$ can also be useful in an attempt to explain at least a part of this difference as an excess of observed b hadrons arising from gluons splitting into $b\bar{b}$.

Prediction from	$\bar{n}_{g \rightarrow c\bar{c}} [10^{-2}]$	$\bar{n}_{g \rightarrow b\bar{b}} [10^{-2}]$
Resummed + leading order ²⁾	1.35	0.177
Leading order ³⁾	0.607	0.100
HERWIG	0.923 ± 0.005	0.227 ± 0.001
JETSET	1.701 ± 0.013	0.160 ± 0.004
ARIADNE	2.177 ± 0.015	0.326 ± 0.006

Table 1: Theoretical predictions of $\bar{n}_{g \rightarrow c\bar{c}}$ and $\bar{n}_{g \rightarrow b\bar{b}}$. The leading order calculation ³⁾ is fully contained in the resummed calculation ²⁾. The Monte Carlo model predictions are taken from Ref. ²⁾.

2 Gluon goes to $c\bar{c}$: D^* -tagging method

The process of gluons splitting into heavy quarks is studied by OPAL in an analysis of D^* production at very low D^* energies ⁴⁾. The study is based on a total of 1.246 million Z^0 hadronic decay events that are selected from data collected from 1990 to 1992. D^* mesons are identified via the decay $D^{*+} \rightarrow D^0\pi^+$ followed by $D^0 \rightarrow K^-\pi^+$. The main contribution from gluon splitting to the D^* signal is expected in the low $x_{D^*} \equiv 2E_{D^*}/E_{\text{cm}}$ region.

Three main sources contribute to the D^* signal: primary c events, primary b events, and gluons splitting into a pair of heavy quarks that hadronize into a D^* meson. Decays of c-quarks are separated from those of b-quarks by a combination of bottom tagging methods using leptons, jet shape variables, and lifetime information. In the resulting differential cross-section, an excess of events is observed at very low x_{D^*} , above the expectations from the primary quark production processes $b \rightarrow D^*$ and $c \rightarrow D^*$. This is interpreted as a signal for $g \rightarrow c\bar{c}$. Using Monte Carlo to predict the shape of this component, the rates of D^* mesons from primary charm and from $g \rightarrow c\bar{c}$ are determined in a fit to this c-like sample. The result of the fit is shown in Fig.1. The final value for the average number of gluons splitting into a $c\bar{c}$ pair per hadronic Z^0 decay event is

$$\bar{n}_{g \rightarrow c\bar{c}} = (4.4 \pm 1.4 \pm 1.5) \times 10^{-2}.$$

The systematic error includes the effects of errors from the b/c separation procedures, errors in the D^* reconstruction, and additional errors which are caused by the above fit having to assume specific functional forms for the $c \rightarrow D^*$ fragmentation function and for the $g \rightarrow c\bar{c}$ spectrum.

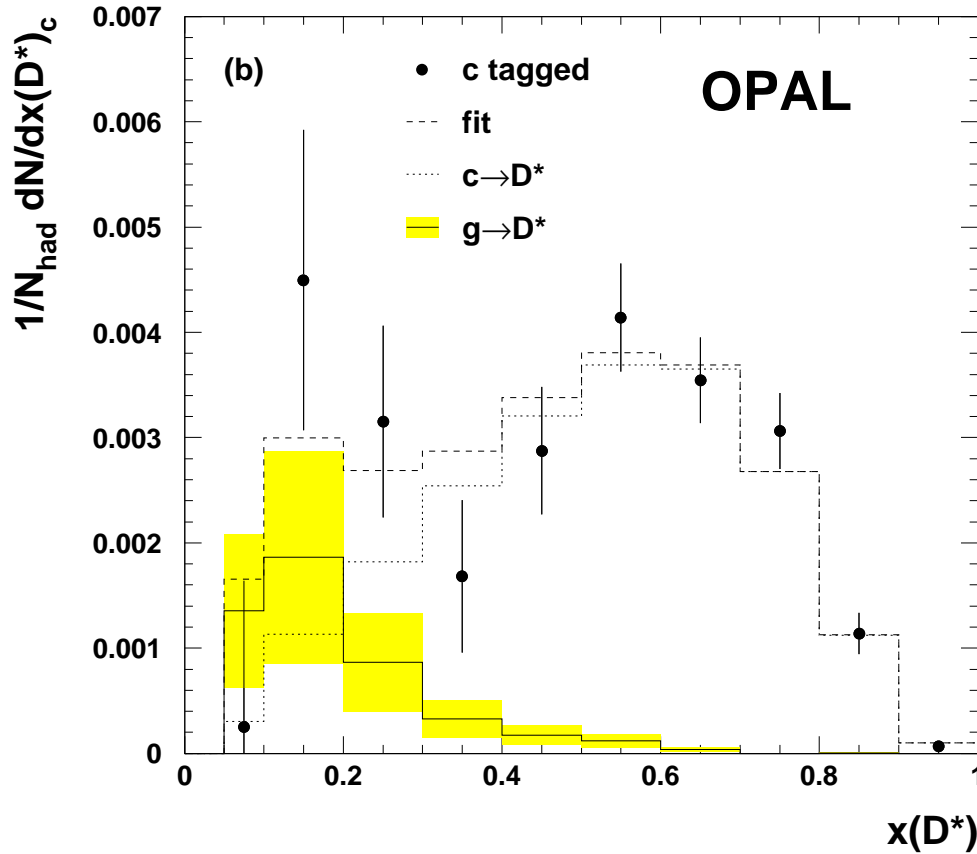


Figure 1: The observed yield of D^* mesons in c -tagged events, normalized to the total number of multihadronic events. The dashed curve is the result from the fit allowing both quark and gluon contributions to vary. The dotted line is the $c \rightarrow D^*$ component, and the solid one indicates the component from gluon splitting. The errors on the latter have been indicated by the shaded area, superimposed on the $g \rightarrow D^*$ curve.

3 Gluon goes to $c\bar{c}$: event topology method

In this approach gluon splitting into heavy quarks is studied by OPAL in an analysis of 3-jet events with a prompt lepton in the lowest energy jet, which is assumed to be the gluon jet ⁵⁾. The study is based on a total of 3.511 million Z^0 hadronic decay events that are selected from data collected from 1990 to 1994. The decay of a charmed hadron is then tagged by selecting events with either an electron or a muon in the gluon jet, and requiring $2 < p_e < 6$ GeV/c and $2 < p_\mu < 6$ GeV/c. The $b\bar{b}$ contribution to this sample is suppressed by requiring an anti-vertex tag and a cut on the invariant mass of the gluon jet. A clear difference between $g \rightarrow c\bar{c}$ and background events is found in the invariant mass distribution of the jet. The background subtracted distribution is shown in Fig. 2.

Monte Carlo is used to correct for the remaining non- $g \rightarrow c\bar{c}$ background, due to jet misassignment, residual photon conversions, lepton misidentifications, Dalitz decays of π^0 and η and leptons from $g \rightarrow b\bar{b}$ that survive the selection cuts. The result for the average number of charm quarks from gluon splitting per hadronic Z^0 decay, after correcting for the reconstruction efficiency and the charm hadron semileptonic branching ratio, is

$$\bar{n}_{g \rightarrow c\bar{c}} = (2.27 \pm 0.28 \pm 0.41) \times 10^{-2},$$

where the first error is statistical and the second is systematic.

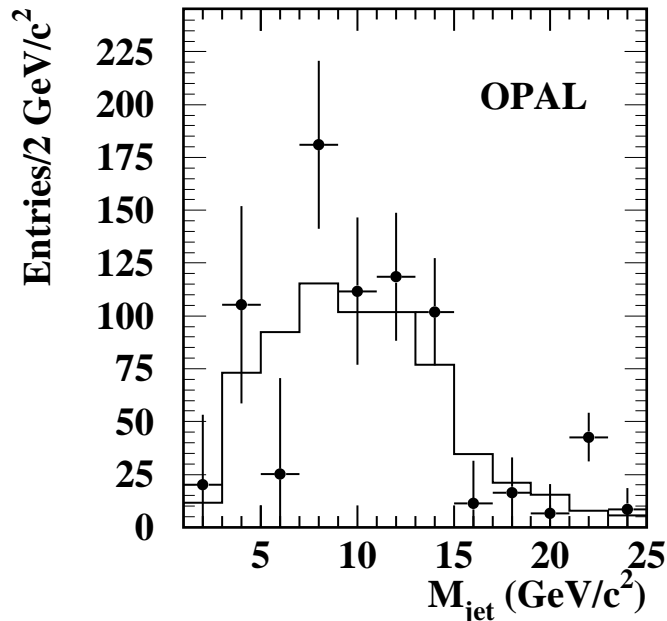


Figure 2: *The invariant mass of the lowest energy jet for background subtracted data (points) and the JETSET spectrum normalized to the measured value of $\bar{n}_{g \rightarrow c\bar{c}}$ (line histogram).*

4 Gluon goes to $b\bar{b}$: b-tagging in 4-jet events

Approximately 1.4×10^6 hadronic Z^0 events, collected by the DELPHI detector at LEP in 1994, were used to establish the presence of $g \rightarrow b\bar{b}$. Two b-jets are identified using a lifetime based tag in events with a 4-jet topology ⁶⁾. The quantity P_J (see Ref. ⁷⁾) was defined for each reconstructed jet of the event as the probability for the jet J to contain no decay products from long lived hadrons. A cut $P_J < 0.003$ was applied on the two jets forming the smallest angle in the event, numbered as jets #1 and #2 (where jet #1 is more energetic than jet #2). This selection maximizes the probability that the jets originated from secondary b quarks, i.e. from gluon splitting. The remaining two jets were numbered #3 and #4.

To reduce the amount of background, two more variables were used: the rapidity η_{TJ} of the jet J with respect to the thrust direction of the event, and the angle α_{1234} between the planes P_{12} , formed by jets #1 and #2, and P_{34} , formed by jets #3 and #4. A cut on η_{TJ} helps in rejecting those selected jets, mainly b-jets, coming from Z^0 decay (primary production). A cut on the rapidity of jet #1 was applied, by requiring $\eta_{T1} < 1.2$. It is also expected that the planes built with the selected jets be more perpendicular in cases of $g \rightarrow b\bar{b}$ occurrence than in background events, where jets #3 and #4 are usually originated by radiated gluons. A $|\cos \alpha_{1234}| < 0.8$ cut is thus used.

After imposing all the cuts, 28 events in data were left, out of which 15.1 were estimated to be background. Relying on JETSET simulation for the efficiency evaluation of the $g \rightarrow b\bar{b}$ signal, and taking into account systematic effects, the average number of beauty quarks from gluon splitting per hadronic Z^0 decay was found to be

$$\bar{n}_{g \rightarrow b\bar{b}} = (0.22 \pm 0.10 \pm 0.08) \times 10^{-2}$$

where the first error is statistical and the second is systematic.

5 Summary and conclusions

The multiplicity of charm quark pairs from gluon splitting was measured by the OPAL collaboration using two independent approaches: the analysis of D^* production at low x_{D^*} and the analysis of 3-jet events with a prompt lepton in the lowest energy jet. The two measurements of $\bar{n}_{g \rightarrow c\bar{c}}$ yield consistent results and are averaged, noting that the dominant part of the systematic uncertainties are uncorrelated, yielding a final average value of

$$\bar{n}_{g \rightarrow c\bar{c}} = (2.38 \pm 0.48) \times 10^{-2}.$$

The error includes the statistical and systematic errors added in quadrature. The DELPHI search for two b-jets in a 4-jet topology gives a measurement of $\bar{n}_{g \rightarrow b\bar{b}}$

$$\bar{n}_{g \rightarrow b\bar{b}} = (0.22 \pm 0.13) \times 10^{-2}$$

The values for both $\bar{n}_{g \rightarrow c\bar{c}}$ and $\bar{n}_{g \rightarrow b\bar{b}}$ are in good agreement with the theoretical calculations. Finally it should be stressed that this value of $\bar{n}_{g \rightarrow b\bar{b}}$ is consistent with the JETSET value of 0.16×10^{-2} and therefore lends support to the LEP method of accounting for $g \rightarrow b\bar{b}$ in the $\Gamma_{b\bar{b}}/\Gamma_{\text{had}}$ measurements 1).

Acknowledgements

It is a pleasure to thank the organizers of the conference for their efforts in arranging such an inspiring and enjoyable meeting. I would like to express my thanks to my OPAL colleagues Ties Behnke and Yoram Rozen, and to the DELPHI $\bar{n}_{g \rightarrow b\bar{b}}$ group, for their help in the preparation of this talk and manuscript.

References

1. LEP Electroweak Working Group, CERN-PPE/95-172.
2. M.H. Seymour, Nucl. Phys. **B 436** (1995) 163.
3. M.L. Mangano, P. Nason, Phys. Lett. **B 285** (1992) 160.
4. OPAL Collaboration, R. Akers et al., Z. Phys. **C 67** (1995) 27.
5. OPAL Collaboration, R. Akers et al., Phys. Lett. **B 353** (1995) 595.
6. DELPHI private communication from A. Baroncelli, P. Branchini, E. Graziani, C. Mariotti.
7. DELPHI Collab., P. Abreu *et al.*, CERN-PPE/94-131

ARE THE LEP AND SLD HEAVY FLAVOUR ELECTROWEAK DATA COMBINED CORRECTLY?

P. S. Wells,
CERN, 1211 Geneva 23, Switzerland

Abstract

This talk forms part of a mini-workshop on R_b and R_c , motivated by the current discrepancy between the measurements and the Standard Model expectation. The question of whether the data are combined correctly is addressed here. The complete averaging procedure used to combine all the heavy flavour electroweak data from LEP and SLD is described with a view to convincing the reader that it is indeed correct. The sensitivity of the averages to the dominant sources of systematic error is also discussed.

1 Introduction

The diverse measurements of electroweak quantities in the heavy quark sector from the four LEP experiments and from SLD have been combined to give the best estimates of the electroweak parameters^{1, 2)}. The average values of R_b and R_c are in poor agreement with the Standard Model expectation. The details of the combination procedure are described here, with a view to convincing the reader that it is correct. The measurements and averages are critically dependent on assumptions made about sources of systematic errors. Their effect is discussed, and some general words of caution are given.

2 The principles of the averaging procedure

2.1 Back to Basics

For a single measurement, $a_1 \pm \sigma_1$, with a Gaussian p.d.f., the χ^2 is given by:

$$\chi^2(x) = (x - a_1)^2 / \sigma_1^2.$$

Given two measurements, the best estimate, a_0 , is a linear combination of a_1 and a_2 with χ^2 given by:

$$\chi^2(x) = (x - a_1)^2 / \sigma_1^2 + (x - a_2)^2 / \sigma_2^2.$$

This has a minimum at $x = a_0$, and the 1 standard deviation error is given by $\Delta\chi^2 = \chi^2(a_0 \pm \sigma_0) - \chi^2(a_0) = 1$ (see figure 1a). Correlations between the measurements can be taken into account via the covariance matrix, \mathcal{C} . For example, if the two measurements have uncorrelated errors u_i and 100% correlated errors c_i , i.e. $a_1 \pm u_1 \pm c_1$ and $a_2 \pm u_2 \pm c_2$, the covariance matrix is given by:

$$\mathcal{C} = \begin{pmatrix} \sigma_1^2 & \rho\sigma_1\sigma_2 \\ \rho\sigma_1\sigma_2 & \sigma_2^2 \end{pmatrix} = \begin{pmatrix} u_1^2 + c_1^2 & c_1c_2 \\ c_1c_2 & u_2^2 + c_2^2 \end{pmatrix}$$

and the χ^2 , with the same properties as before, becomes:

$$\chi^2(x) = \sum_{ij=1,2} (x - a_i) \mathcal{C}_{ij}^{-1} (x - a_j).$$

If there are several sources of correlated errors, c_i^p , the off-diagonal terms are $\sum_p c_1^p c_2^p$. This method can be trivially extended to many measurements of the same parameter³⁾.

2.2 More than one parameter

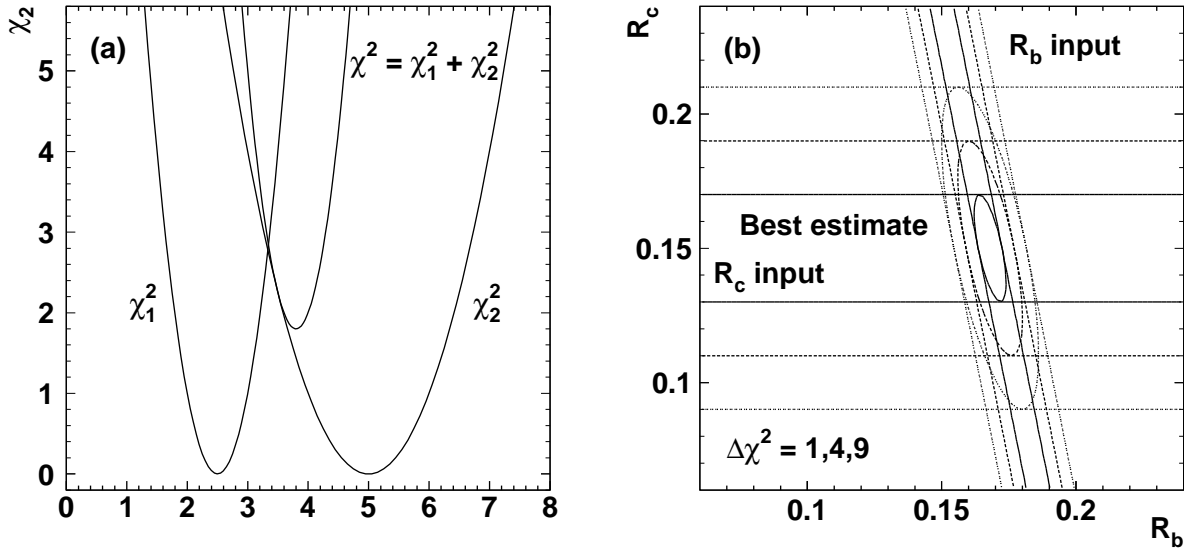
In the case of the electroweak heavy flavour analyses, we want the best estimates of 10 heavy flavour quantities¹⁾, denoted x^μ (where index μ corresponds to the parameter)

$$x^\mu = R_b, R_c, A_{\text{FB}}^{b\bar{b}}, A_{\text{FB}}^{c\bar{c}}, \mathcal{A}_b, \mathcal{A}_c, \\ \text{BR}(b \rightarrow \ell^-), \text{BR}(b \rightarrow c \rightarrow \ell^+), \bar{\chi}, \text{BR}(c \rightarrow D^{*+} \rightarrow \pi^+ D^0).$$

The mixing parameter $\bar{\chi}$ and the three branching ratios are included because they are measured simultaneously in several of the analyses. Individual measurements are denoted by r_i^μ , where the index i runs over the 76 measurements, and the index μ indicates which of the 10 parameters this measures. The χ^2 to be minimised w.r.t. the best estimates x^μ is given by:

$$\chi^2 = \sum_{ij} (r_i^\mu - x^\mu) \mathcal{C}_{ij}^{-1} (r_j^\nu - x^\nu)$$

Figure 1: The curves in (a) illustrate the combination of two uncorrelated measurements. In (b), a fictitious measurement of R_b which depends on R_c (eg. from double-tagging) is combined with a fictitious measurement of R_c which is independent of R_b (eg. using b-c separation in a D meson measurement). This illustrates the main source of the correlation between the combined values of R_b and R_c .



where C is the 76×76 covariance matrix for all the heavy flavour measurements. The 1 standard deviation error for a parameter is defined by $\Delta\chi^2 = 1$, minimising the χ^2 w.r.t. all other parameters.

The calculation of the full covariance matrix, $C = C^{\text{stat}} + C^{\text{syst}}$, is an essential part of the procedure. The statistical covariance matrix, C^{stat} , includes off-diagonal terms from multiparameter fits, and looks something like this:

$$\begin{pmatrix} a & 0 & 0 & 0 & 0 & 0 & .. \\ 0 & b & 0 & 0 & 0 & 0 & .. \\ 0 & 0 & c & x & y & 0 & .. \\ 0 & 0 & x & d & z & 0 & .. \\ 0 & 0 & y & z & e & 0 & .. \\ 0 & 0 & 0 & 0 & 0 & f & .. \\ : & : & : & : & : & : & g \end{pmatrix}$$

The systematic covariance matrix has the square of each total systematic error on the diagonal, C_{ii}^{syst} . The off-diagonal terms are calculated from a detailed breakdown of systematic errors (whose relative signs are important):

$$C_{ij}^{\text{syst}} = \sum_p c_i^p c_j^p$$

where the sum is over all sources of uncertainty, p , which affect both results i and j .

2.3 Interdependence of parameters

If a measurement r_i^μ of parameter x^μ depends on the value of some other parameter x^ν , $\nu \neq \mu$, this is taken into account explicitly in the χ^2 . For example, if the k th measurement is a precise double-tag value of R_b which depends on R_c and was evaluated with $R_c = R_c^{\text{used}}$, the following expression can be

included in the χ^2 :

$$r_k^{R_b} = R_b^{\text{meas}} + a_k^{R_c} \frac{(x^{R_c} - R_c^{\text{used}})}{x^{R_c}},$$

with the strength of the dependence given by the constant $a_k^{R_c}$ (see figure 1b).

2.4 Cross checks

Many cross checks can be made to verify that the combination procedure is correctly implemented. These are facilitated by the flexible framework in which the code runs. The χ^2 is well behaved with a unique minimum for each parameter. Comparing results from independently written code gives confidence that they are technically correct, while the input tables for complicated multiparameter fits can be checked for consistency by ensuring that they reproduce the individual fit results. In addition, averages made from subsets of results are consistent with those from simpler methods.

3 Common systematic errors

Sources of systematic uncertainty which are common to all the experiments, and which give a significant contribution to the total error in R_b or R_c , are listed in table 1. The present errors and possible improvements are indicated ^{4, 5}). The ‘‘pulls’’ indicate how many sigma ‘‘wrong’’ each input would have to be if it were the sole cause of the discrepancy with the Standard Model expectation.

3.1 Use of results from lower energy experiments at the Z

The validity of applying results from lower energy experiments at the Z energies is often questioned because the mixture of heavy hadrons produced may be different. A few comments are in order:

Semileptonic branching ratios: BR($b \rightarrow \ell^-$) and BR($b \rightarrow c \rightarrow \ell^+$) are now taken from LEP measurements, but CLEO data (including only B^0 and B^+) are still used for the decay spectra, while BR($c \rightarrow \ell$) also relies on lower energy data ¹).

Charm background for R_b : It is assumed that lower energy measurements of D fractions produced in $c\bar{c}$ events are valid at the Z. This is born out by the consistency of lower energy and LEP results (see table 1).

For measurements of R_c : Assumptions on the rates of D^0 , D^+ are not needed. There is still a gain in precision from using the lower energy average of BR($c \rightarrow D^* \rightarrow \pi D^0$) = 0.178 ± 0.013 in addition to the (consistent) LEP measurement of 0.164 ± 0.008 .

3.2 Hemisphere correlations

The equations for the number of tagged hemispheres and double tagged events have been seen many times in this workshop. They can be written as:

$$\begin{aligned} N_t/2N_{\text{had}} &= \varepsilon_b R_b + \varepsilon_c R_c + \varepsilon_{\text{uds}}(1 - R_b - R_c), \\ N_{tt}/N_{\text{had}} &= C_b \varepsilon_b^2 R_b + \varepsilon_c^2 R_c + \varepsilon_{\text{uds}}^2(1 - R_b - R_c), \end{aligned}$$

where $C_b = \varepsilon_b^d / \varepsilon_b^2$ accounts for the fact that the tagging efficiencies in the two hemispheres of the event may not be independent (ε_b^d is the double-tagging efficiency for a $b\bar{b}$ event). Neglecting background,

Table 1: Common systematic errors, with currently used “Value and range” (corresponding to PDG92), reasonable “New Values” (unofficial LEP average or PDG95) and the “Pull”, which is defined by: (Average–Standard Model)/(Signed error from this source).

Error source	Value and range	New value	R_b pull	R_c pull
Decay model $b \rightarrow \ell$	ACMM ^{+ISGW} _{-ISGW**}		-47	-34
Decay model $c \rightarrow \ell$	CL1 ^{+CL2} _{-CL3}		-88	∞
BR($c \rightarrow \ell$)	$(9.8 \pm 0.5)\%$		+21	+5
BR($b \rightarrow \bar{c} \rightarrow \ell^-$)	$(1.3 \pm 0.5)\%$		-161	+168
$\langle x_E(b) \rangle$ (if not in fit)	0.70 ± 0.02	0.695 ± 0.010 LEP	-129	+16
$\langle x_E(c) \rangle$ (if not in fit)	0.51 ± 0.02	0.515 ± 0.013 LEP	-100	+13
b fragmentation model	Peterson, Kartvelishvelli, Collins–Spiller		∞	+67
c fragmentation model	”		-135	-8
BR($D^0 \rightarrow K^- \pi^+$)	$(3.84 \pm 0.13)\%$	PDG’95	+61	+9
BR($D^+ \rightarrow K^- \pi^+ \pi^+$)	$(9.1 \pm 0.6)\%$	PDG’95	+168	+25
BR($D_s^+ \rightarrow \phi \pi^+$)	$(3.5 \pm 0.4)\%$	PDG’95	+178	+34
BR($\Lambda_c \rightarrow p K^- \pi^+$)	$(4.4 \pm 0.6)\%$	PDG’95	+198	+30
c baryon/ Λ_c	1.15 ± 0.05		∞	-94
D^0 fraction in $c\bar{c}$ events	0.557 ± 0.053	0.583 ± 0.035 LEP	-132	∞
D^+ fraction	0.248 ± 0.037	0.233 ± 0.024 LEP	-11	+55
$(D^0 + D^+)$ fraction	0.80 ± 0.07		-19	+124
D_s fraction	0.12 ± 0.05	0.097 ± 0.022 LEP	-18	+119
Λ_c fraction	0.08 ± 0.05	0.076 ± 0.033 LEP	-198	∞
D^0 lifetime (ps)	0.420 ± 0.008	0.415 ± 0.004 PDG’95	-35	-76
D^+ lifetime (ps)	1.066 ± 0.023	1.057 ± 0.015 PDG’95	-31	-52
D_s lifetime (ps)	$0.450^{+0.030}_{-0.026}$	0.467 ± 0.017 PDG’95	-44	-96
Λ_c lifetime (ps)	$0.191^{+0.015}_{-0.012}$	0.206 ± 0.012 PDG’95	-323	-30
B decay multiplicity	5.5 ± 0.5 OPAL	5.7 ± 0.3 OPAL, DELPHI	-263	+52
D decay multiplicity	2.53 ± 0.06		-15	+101
BR($D \rightarrow K_s^0 X$)	0.46 ± 0.06		+17	-109
$N(g \rightarrow b\bar{b})$	$(0.16 \pm 0.08)\%$		-41	∞
$N(g \rightarrow c\bar{c})$	$(1.6 \pm 0.8)\%$ theory	$(2.38 \pm 0.48)\%$ OPAL	-28	-24
Rate long-lived light h	JETSET $\pm 10\%$		-26	+118
Light quark frag.	JETSET \pm small		+20	-72

these equations give $R_b \approx C_b N_t^2 / 4 N_{tt} N_{\text{had}}$, i.e. R_b is very sensitive to the hemisphere correlations, with the relative change in R_b directly proportional to $C_b - 1$. Estimates of the error in $C_b - 1$ are between 0.3% and 1.3% and to date have been dominated by statistics (Monte Carlo or data). For this reason the uncertainty has been taken to be uncorrelated between measurements. Varying the assumptions on the correlated uncertainty due to C_b has a tiny effect on the R_b value or error. The result would be much more sensitive to a change in the evaluation of $C_b - 1$ or the error in this quantity. This is an area of intense study, whose treatment is expected to be refined in the near future.

4 Electroweak results

The combination procedure is applied to physical observables. Small corrections are applied to give the corresponding parameters for pure Z exchange. Defining $R_b \equiv \sigma(e^+e^- \rightarrow b\bar{b})/\sigma(e^+e^- \rightarrow \text{hadrons})$, $R_b^0 \equiv \Gamma(Z \rightarrow b\bar{b})/\Gamma(Z \rightarrow \text{hadrons})$, and similarly R_c and R_c^0 , the corrections for photon exchange are given by $R_b^0 = R_b + 0.0003$ and $R_c^0 = R_c - 0.0003$. The combined results are given below. The overall $\chi^2/\text{d.o.f.} = 41/(76-10)$, indicating that the measurements are self-consistent.

	Result	Correlation Matrix									
R_b^0	0.2211 ± 0.0016	1.0	-.30	.01	-.03	-.06	.05	-.11	-.07	.06	.10
R_c^0	0.1598 ± 0.0070	-.30	1.0	.05	.02	.07	-.06	.02	.15	-.03	-.43
$A_{\text{FB}}^{0,b}$	0.1002 ± 0.0028	.01	.05	1.0	.10	.04	.00	.02	-.15	.28	-.05
$A_{\text{FB}}^{0,c}$	0.0759 ± 0.0051	-.03	.02	.10	1.0	-.01	.06	-.01	-.06	.06	.00
\mathcal{A}_b	0.842 ± 0.052	-.06	.07	.04	-.01	1.0	.07	.00	-.06	.03	-.03
\mathcal{A}_c	0.618 ± 0.091	.05	-.06	.00	.06	.07	1.0	.09	-.13	.15	.01
$\text{BR}(b \rightarrow \ell^-)\%$	11.11 ± 0.23	-.11	.02	.02	-.01	.00	.09	1.0	-.31	.39	-.01
$\text{BR}(b \rightarrow c \rightarrow \ell^+)\%$	7.81 ± 0.40	-.07	.15	-.15	-.06	-.06	-.13	-.31	1.0	-.45	-.06
$\bar{\chi}$	0.1221 ± 0.0051	.06	-.03	.28	.06	.03	.15	.39	-.45	1.0	.00
$\text{BR}(c \rightarrow D^* \rightarrow \pi D^0)$	0.1681 ± 0.0071	.10	-.43	-.05	.00	-.03	.01	-.01	-.06	.00	1.0

5 Conclusion

The aim of this paper has been to demonstrate that the combination of data is correct, in that the averaging procedure is sensible, and performs as expected. Of course, the combined results are only as correct as individual input measurements. Unknown sources of error are not taken into account and any mistakes or incorrect assumptions in the input results are still present in the averages. It should be remembered that all dependences are assumed to be linear and all errors are assumed to be Gaussian. The input values and ranges for systematic errors will be updated in the near future, but no big deviations are expected.

Acknowledgements

It is a pleasure to thank the organisers for arranging such a fruitful and enjoyable conference, the LEP electroweak working group and LEP and SLD heavy flavour groups for their careful studies and collaboration, and in particular Mike Hildreth and Dave Charlton for input to this review.

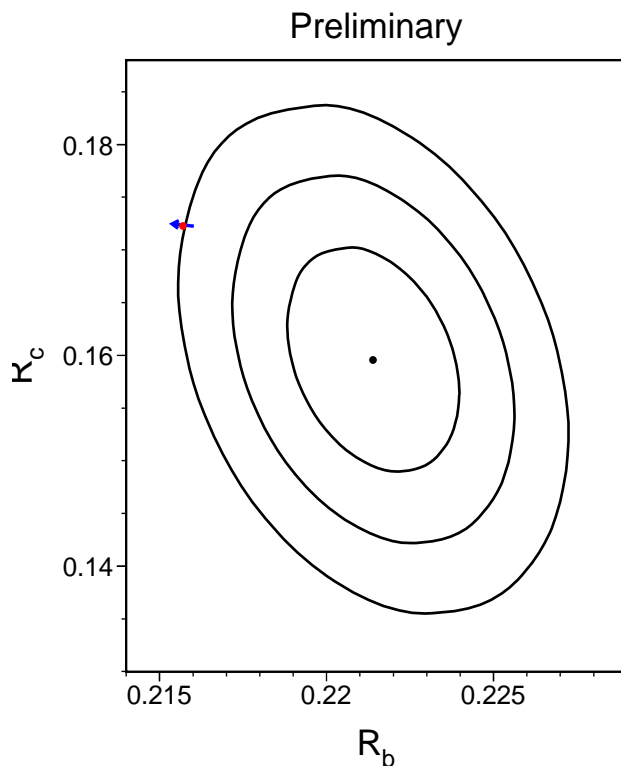
References

1. The LEP Experiments, Combining Heavy Flavour Electroweak Measurements at LEP, CERN-PPE/96-017, Submitted to NIM.
2. The LEP Experiments and the LEP Electroweak Working Group, A Combination of Preliminary LEP Electroweak Measurements and Constraints on the Standard Model CERN-PPE/95-172
3. L. Lyons, D. Gibaut and P. Clifford, Nucl. Instr. Meth. **A270** (1988) 110.
4. K. Hikasa *et al.*, Phys. Rev. **D45**(1992)S1.
5. L. Montanet *et al.*, Phys. Rev. **D50**(1994)1173, 1995 update (URL: <http://pdg.lbl.gov/>).

EFFECTS OF QCD IN R_b AND R_c

James G. Branson

University of California, San Diego



Abstract

The combined LEP and SLD measurements of R_b are about three standard deviations above the standard model. The measurement techniques employed are claimed to be highly reliable and systematically safe. R_c , which is measured using different and inherently less reliable techniques, is found to be 1.7 standard deviations low. In this paper, I will examine what constraints the measurements of α_s put on these measurements. I will also explore possible sources of systematics related to the models used to account for QCD effects in the processes measured.

1 Introduction

The LEP electroweak working group^{1, 2)} has made a careful combination of the measurements of R_b and R_c . Some of these results are preliminary but most have been published. The two measurements are slightly correlated. When the two are determined simultaneously the result is $R_b = 0.2211 \pm 0.0016$ compared to 0.2156 expected in the Standard Model and $R_c = 0.1598 \pm 0.0070$ compared to 0.172 expected in the Standard Model. R_b is 3.4 standard deviations or 2.6% high while R_c is 1.7 standard deviations or 7.0% low. This combined result is shown in Figure 1. Since the deviation in R_c is rather large and less significant statistically, they have also quoted the best value of R_b assuming that R_c takes on its standard model value. They find $R_b(R_c = 0.172) = 0.2202 \pm 0.0016$, which is still 2.9 standard deviations or 2.1% high compared to the Standard Model.

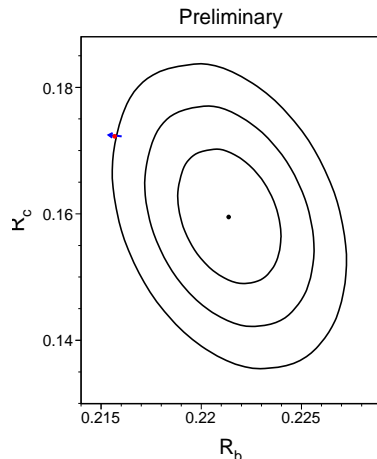


Figure 1: The measurement of R_b and R_c is shown as the point at the center of this figure. Confidence level contours are shown from 68% CL, 95% CL, and 99.7% CL. The Standard Model prediction is shown as the point at the upper left. The arrow represents the uncertainty on the standard model prediction and points in the direction of increasing top mass.

If the deviations in R_b and R_c are due to new physics beyond the standard model, they require a **change in the value of α_s measured from R_{had} on the Z^0** . If this α_s measurement becomes inconsistent with the other α_s determinations, we must be skeptical of changes in R_b and R_c .

As the other speakers in this session have made clear, **the measurement of R_b is designed to be insensitive to models**. The b tagging efficiency is measured in the data principally by comparing doubly tagged events to single tags. Models are only needed to calculate small backgrounds and to determine the efficiency correlation in the double tags. QCD effects play a role in this correlation.

Hard gluon emission can put both b and \bar{b} in the same hemisphere precluding a double tag. If this process is not modeled correctly, an error could result. Gluon emission also introduces correlations in the momenta of the two B particles. Since the efficiency is momentum dependent, this translates into an efficiency correlation which is sensitive to the fragmentation model. **Gluon splitting**, the process in which a radiated gluon produces an additional quark pair in the event can give rise to additional heavy quarks in the event and if not modeled correctly will produce an error in the result. Finally, other, perhaps nonperturbative, aspects of the QCD might not be modeled correctly.

2 New Physics in R_b and R_c Changes α_s

When, due to new physics, R_b and R_c are found to be different from their standard model value, the partial widths of the Z into b and c quarks, Γ_b and Γ_c , must change. This in turn will mean a change in the total width into hadrons, Γ_{had} . This is a very well determined quantity at LEP based on measurements of the Z^0 peak cross section and total width. Figure 2 shows an example of the detailed lineshape data used to determine Γ_{had} . The Γ_{had} measurement and Standard Model prediction can be summarized as follows:

$$\Gamma_{had} = \sum_q \Gamma_q = 1745.0 \pm 3.0 \text{ MeV vs. } 1744.8 \text{ in SM,}$$

$$\Gamma_q = \frac{\sqrt{2}}{4\pi} G_\mu M_Z^3 [\bar{g}_v^2 + \bar{g}_a^2] (1 + \delta_{QED}^q) (1 + \delta_{QCD}^q) \equiv \Gamma_q^0 (1 + \delta_{QCD}^q).$$

If Γ_b and Γ_c change, we need to adjust^{3, 4)} α_s and hence δ_{QCD}^q to maintain consistency with the measured value of Γ_{had} . Note that the LEP Electroweak group uses $\alpha_s = 0.123$ as measured from event shapes at LEP and finds good agreement between the measured Γ_{had} and the Standard Model without modified heavy quark partial widths. The dependence of the QCD radiative correction, δ_{QCD}^q , is given by

$$\delta_{QCD}^q = 1.06\left(\frac{\alpha_s}{\pi}\right) + 0.85\left(\frac{\alpha_s}{\pi}\right)^2 - 15\left(\frac{\alpha_s}{\pi}\right)^3 \cong 0.042 \text{ (for } \alpha_s = 0.123\text{)}.$$

This correction will be a small amount (0.002) larger for b quarks due to mass effects.

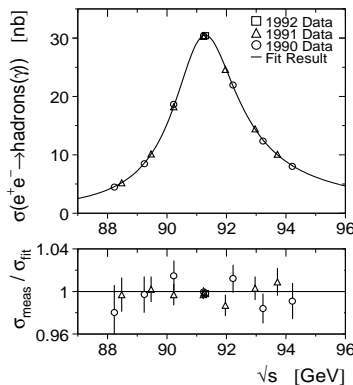


Figure 2: Z^0 lineshape data from L3 compared to the Standard Model fit. In the bottom graph, the deviation from the standard model is shown.

To understand the shift in α_s needed to agree with the new heavy quark partial widths, let us define $\Delta\Gamma_q \equiv \Gamma_q - \Gamma_q^{SM}$. Let us then examine several scenarios.

- Assume $\Delta\Gamma_u = \Delta\Gamma_d = \Delta\Gamma_s = 0$ and $\Delta\Gamma_c, \Delta\Gamma_b$ are **exactly** as measured. This implies that $\Delta\Gamma_{had} = -18.9$ MeV and hence α_s from Γ_{had} becomes 0.156 ± 0.006 which is in gross disagreement with other measurements of α_s . If we adjust R_c to be in agreement with α_s measurements, it is only a fraction of a standard deviation from the standard model. Therefore the large fractional deviation in Γ_c seems unlikely in this scenario.
- Assume universality: $\Delta\Gamma_u = \Delta\Gamma_c$ and $\Delta\Gamma_d = \Delta\Gamma_s = \Delta\Gamma_b$. This would make α_s even higher!
- Assume $\Delta\Gamma_u = \Delta\Gamma_d = \Delta\Gamma_s = \Delta\Gamma_c = 0$ and $\Delta\Gamma_b$ is **exactly** as measured. This calls for $\Delta\Gamma_{had} = 10.3$ MeV and $\alpha_s = 0.105 \pm 0.006$. Here we get into tough discussions on

the correct value of α_s . Low energy experiments tend to prefer values in the region of 0.113 (DIS). All the best LEP event shape measurements average 0.123. Which one is right for $\alpha_s(M_Z)$?

There are many other ways to set the partial widths to get any value of α_s in the region of 0.12. But there is no **experimental** motivation for any of them. If the partial widths into quarks are all at variance with the SM, why are the leptonic widths ok?

One possible scenario is that there is new physics in R_b and a fluctuation and/or a systematic problem in R_c . Perhaps the true R_b deviation from the SM is $\sim 1\sigma$ smaller than measured now giving and α_s which is very reasonable. The other scenario would be that there are systematic problems in both R_b and R_c , and no new physics. We will look for some problem in the measurement of R_b below.

3 Simulation of B Jets

It is important to study the basic simulation of b quark jets and a good deal of work has gone into this at LEP. Figure 3 shows three comparisons⁵⁾ between b jets and models. The first graph compares the energy distribution relative to the jet axis for b jets versus jets from light quarks. The second graph shows a similar distribution comparing b jets with gluon jets. The third shows the number of charged tracks which are significantly displaced from the primary vertex. The model agrees well with the data in all of these distributions.

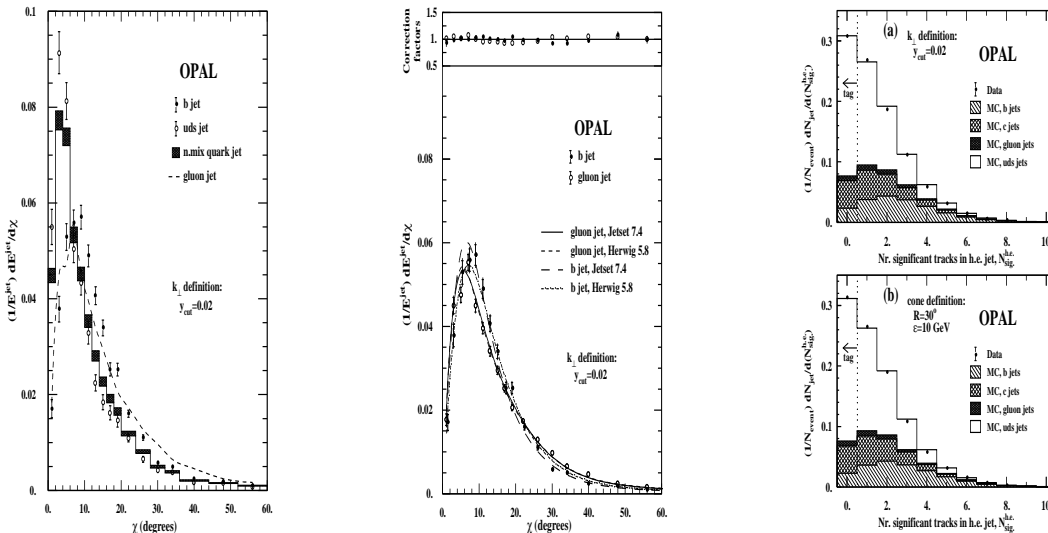


Figure 3: A comparison of the energy flow in b jets with (a) light quark jets, and (b) gluon jets. In (c) the number of lifetime significant tracks is checked in the MC model.

4 Gluon Emission

Hard gluon emission that causes both b and \bar{b} to be in the same hemisphere implies changes in the rate of double tagging. This process should be fairly well measured and modeled. Experiments have looked at the (negative) correlation this effect should induce. That is, since both b's are in the same hemisphere, double tagging becomes much less likely. Gluon radiation will also induce a positive correlation by softening momenta and increasing multiple scattering, thus reducing tagging probabilities in both hemispheres. Figure 4 shows

the general correlation studies done by ALEPH and DELPHI. They each include a study of correlation due to gluon emission using variables like thrust. The third part of Figure 4 shows a correlation computed by Delphi for data and Monte Carlo based on the thrust of the event. Data events were selected by tagging in the opposite jet to reduce light quark background. The agreement between data and Monte Carlo is impressive.

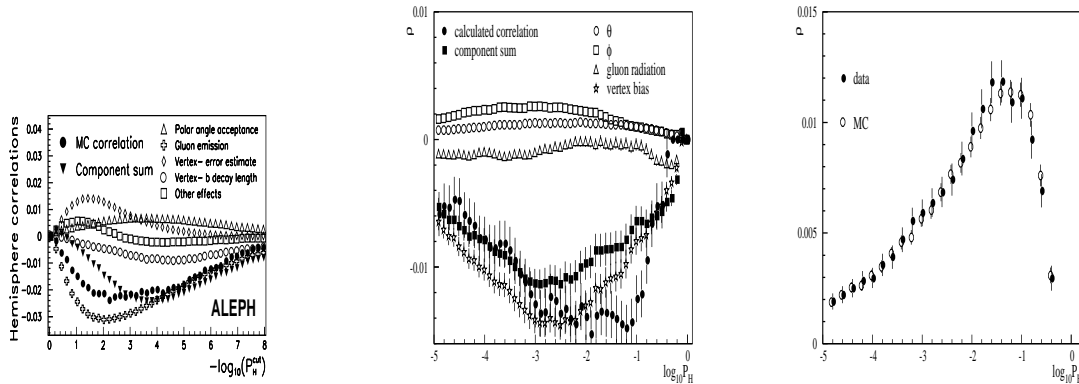


Figure 4: Hemisphere correlations calculated by ALEPH, calculated by DELPHI, and correlations due to gluon radiation obtained from the signed thrust in DELPHI data and MC.

5 Fragmentation Correlation

QCD predicts a correlation between the momenta of the two B mesons which is due to gluon emission. Hard gluon emission is simulated fairly well. It is less clear what happens in the fragmentation process. JETSET has some positive correlation. The size of this correlation is not sufficient to change R_b by very much. If the correlation were actually larger than simulated, R_b should increase.

Figure 6 shows the correlations in the SLD experiment in data and Monte Carlo. In particular the B momentum correlation is small and well reproduced in the Monte Carlo. The second part of Figure 6 shows a scatter plot of the two B momenta as produced in JETSET. A clear correlation is visible at both high momentum and low momentum. A larger correlation at low momentum would be quite dangerous but would move R_b even further from the Standard Model. Opal estimates a 4 per mille effect due to this momentum correlation.

It has been pointed out⁶⁾ at this conference, that the fragmentation models used may be far from correct in some regions, for example if two heavy quarks have very low momentum. This is also a region where detection is very difficult.

6 Gluon Splitting

Gluon splitting, which produces additional heavy quarks in an event, affects the tagging efficiency for light quarks. This has been discussed in the talk of Helenka Przywiecniak at this conference. The measured values are $g \rightarrow b\bar{b} = (0.22 \pm 0.13)\%$ and $g \rightarrow c\bar{c} = (2.38 \pm 0.48)\%$. These are now rather solid numbers. The LEP electroweak group assumes that gluon splitting is as in JETSET with an uncertainty of 50%: $F(g \rightarrow b\bar{b}) \approx (0.16 \pm 0.08)\%$, and $F(g \rightarrow c\bar{c}) \approx (1.6 \pm 0.8)\%$. With these assumptions, ALEPH, DELPHI and SLD derive a systematic error on R_b of about ± 0.0002 . Clearly, the measurements give us confidence that gluon splitting is not a major problem with the R_b measurement.

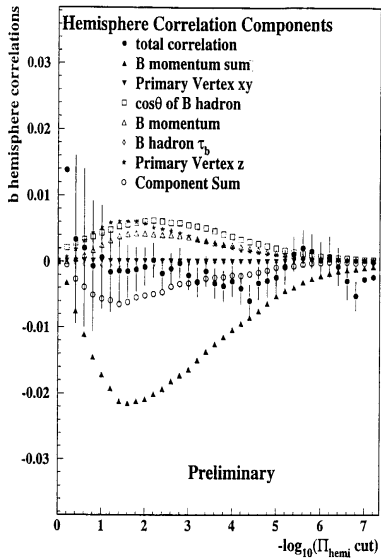


Figure 16: b -hemisphere correlation components

Figure 5: SLD correlations.

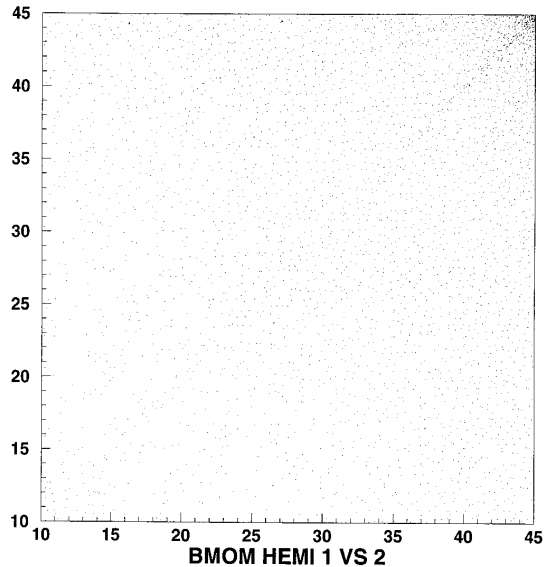


Figure 6: Momentum correlation in JETSET.

7 CONCLUSIONS

In summary, we can draw the following conclusions. The measured value of R_c , which deviates from the standard model by a large fraction (7% but only 1.7σ) would require an unacceptably large value of α_s in order to agree with the precise lineshape measurements from LEP. Assuming R_c takes on its standard model value, the measured value of R_b requires a rather low value of α_s which agrees with low energy measurements but disagrees with event shape measurements at high energy. While many combinations of the partial decay widths of the Z into quarks could fit all the data, we have no experimental motivation for anything except a large value or R_b .

Jets from b quarks are well described in the Monte Carlo. Gluon emission can give a large negative correlation but should be well modeled. B energy correlations are small and positive. Gluon splitting corrections are small and the processes have now been measured.

While the R_b measurements appear to be very solid, it is still unclear whether there is new physics behind them. The next round of measurements will hopefully give us a much clearer picture.

I would like to thank the organizers for an informative and enjoyable conference, and the LEP electroweak working group and LEP and SLD heavy flavor groups for their careful summaries.

References

1. The LEP Experiments, Combining Heavy Flavour Electroweak Measurements at LEP, CERN-PPE/96-017, Submitted to NIM.
2. The LEP Experiments and the LEP Electroweak Working Group, A Combination of Preliminary LEP Electroweak Measurements and Constraints on the Standard Model CERN-PPE/95-172
3. Kaoru Hagiwara, KEK preprint 95-184.
4. J. Field, Private communication
5. OPAL Collaboration, CERN-PPE/95-126.
6. V. Khoze, Private communication.

R_b IN THE MINIMAL SUPERSYMMETRIC STANDARD MODEL: HOW BIG CAN IT BE?

Piotr H. Chankowski
Institute of Theoretical Physics, Warsaw University,
ul. Hoża 69, 00-681 Warsaw, Poland.

Abstract

The possible magnitude of the supersymmetric contribution to R_b with imposed all available phenomenological constraints and demanding good quality of the global fit to the precision electroweak data is summarized. For small $\tan\beta$ and $M_2 \approx |\mu|$ and $\mu < 0$, R_b remains large, ~ 0.2180 even for the lighter chargino mass ~ 90 GeV. It is an interesting mixture of the up-higgsino and gaugino. The large $\tan\beta$ option (still not ruled out) for enhancement of R_b is also reviewed. In this case R_b up to ~ 0.2186 can be obtained.

1. The successful tests of the Standard Model (SM) to a per mille level are challenged by the measurements of the partial Z^0 widths into $\bar{b}b$ and $\bar{c}c$ quarks. The recent values of these quantities [1], $R_b = 0.2211 \pm 0.0016$ and $R_c = 0.1598 \pm 0.0070$ disagree with the SM prediction for $m_t = 170(180)$ GeV at the level of $3.1(3.4)\sigma$ and $1.7(1.7)\sigma$ respectively. It is therefore tempting to interpret these discrepancies as a first signal of physics beyond the SM.

As is well known, the value of the strong coupling, $\alpha_s(M_Z) = 0.123 \pm 0.005$, obtained from the SM fit to the electroweak data is strongly correlated with the values of R_b and R_c predicted in that model [2] and apparently does not agree with the value of $\alpha_s(M_Z)$ extracted at low energies e.g. DIS or lattice calculations. In a model which predicts R_b and R_c different by δR_b and δR_c than the SM we would get from the fit $\alpha_s(M_Z)$ different by $\delta\alpha_s = -4(\delta R_b + \delta R_c)$. This means that if both R_b and R_c anomalies were to be fully explained by some sort of "new physics" we would get $\alpha_s(M_Z) \approx 0.16$ which is unacceptably large and one would have to modify also Z^0 couplings to light quarks [3]. On the other hand, if the experimental result for R_c is due to a large statistical fluctuation then the full explanation of R_b by "new physics" would bring $\alpha_s(M_Z)$ down to $\alpha_s(M_Z) \approx 0.108$ which is also hard to accept. In view of that it seems reasonable to take measured R_b as a statistical hint for value of R_b somewhat larger than predicted by the SM and investigate other models to see how big R_b they can accommodate. In this note (based on ref. [4]) we do that for the MSSM which is the most popular and well motivated extension of the SM.

Any improvement in R_b must not destroy the perfect agreement of the SM with the other precision LEP measurements and must be consistent with several other experimental constraints (which will be listed later on). It is, therefore, important to discuss the changes in R_b in the context of global fits to the electroweak data. It has been shown [5] that the best fit of the MSSM single out either very small (~ 1) or very large ($\sim m_t/m_b$) values of $\tan\beta$ ($\tan\beta \equiv v_2/v_1$ where $v_{1,2}$ are the VEV of the two Higgs doublets). Therefore, our presentation will be divided into small and large $\tan\beta$ cases. In both cases, in order to maintain excellent agreement with the bulk of the precision data (i.e. to avoid new sources of the custodial $SU_V(2)$ symmetry breaking in the left currents) the superpartners of the left handed quarks of the third generation (and all left leptons) must be sufficiently heavy [6, 5], say, $M_{\tilde{q}_L}, M_{\tilde{l}_L} > \mathcal{O}(500 \text{ GeV})$. At the same time, R_b is sensitive mainly to the masses and couplings of the superpartner of the right handed top quark, charginos and - in the case of large $\tan\beta$ - superpartner of the right handed bottom and CP -odd Higgs boson A^0 [7]. The latter do not affect $SU_V(2)$ too much. Therefore, the requirement of good overall fit is not essentially in conflict with requirement of enhancement of R_b [5].

2. We begin with the low $\tan\beta$ case. When the lighter stop, \tilde{t}_1 , is dominantly right-handed, as required for a large $b\tilde{t}_1 C$ coupling, its coupling to Z^0 is suppressed (it is proportional to $g \sin^2 \theta_W$). Therefore, significant contribution can only come from diagrams in which charginos are coupled to Z^0 . Their actual magnitude depend on the interplay of the couplings in the $C_i^- \tilde{t}_1 b$ vertex and the $Z^0 C_i^- C_j^-$ vertex. The pattern of the chargino masses (which are mixtures of winos \tilde{W}^\pm and the two higgsinos \tilde{H}_1 and \tilde{H}_2) and couplings is determined by the ratio $r \equiv M_2/|\mu|$ (of the wino and higgsino masses) and depends crucially on the sign of μ [4]. The $C_i^- \tilde{t}_1 b$ coupling is large only for charginos with large \tilde{H}_2 component (it is then dominated by the top Yukawa coupling), the second - for charginos with large \tilde{W}^\pm component in at least one of its two-component spinors. This combination never happens for $\mu > 0$. Large R_b can then only be achieved at the expense of extremely light C_j^- and \tilde{t}_1 , either already ruled out by the existing mass limits or in conflict with global χ^2 . In addition, R_b is larger for $r > 1$ i.e. for higgsino-like chargino as the enhancement of the $C_1^- \tilde{t}_1 b$ coupling is more important than

of the $Z^0 C_1^- C_1^-$ coupling.

For $\mu < 0$ the situation is much more favourable. In the range $r \approx 1 \pm 0.5$ the second chargino which for low $\tan\beta$, is very close in mass to the lighter one, has large \tilde{H}_2 higgsino component and \tilde{W}^\pm component. Large couplings in both types of vertices of the diagram with charginos coupled to Z^0 give significant increase in R_b even for the lighter chargino as heavy as 80 – 90 GeV.

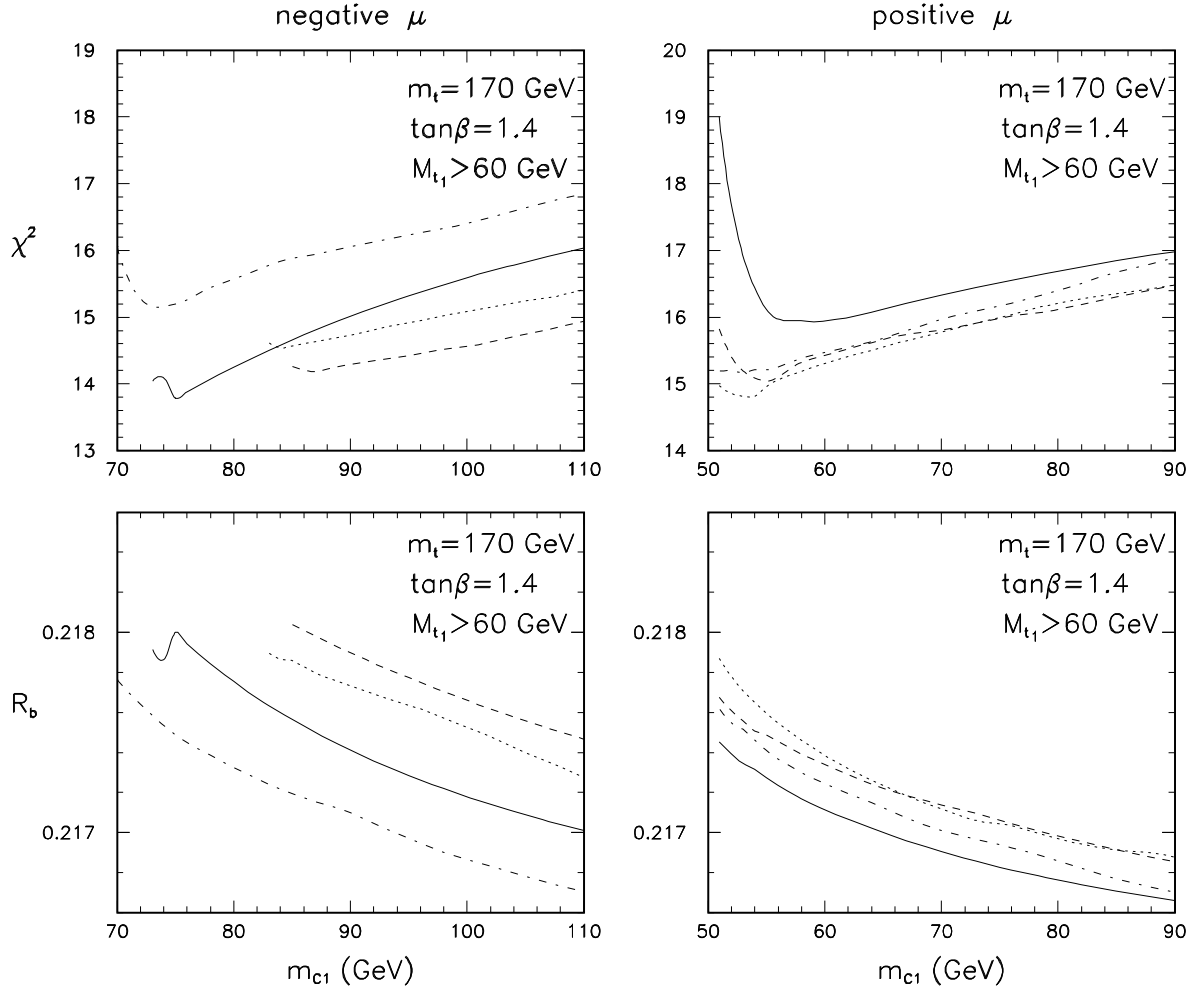


Figure 1: χ^2 as a function of m_{C_1} for $r \equiv M_2/|\mu| = 0.5$ (solid lines), 1 (dashed), 1.5 (dotted), and 3 (dash-dotted) for both signs of μ for $m_t = 170$ GeV, $\tan\beta = 1.4$, $M_A = M_{\tilde{t}_2} = 1$ TeV. In lower panels the best values of R_b with the restriction $\chi^2 < \chi^2_{min} + 1$ (here χ^2_{min} denotes the best χ^2 for fixed value of m_{C_1}) are shown. In addition we required $M_{\tilde{t}_1} > 60$ GeV.

We now turn our attention to a global fit to the precision. We impose the following constraints: 1) $\Gamma(Z^0 \rightarrow N_1^0 N_1^0) < 4$ MeV (N_i^0 are the four neutralinos), 2) $BR(Z^0 \rightarrow N_1^0 N_2^0) < 10^{-4}$, 3) $M_h > 60$ ($M_A > 55$) GeV for small (large) $\tan\beta$ [10], 4) $BR(b \rightarrow s\gamma)$ in the range $(1.2 - 3.4) \times 10^{-4}$ 5) $BR(t \rightarrow new) < 45\%$ (following ref. [8]) 6) Recent exclusion curves in the $(m_{N_1}, M_{\tilde{t}_1})$ plane from $D0$ obtained under the assumption $m_{C_1} > M_{\tilde{t}_1}$ [9].

The rôle of the lower limit on the Higgs boson mass depends on the mass of the heavier stop \tilde{t}_2 and the left-right mixing angle. For $M_{\tilde{t}_2} > 500$ GeV (as required for good quality of the global fit) and small mixing angles (necessary for large R_b) M_h is above the experimental limit in a large range of the parameter space. Very small and large left-right mixing angles are, however, ruled out by this constraint.

The $b \rightarrow s\gamma$ decay is a very important constraint on the parameters space [11]. In the MSSM an acceptable value of $BR(b \rightarrow s\gamma)$ can be obtained in two ways. One is a cancellation

between the H^\pm and supersymmetric contributions. This mechanism is however in conflict with the increase of R_b . The other mechanism is based on the choice of the proper range of the left-right mixing angles. It turns out [4] that for small $\tan\beta$ the region of acceptable $BR(b \rightarrow s\gamma)$ partly overlaps with the region of large R_b .

The results of a global fit are presented in Fig. 1 as projections of χ^2 as a function of m_{C_1} for several values of r . We also show the best values of R_b obtained with the restriction $\chi^2 < \chi_{min}^2 + 1$ where χ_{min}^2 is the minimum of the χ^2 for fixed m_{C_1} .

The value of $m_t = 170$ GeV chosen for the plots is close to the best value obtained from the fit. Larger values of m_t give worse χ^2 and this is a reflection of the well known from the SM fits correlation between the Higgs boson and the top quark masses [1]. Here M_h is constrained by supersymmetry and cannot follow the increase of m_t . In our fit $\tan\beta$ is bounded so that the top quark Yukawa coupling remains perturbative up to the GUT scale (we take $\tan\beta \geq 1.4$ for $m_t = 170$ GeV). We impose this theoretical constraint to remain on the conservative side, as lower values of $\tan\beta$ (for the same m_t) give larger R_b .

For $\mu > 0$, the best fit is obtained for $m_{C_1} \sim 50$ GeV, well below the new experimental limit from LEP1.5, $m_{C_1} > 65$ GeV [10]. This limit is valid for $m_{C_1} - m_{N_1} > 10$ GeV. In principle, the degeneracy of the chargino and neutralino masses can be better than 10 GeV. This occurs for $r > 10$ with $M_1 \approx 0.5M_2$ (note however, that supersymmetric contribution to R_b decreases for very large values of r) or for any value of r for sufficiently large M_1 (M_1 being the bino mass). On the other hand, for $m_{C_1} = 65$ GeV the maximal reachable value of R_b is only $R_b = 0.2173$.

For $\mu < 0$ χ^2 (R_b) is small (large) for much larger values of m_{C_1} . In fact the new LEP1.5 limit is totally irrelevant in this case. A chargino with mass $70 - 90$ GeV and with the composition described by $M_2 \approx |\mu|$ remains an interesting potential possibility. Supersymmetric contribution to R_b decreases with the stop mass but even for $M_{\tilde{t}_1} = m_{C_1} = 90$ GeV, $R_b > 0.2175$. Moreover, a significant enhancement in R_b is consistent with both configurations: $M_{\tilde{t}_1} > m_{C_1}$ and $M_{\tilde{t}_1} < m_{C_1}$.

3. Significant enhancement of R_b is also possible for large $\tan\beta$ values, $\tan\beta \approx m_t/m_b$. In this case, in addition to the stop - chargino contribution there can be even larger positive contribution from the h^0 , H^0 and A^0 Higgs boson exchanges in the loops, provided those particles are sufficiently light and non-negligible sbottom-neutralino loop contributions.

The discussion of large $\tan\beta$ case is relatively simpler as most of the results is symmetric under the simultaneous change of sign of μ and θ_t . In this case, for both signs of μ the chargino composition is the same in the up and down Weyl spinors and is a monotonic function of the ratio r . For enhancement in R_b the $b\tilde{t}_1C^-$ coupling is more important than the Z^0CC coupling, so higgsino-like chargino ($r \gg 1$) is more favourable.

For large $\tan\beta$, the $b \rightarrow s\gamma$ rate does not constrain the value of R_b at all due to the cancellation between H^+ and chargino/stop contributions [4]. The lower experimental bound on the lightest Higgs boson mass in the large $\tan\beta$ scenario is ~ 40 GeV. Since in the MSSM $M_{A^0} \approx M_{h^0}$, our results are not constrained by this bound.

In the parameter space which gives enhancement in R_b , also the decays $t \rightarrow new$ are enhanced. In addition to $t \rightarrow \tilde{t}_1 N_i^0$, important is also the decay $t \rightarrow bH^+$. For instance, for $m_t = 170$ GeV, $\tan\beta = 50$, $m_{C_1} = 65$ GeV and $M_A = 55(65)$ GeV we get $BR(t \rightarrow bH^+)$ ranging from 37(34)% up to 49(46)% depending on the stop sector parameters. However, the decay $t \rightarrow bH^+$ is not easily distinguishable from the standard one, $t \rightarrow bW^+$, for M_{H^+} close to M_W [8] and we do not impose this constraint in the global fit.

In Fig. 2 we present the results of a global fit in the large $\tan\beta$ case, together with the

corresponding values of R_b . Important feature of the global χ^2 is the decrease in the quality of the fit for $m_t = 180$ GeV (compared to the best fit for $m_t = 170$ GeV). This effect is stronger than similar effect for low $\tan\beta$.

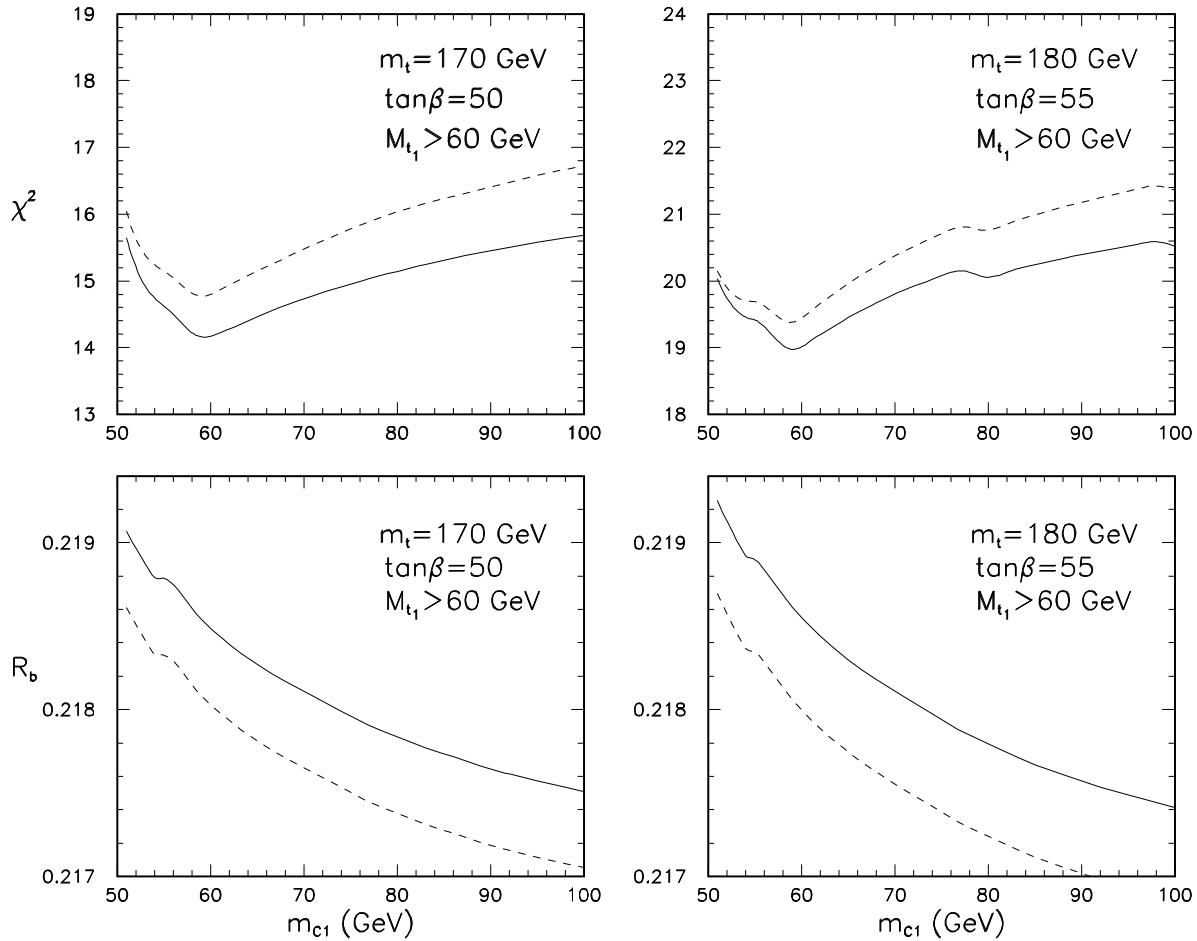


Figure 2: χ^2 as a function of m_{C_1} ($\mu > 0$) for $M_A = 55$ GeV (solid) and $M_A = 65$ GeV (dashed) for $m_t = 170$ GeV, $\tan\beta = 50$ and 180 GeV, $\tan\beta = 55$. $M_{\tilde{t}_2} = 1$ TeV, $M_{\tilde{b}_R} = 130$ GeV. In lower pannels the best values of R_b with the restriction $\chi^2 < \chi^2_{min} + 1$ (here χ^2_{min} denotes the best χ^2 for fixed value of m_{C_1}) are shown. In addition we required $M_{\tilde{t}_1} > 60$ GeV.

The values of R_b are almost insensitive to the value of $M_{\tilde{t}_1}$ in the range $50 - 100$ GeV and show the expected dependence on M_A and m_{C_1} with the maximal values for very light charginos. It is, therefore, worth recalling that the new limit $m_{C_1} > 65$ GeV is based on the assumption $m_{C_1} - m_{N_1} > 10$ GeV. As for low $\tan\beta$, better degeneracy of the two masses is achieved for $r > 10$ (and/or for $M_1 > 0.5M_2$) and the best fits for $m_{C_1} < 65$ GeV is obtained just for such values of r . Still, the quality of the fit with charginos below 60 GeV decreases significantly mainly due to the chargino contribution to the Z^0 wave function renormalization which affects Γ_Z [12]. Thus, the largest R_b which can be obtained requiring good quality of the fit is ~ 0.2186 . It is also remarkable, that due to the combined effect of neutral Higgs exchange and the chargino-stop together with the neutralino - sbottom contributions, the R_b remains greater than 0.2175 for masses well above the present experimental limits. E.g., for $m_{C_1} \approx M_{\tilde{t}_1} \approx M_A \approx 70$ GeV, $R_b = 0.2178$.

4. We conclude that the new LEP1.5 limit, $m_{C_1} > 65$ GeV still leaves open the possibility of a supersymmetric explanation of R_b up to $0.2180(2186)$ for small (large) $\tan\beta$. We also

conclude that $R_b > 0.2175$ (which is still interesting - see [13]) even for $m_{C_1} = M_{\tilde{t}_1} = 90$ GeV both in the small and large $\tan\beta$ cases. Thus LEP2 may not resolve this question. It is also worth noting that the best fit in the MSSM give $\chi^2 \approx 14.5$ for $m_t = 170$ GeV whereas similar fit in the SM gives at the minimum (arising for $m_t = 169$ GeV and $M_{H^{SM}} = 70$ GeV) $\chi^2 \approx 18.4$.

Finally, we stress that a good quality of the global fit requires the hierarchy $M_{\tilde{t}_1} \ll M_{\tilde{t}_2}$ (i.e. $M_{\tilde{t}_R} \ll M_{\tilde{t}_L}$). This hierarchy is natural if the low energy values of the soft squark masses have their origin in the renormalization group evolution from the GUT scale with the initial condition $m_0^2 \gg M_2^2$.

References

- [1] The LEP Electroweak Working Group, CERN preprint LEPEWWG/96-01.
- [2] A. Blondel, C. Verzegnassi *Phys. Lett.* **311B** (1993) 346,
J. Erler, P. Langacker *Phys. Rev.* **D52** (1995) 441.
- [3] P. Chiapetta these proceedings.
- [4] P.H. Chankowski, S. Pokorski hep-ph/9603310.
- [5] P.H. Chankowski, S. Pokorski *Phys. Lett.* **366B** (1996) 188.
- [6] P.H. Chankowski et al. *Nucl. Phys.* **B417** (1994), 101.
- [7] M. Boulware, D. Finnell *Phys. Rev.* **D44** (1991) 2054.
- [8] S. Mrenna, C.-P. Yuan *Phys. Lett.* **367B** (1996) 188.
- [9] S. Abachi et al. (D0 Collaboration) preprint FERMILAB-PUB-95-380-E (1995).
- [10] L. Rolandi, H. Dijkstra, D. Strickland and G. Wilson (ALEPH, DELPHI, L3 and OPAL collaborations) Joint Seminar on the First Results from LEP1.5, CERN, Dec. 1995.
- [11] R. Barbieri, G.F. Giudice *Phys. Lett.* **309B** (1993) 86.
- [12] R. Barbieri, F. Caravaglios, M. Frigeni *Phys. Lett.* **279B** (1992) 169.
- [13] A. Blondel these proceedings.

HADROPHILIC Z' : AN EXPLANATION OF LEP1, SLC AND CDF ANOMALIES?

P. Chiappetta

Centre de Physique Théorique, UPR 7061,
CNRS Luminy, Case 907, F-13288 Marseille Cedex 9.

Abstract

In order to explain possible departures from the Standard Model predictions of $b\bar{b}$ and $c\bar{c}$ production at Z peak, we propose the existence of a Z' vector boson with enhanced couplings to quarks. We first show that this proposal is perfectly consistent with the full set of LEP1/SLC results. We then show that there is a predicted range for enhanced $Z'q\bar{q}$ couplings which explains, for Z' masses in the TeV range, the excess of dijet events seen at CDF and leads to visible deviations at LEP2.

LE Z' HADROPHILE EXPLIQUE-T-IL LES ANOMALIES OBSERVÉES A LEP1, A SLAC ET A CDF ?

P. Chiappetta
Centre de Physique Théorique, UPR 7061,
CNRS Luminy, Case 907, F-13288 Marseille Cedex 9.

Résumé

Afin d'expliquer les déviations par rapport aux prédictions du Modèle Standard observées à LEP et au SLC dans le secteur des quarks lourds ($b\bar{b}$ et $c\bar{c}$), nous proposons l'existence d'un boson vectoriel Z' dont le couplage aux quarks est renforcé. Nous montrons tout d'abord que cette hypothèse est parfaitement consistante avec les données de LEP et du SLC. Nous établissons ensuite l'existence d'un domaine de valeurs des couplages $Z'q\bar{q}$ capable d'expliquer, pour des masses du Z' autour du TeV, l'excès d'évènements à deux jets observé à CDF et d'induire des effets visibles à LEP2.

1 Introduction

Through measurements of the $Z \rightarrow b\bar{b}$ and $Z \rightarrow c\bar{c}$ widths and asymmetries, LEP and SLC have given¹⁾ indications for possible departures from the SM predictions for b and c couplings at the level of a few percent. In the $b\bar{b}$ case such anomalies could be interpreted as a signal for NP in the heavy quark sector: anomalous top quark properties^{2),3)}, ETC models⁴⁾, Anomalous Gauge boson couplings⁵⁾, Supersymmetry contributions, new Higgses^{6),7)}. A common feature of all these explanations is that they fail to explain the possible existence of $c\bar{c}$ anomalies.

We would like to propose⁸⁾ a simple explanation based on the existence of a hadrophilic Z' vector boson, i.e. one which would couple universally to quarks more strongly than to leptons. We shall not propose here a specific model. We shall be limited to extracting from LEP1/SLC experiments several suggestions about the required Z' properties. To achieve this, we shall first rely on a model independent framework for the analysis of $Z - Z'$ mixing effects⁹⁾, in which the $Z'f\bar{f}$ couplings were left free. We will then derive experimental informations on the $Z - Z'$ mixing angle θ_M and on the $Z'f\bar{f}$ couplings showing that, indeed, the anomalies in $b\bar{b}$ and $c\bar{c}$ production can be described by such an hadrophilic Z' .

The next relevant question to be answered is that of whether the values of the Z' couplings that we determined in this way do not contradict any already available experimental constraint and in particular, the significant excess of dijet events for large masses (above 500 GeV) seen at CDF¹⁰⁾. We shall show that this phenomenon could be naturally explained in terms of an hadrophilic Z' , whose mass lies in the range between 800 GeV and 1 TeV. In Ref.¹¹⁾ more restrictions have been imposed on the Z' couplings, namely from assuming equality of left-handed couplings within $SU(2)_L$ doublets and leaving free the right handed couplings. Our next step will then consist of examining the consequences of this solution for other processes, in particular possible Z' effects in $e^+e^- \rightarrow f\bar{f}$ at LEP2.

2 Analysis of LEP1/SLC results.

We consider $Z - Z'$ mixing effects at the Z peak in a model independent way following the procedure given in ref.⁹⁾. As well-known, the two relevant effects consist in a modification of the Z couplings to fermions, proportional to a mixing angle $\equiv \theta_M$, and in a Z mass shift which induces a contribution to the δ_ρ parameter:

$$\delta_\rho^{Z'} \simeq \theta_M^2 \frac{M_Z^2}{M_{Z'}^2} \quad (1)$$

From the latest available data¹⁾, we derive an upper value for the mixing angle at two standard deviations:

$$|\theta_M| < \sqrt{0.005} \frac{M_Z}{M_{Z'}} \quad (2)$$

We then normalize the $Z' f \bar{f}$ couplings in the same way as the $Z f \bar{f}$ ones:

$$-i \frac{e(0)}{2s_1 c_1} \gamma^\mu [g'_{Vf} - g'_{Af} \gamma^5] \quad (3)$$

(for Z couplings: $g_{Vl} = -\frac{v_1}{2}$; $g_{Al} = -\frac{1}{2}$; $v_1 = 1 - 4s_1^2$; $s_1^2 c_1^2 = \pi\alpha(0)/\sqrt{2}G_\mu M_Z^2$).

We measure the magnitude of the $Z' f \bar{f}$ couplings by defining the ratios $\xi_{Vl} \equiv \frac{g'_{Vl}}{g_{Vl}}$ and $\xi_{Al} \equiv \frac{g'_{Al}}{g_{Al}}$. The Z' couplings are summarized below in the form of allowed bands, at two standard deviations, assuming that $|\theta_M|$ saturates the bound, eq. (2), with the two possible signs: $\eta_M = \pm 1$.

$Z' l \bar{l}$ couplings

$$\eta_M \xi_{Vl} \simeq (-2.25 \pm 6.25) \left(\frac{M_{Z'}}{1 \text{TeV}} \right) \quad (LEP) \quad \eta_M \xi_{Vl} \simeq (+1.75 \pm 6.25) \left(\frac{M_{Z'}}{1 \text{TeV}} \right) \quad (SLC) \quad (4)$$

$$\eta_M \xi_{Al} \simeq (-0.2 \pm 0.5) \left(\frac{M_{Z'}}{1 \text{TeV}} \right) \quad (5)$$

$Z' b \bar{b}$ couplings

$$\eta_M \xi_{Vb} \simeq (-3.45 \pm 20.72) \left(\frac{M_{Z'}}{1 \text{TeV}} \right) \quad (LEP) \quad \eta_M \xi_{Vb} \simeq (-24.24 \pm 25.98) \left(\frac{M_{Z'}}{1 \text{TeV}} \right) \quad (SLC) \quad (6)$$

$$\eta_M \xi_{Ab} \simeq (+4.58 \pm 9.84) \left(\frac{M_{Z'}}{1 \text{TeV}} \right) \quad (LEP) \quad \eta_M \xi_{Ab} \simeq (+14.54 \pm 12.47) \left(\frac{M_{Z'}}{1 \text{TeV}} \right) \quad (SLC) \quad (7)$$

$Z' c \bar{c}$ couplings

$$\eta_M \xi_{Vc} \simeq (-6.94 \pm 26.60) \left(\frac{M_{Z'}}{1 \text{TeV}} \right) \quad (LEP) \quad \eta_M \xi_{Vc} \simeq (-20.38 \pm 40.62) \left(\frac{M_{Z'}}{1 \text{TeV}} \right) \quad (SLC) \quad (8)$$

$$\eta_M \xi_{Ac} \simeq (-7.88 \pm 8.46) \left(\frac{M_{Z'}}{1 \text{TeV}} \right) \quad (LEP) \quad \eta_M \xi_{Ac} \simeq (-6.01 \pm 9.70) \left(\frac{M_{Z'}}{1 \text{TeV}} \right) \quad (SLC) \quad (9)$$

From SLC data, a definite non zero value for ξ_{Ab} is suggested. A priori we would not trust values larger than the QCD strength ($\alpha_s \simeq 0.12$).

From the very precise measurement of Γ_{had} we can derive a strong correlation between $\delta\Gamma_b$ and $\delta\Gamma_c$, that is peculiar of our Z' hypothesis. Our universality assumptions lead to:

$$\frac{\delta\Gamma_b}{\Gamma_b} \simeq -0.5 \frac{\delta\Gamma_c}{\Gamma_c} \quad (10)$$

Thus, in a natural way, the relative shifts in Γ_b and in Γ_c are predicted to be of opposite sign, with a ratio consistent with the experimental data and errors.

3 Analysis of CDF dijet events in terms of a Z' .

The CDF collaboration¹⁰⁾ has reported the observation of an excess of events with two-jet mass above 500 GeV, compared to the QCD prediction. The two jet production in hadronic collisions has been computed at next to leading order in QCD¹²⁾. We shall now investigate whether the observed dijet excess may be explained in terms of a hadrophilic Z' . We have therefore to add to the dominant QCD component the weak contributions arising from W,Z, γ exchanges and from the Z' with couplings taken within the range suggested by the LEP/SLC analysis. Since the weak contribution due to SM bosons has been evaluated at leading order¹³⁾, we shall therefore restrict our calculation to leading order.

The result of our investigation is shown in figure 1. As one can see, the observed dijet excess can be satisfactorily explained for $M_{Z'}$ around 800–900 GeV and for typical values of couplings $|\xi_{Ab}| = |\xi_{Vb}| \simeq 3$. The excess of dijet events has been fitted in Ref.¹¹⁾ by a Z' of mass 1 TeV provided that its quark couplings are large and its width lies below 500 GeV. The uncertainty due to our imperfect knowledge of the structure functions is small since we calculate a ratio. The dominant weak contribution is due to the Z' pole: we are therefore not sensitive to the sign of $Z'q\bar{q}$ couplings.

4 Z' Effects in hadronic production at LEP2

We shall examine possible visible consequences at LEP2 of our assumption that a hadrophilic Z' exists. Since there is no indication for large $Z'l\bar{l}$ couplings, we shall concentrate our attention on the three hadronic observables that will be measured at LEP2, i.e. the $b\bar{b}$ cross section $\sigma_b(q^2)$, the $b\bar{b}$ forward backward asymmetry $A_{FB,b}(q^2)$ and the total hadronic production cross section $\sigma_h(q^2)$, where $\sqrt{q^2}$ is the total center of mass energy¹⁴⁾. The calculated shifts on these three quantities due to a Z' will depend on products of Z' quark couplings with Z' lepton couplings. Following a conservative attitude, we shall assume therefore that the leptonic Z' couplings lie in the domain of non observability at LEP2¹⁵⁾, corresponding for $q^2 = (175\text{GeV})^2$ to the following limitations on the leptonic ratios:

$$|\xi_{Vl}| \lesssim 8.02 \left(\frac{M_{Z'}}{1\text{TeV}} \right) \quad |\xi_{Al}| \lesssim 1.01 \left(\frac{M_{Z'}}{1\text{TeV}} \right) \quad (11)$$

Using as input the upper bounds, we shall first compute the relative shifts $\frac{\delta\sigma_b(q^2)}{\sigma_b}$ and $\frac{\delta A_{FB,b}(q^2)}{A_{FB,b}}$, using a theoretical approach proposed very recently¹⁶⁾. In figure 2 we present our results for the $Z'b\bar{b}$ couplings rescaled by the factor $\frac{M_{Z'}}{1\text{TeV}}$. The observability regions of figure 2 correspond

to a relative Z' effect in $\frac{\delta\sigma_b}{\sigma_b}$ of at least five percent (dark area) and ten percent (grey area). As one can see from an inspection of the figure, values of the couplings lying in the neighbourhood of $|\xi_{Ab}| = |\xi_{Vb}| \simeq 3$ should not escape indirect experimental detection in the final $b\bar{b}$ channel at LEP2 according to the analysis presented in ref.¹⁵⁾. These values of the Z' couplings would also be able to generate a clean effect in the total hadronic observables.

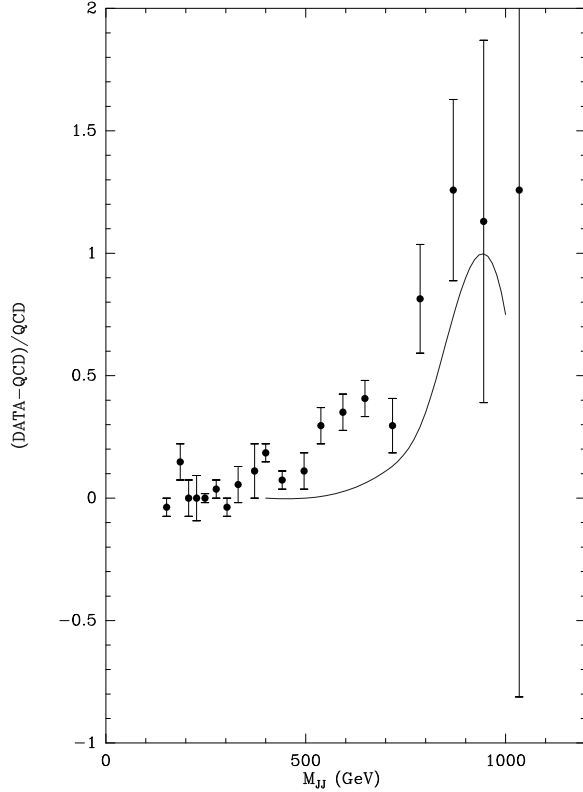


Fig. 2

Fig. 1 Fractional difference between dijet CDF data¹⁰⁾ and QCD compared to a hadrophilic Z' of mass $M_{Z'} = 900$ GeV for $\xi_{Vb} = 4$, $\xi_{Ab} = 3$, $\xi_{Vc} = 4$ and $\xi_{Ac} = 3$.

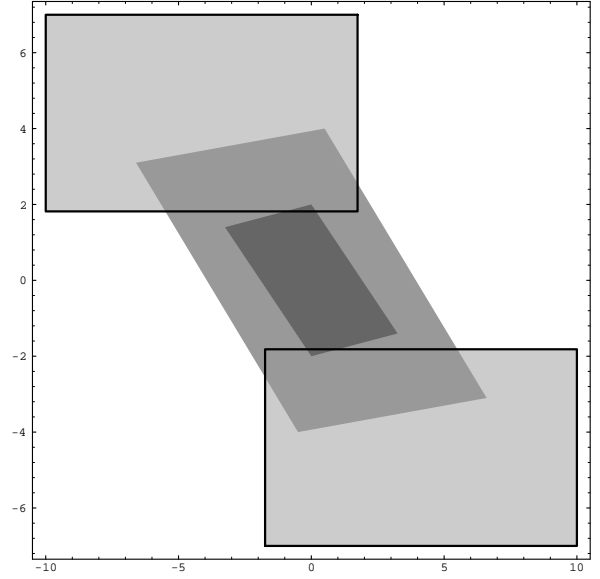


Fig. 2 Domains in $Z'bb$ vector (abscissa) and axial (ordinate) coupling ratios scaled by the factor $(M_{Z'}/1TeV)$. Observability limits from σ_b at LEP2 with two possible accuracies, 5% (Central dark), 10% (Central grey).

5 Conclusions

The presence of anomalous effects in heavy quarks decay channels at Z peak could be explained by a Z' more strongly coupled to quarks than to leptons, a hadrophilic Z' . It can also naturally explain the observed excess of high mass dijet events at CDF provided that its couplings to quarks are quite large, its mass range lies around 800 – 1000 GeV and it is wide. The existence of a hadrophilic Z' with couplings and mass range constrained to produce LEP1/SLC and CDF anomalies could be confirmed by hadronic measurements at LEP2.

References

- [1] P.B. Renton, Rapporteur talk at the Int. Conf. on High Energy Physics, Beijing (1995); see also P. Langacker, hep-ph/9511207; see also LEP and SLC contributions in these proceedings.
- [2] E. Malkawi and C.P. Yuan, Phys. Rev. **D50** (1994) 4462.
- [3] G.J. Gounaris, F.M. Renard and C. Verzegnassi, Phys. Rev. **D52** (1995) 451.
- [4] E.H. Simmons, R.S. Chivukula and J. Terning, BU-HEP-95-3x(1995).
- [5] F.M. Renard and C. Verzegnassi, Phys. Lett. **B345** (1995) 500 .
- [6] J.D. Wells and G.L. Kane, SLAC-PUB-7038(1995); P. Chankowski in these proceedings.
- [7] D. Comelli, F.M. Renard and C. Verzegnassi, Phys. Rev. **D50** (1994) 3076.
- [8] P. Chiappetta, J. Layssac, F.M. Renard and C. Verzegnassi, hep-ph 9601306, to appear in Phys. Rev. D.
- [9] J. Layssac, F.M. Renard and C. Verzegnassi, Phys. Lett. **B287** (1992) 267 , Z. Phys. **C53** (1992) 97.
- [10] E. Buckley-Geer, FERMILAB-Conf-95/316-E (1995), to appear in Proceedings of International EPS Conference on HEP, Brussels.
- [11] G. Altarelli, N. Di Bartolomeo, F. Feruglio, R. Gatto and M. Mangano, hep-ph 9601324.
- [12] S. D. Ellis, Z. Kunszt and D. E. Soper, Phys. Rev. Lett. **69** (1992) 1496.
- [13] C. Bourrely, J. Ph. Guillet and J. Soffer, Nucl. Phys. **B361** (1991) 86.
- [14] Proceedings of LEP2 workshop (1995), CERN report 96-01 (G. Altarelli, T. Sjostrand and F. Zwirner eds).
- [15] P. Chiappetta, C. Verzegnassi et al, in Proceedings of LEP2 workshop (1995), CERN report 96-01 vol 1 p577 (G. Altarelli, T. Sjostrand and F. Zwirner eds).
- [16] F.M. Renard and C. Verzegnassi, Phys. Rev. **D52** (1995) 1369 and Phys. Rev. **D53** (1996) 1290 .

Summary: R_b , R_c and QCD

Alain BLONDEL

L.P.N.H.E. Ecole Polytechnique, IN²P³-CNRS, 91128 Palaiseau France; and CERN, PPE division

The Standard Model (SM) is ruled out at 99.7% C.L. by the measurements of R_b and R_c , if one assumes Gaussian errors. Experiments are in good agreement with each other, all on the same side of the SM. Systematic errors dominate the average. The averaging procedure is mechanically correct, and could not be incriminated for a bias in the average or for too small errors. Of course, it could not inject systematic uncertainties that would have been underestimated or overlooked by all experiments.

New results were presented: i) a new method by SLD uses a tag based on secondary vertex with a high invariant mass; ii) new measurements of $c \rightarrow D^*$ production rate make single tag measurements of R_c less model-dependent; iii) gluon splitting $g \rightarrow b\bar{b}$ is measured in agreement with the assumed theoretical values, and cannot explain the R_b discrepancy.

Possible correlations of tagging efficiency between hemispheres were identified as the weakest item in the experimental procedure. At present, these correlations are calculated from hadronization Monte-Carlos, errors are MC statistics only, and, consequently, assumed uncorrelated between experiments. A negative correlation of -2%, common to all methods and experiments, would be necessary to bring R_b in agreement with SM – and with the measurement of the hadronic width. A particularly vicious possibility was discussed during the Rencontres: b -hadron momentum correlations from fragmentation. The subject is an area of intense study.

Meanwhile, Supersymmetry volunteers to explain part of the R_b effect, but no discrepancy in R_c , please. To explain both, one has to call in the Hadrophilic or Leptophobic Z' .

With a large fraction of LEP Z peak data not yet analysed, more data to come from SLD, and systematic error studies going on, the situation might change dramatically in the next year.

1 Introduction

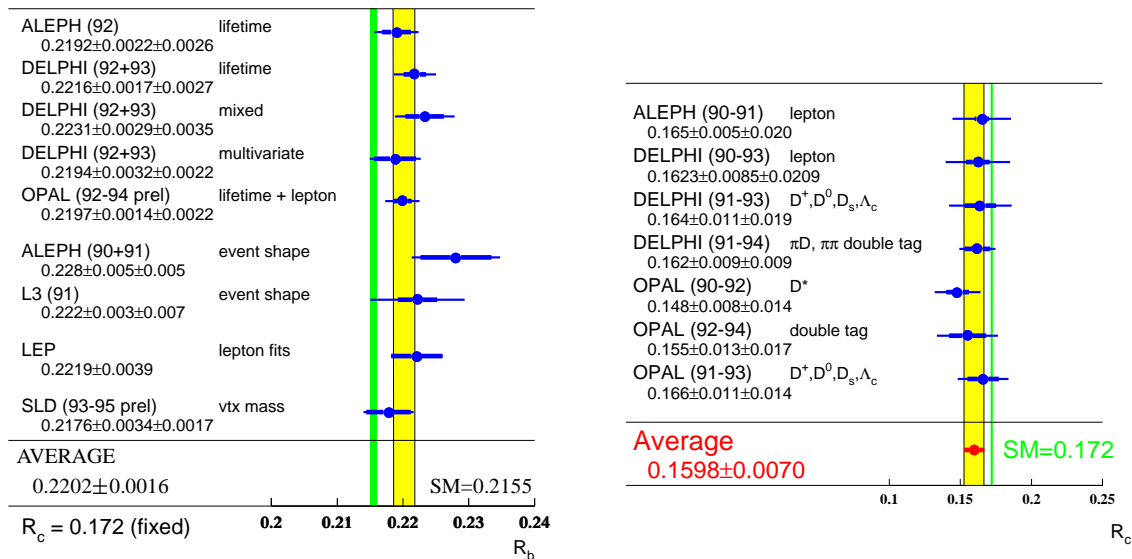


Figure 1: Measurements of R_b and R_c .

This paper summarizes the results of the R_b , R_c mini-workshop [1] that took place in XXXI rencontres de Moriond, QCD and hadronic interactions. The measured values of R_b and R_c are shown in figure 1. The various determinations agree well with each other. The averages are dominated by systematics:

$$R_b = 0.2211 \pm 0.0010_{\text{stat}} \pm 0.0014_{\text{syst}} \quad (1)$$

$$R_c = 0.1598 \pm 0.0038_{\text{stat}} \pm 0.0059_{\text{syst}} \quad (2)$$

with a -30% correlation. Consequently, the SM exclusion confidence level of 99.7%, which assumes Gaussian errors, should be taken with a grain of salt. Many systematic errors are common, and the first accomplishment of the Heavy Flavour team of the LEP electroweak Working Group (LEPEWWG) was to unify the terminology for sources of systematic errors. Indeed, uncertainties of similar physical origin could be termed differently. A well known example is given by the charm leptonic branching ratio (which affects the lepton tags) and the charm lifetime (which affects the lifetime tags). They are both governed by the D^0/D^+ production ratio, itself driven by the D^* rate. These sources properly labeled, the variation of the corresponding parameters were unified between experiments. The rest of the job is heavy but straightforward use of correlation matrices. However, as P. Wells pointed out, the LEPEWWG, consisting of members of the experiments, could not have discovered sources of systematics that everyone ignored. It was indeed the point of this workshop to expose the analysis in detail, so that such possible problems could be pointed out.

2 Progress in the charm sector

Understanding charm production and decays is critical to measure R_c , but also as a background in the measurement of R_b . Individual charmed hadrons have different leptonic BRs, lifetimes, decay multiplicities and possibly fragmentation functions, all of which affect detection efficiency of both charm- and b-tags.

There are two ways out of this problem.

1. Eliminate charm background

By cutting on the invariant mass of particles originating from a secondary vertex, at around 2 GeV, charm background can efficiently be removed. This was first shown by the SLD collaboration, and will certainly be done at LEP. The interaction point at SLC is so small and well determined, that the line of flight between the primary and secondary vertices can be determined well enough to reconstruct the missing transverse momentum at the secondary vertex, which can be added in the invariant mass determination. This allows further improvement in the tag, but might be difficult at LEP.

2. Measure charm properties at LEP

Substantial progress has been achieved in the measurement of charmed hadron production rates.

–Double-tagging measurements of R_c using D^* tagging also determine $P(c \rightarrow D^*)$. So far, it was **assumed** that this probability was center-of-mass independent, and the value 0.178 ± 0.013 from the Υ region were used. The new average from LEP is 0.164 ± 0.008 . Although the average of these two numbers is presently used, LEP could now certainly use the LEP value alone, avoiding this assumption altogether. The new input raised the value of R_c from the single D^* tag analysis, which incidently is the only individual measurement of R_c that disagrees with the SM value.

–Measurements of D^+ , D^0 , D_s , Λ_c production rates allow by straight summation a rather solid determination of R_c .

So far these improvements have been performed only by some of the SLD/LEP experiments, and with partial statistics. The situation should still improve considerably. The charm sector constitutes the bulk of the given systematic error on R_b .

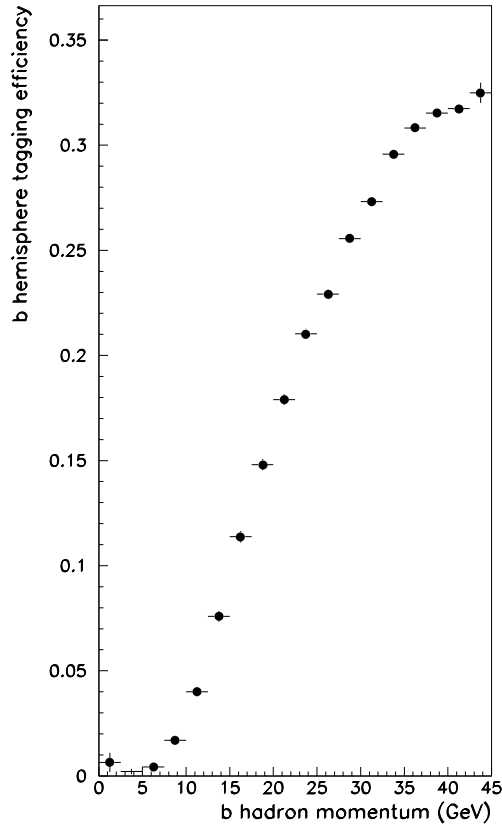
3 Correlations

A large amount of discussion was devoted to the question of correlations of b-tagging between hemispheres. There are several identified sources of correlations:

- geometry produces positive correlations.
- gluon radiation: very hard radiation brings both bs in the same hemisphere, leading to negative correlation. Hard radiation leaves the two bs in opposite hemispheres, with softer momenta, leading to positive momentum and efficiency correlation.
- sharing a common primary vertex leads to negative correlations.

The size of these effects is typically 5% or so. With the double tagging technique, R_b is directly affected by correlations. A characteristic common to all tagging techniques is a very strong sensitivity of the b -tagging efficiency with b -hadron momentum. This is shown in figure 2. Consequently, the method is very sensitive to proper description by the hadronization Monte-carlos of the b -hadron momentum correlations. This point was addressed by Branson, and lead to intense discussion, in particular by Khoze. A negative

Figure 2: *Momentum dependence of the b-tagging efficiency in the ALEPH published analysis [2]. This momentum dependence is very similar for all experiments.*



correlation of -2%, common to all methods and experiments, would be necessary to bring R_b in agreement with SM. Priority will undoubtedly be given to gathering experimental information on this point, and should lead to exciting experimental results in the near future.

In the present averaging, indeed, the tagging correlations are calculated by hadronization MC's, errors are MC statistics only, and therefore averaged as independent. Of course this is a weak point, which will require clarification before the R_b discrepancy is finally established.

4 Gluon splitting

The first idea to explain the observed R_b discrepancy was that $e^+e^- \rightarrow q\bar{q}b\bar{b}$ or $e^+e^- \rightarrow q\bar{q}c\bar{c}$, although accounted for in the analysis, had been underestimated. These processes have now been identified and measured by OPAL and DELPHI, and found to agree with the expected values. Using the measured values instead off the JETSET predictions would shift R_b by -0.0002 ± 0.0003 . **Gluon splitting cannot explain the discrepancy.**

5 True exciting new physics

If your enthusiasm has survived the previous sections, you might imagine that R_b is indeed signal for new physics. There are two classes of possible explanations, new interaction at tree level or radiative effects in the $Z \rightarrow b\bar{b}$ vertex.

New interaction at tree level

Since the $SU(2)_L \times U(1)$ gauge symmetry completely determines neutral current couplings with one parameter $\sin^2 \theta_w^{\text{eff}}$ with a level of precision far superior to the observed discrepancy, one has to turn to an additional intermediate boson, e.g. a Z' . This object has to be rather heavy to have escaped detection so far. The Z' couplings to hadrons must be rather large to affect R_b, R_c , but respect of leptonic observables requires small couplings to leptons. Thus the name hadrophilic [3] or leptophobic [4]. Excitement grew around this possibility when the high E_t anomaly –another effect in the 2-3 σ range – was reported. Although this could possibly be due to our limited knowledge of the gluon structure function, it is incredibly tempting to see it as the foothill of a Z' resonance.

The Z' models assume family universality. The typical number of parameters is 10: Z' mass, Z - Z' mixing angle ξ , and 8 couplings, g_b^f, g_a^f for $f = e, \nu, u, d$. A solution with $M_{Z'} \simeq 1000$ GeV, $\xi = 2 \cdot 10^{-3}$, small lepton couplings, and large couplings to quarks, is found to agree very well with all experimental data, reducing the χ^2 of the fit by about 10 units. The constraint set by the hadronic Z width forces the deviations to R_b and R_c to be in the proportion $\delta R_b \simeq -0.5 \delta R_c$, in agreement with observation within errors. This anticorrelation ensures that the Z' scenario does not spoil the SM agreement with the more precise chiral couplings measurements from neutrino scattering by more than 1.6 σ [5].

Although this scenario explains most of the 1-3 σ anomalies presently observed, it is rather unnatural and implies a rather large number of additional parameters.

New Physics in $Z \rightarrow b\bar{b}$ vertex corrections

A large number of scenarios [6] have been proposed to explain the R_b anomaly by $Z \rightarrow b\bar{b}$ vertex corrections. Since the b is isopartner of the top, it attracts naturally interactions with non-SM Higgses or other symmetry breaking objects. As a consequence all non- b physics remains untouched, in particular the charm quark couplings. The correction to R_b can then be inferred either i) from the direct measurement of R_b with R_c fixed to SM, or ii) from the measurement of the hadronic width using the 1995 PDG average $\alpha(M_Z^2) = 0.118 \pm 0.003$:

$$\text{Direct, } R_c \text{ fixed : } R_b = 0.2202 \pm 0.0016 \quad \delta R_b = +0.0047 \pm 0.0016 \quad (3)$$

$$\text{from } \Gamma_{\text{had}} \text{ : } R_b = 0.2167 \pm 0.0013 \quad \delta R_b = +0.0012 \pm 0.0013 \quad (4)$$

$$\text{average : } (\chi^2 = 2.9) \quad R_b = 0.2181 \pm 0.0017 \quad \delta R_b = +0.0026 \pm 0.0017. \quad (5)$$

These two values being somewhat inconsistent, the error on the average has been increased as usual by $\sqrt{\chi^2} = 1.7$. It follows that the R_b discrepancy is reduced to 1.2%, with a significance of only 1.5 σ .

The most appealing scenario is Minimal Supersymmetry (MSSM), as described by Chankowski. Again, the parameter space is very large. Although most authors were a priori expecting negative values of δR_b , there are regions of the supersymmetric parameter space where positive corrections occur.

a) the low $\tan \beta$ region. Loops with light chargino C_1 and s-top \tilde{t} can generate δR_b of the right sign and magnitude, up to $R_b \leq 0.2180$, obtained in the vicinity of the constraints

$m_{C_1} > 65$ GeV, $m_{\tilde{t}} > 60$ GeV, imposed by the non-observation of these particles at LEP 1.5 [7].

b) the large $\tan \beta$ region. Interestingly this solution would imply a large $t \rightarrow H^+ b$ decay rate, which might be visible in further investigations of top decays. An even larger value of $R_b \leq 0.2186$ could be obtained at the edge of the present LEP1.5 limits.

These MSSM solutions require chargino and s-top that are within reach of LEP2, a very exciting feature. Nevertheless, they cannot produce effects as large as that suggested by the direct measurement of R_b .

6 Conclusions

The situation of R_b and R_c has been reviewed extensively. Beautiful new methods were shown. New results on charm have reduced the R_c discrepancy to 1.7σ . The new SLD measurements of R_b leads the way to charm-background free measurements. A potentially dangerous weakness in the treatment of efficiency correlations between event hemispheres has been identified. A rather large effect would be necessary to explain the R_b discrepancy, but this topic will certainly be studied further. With a large fraction of LEP1 data not yet analysed, more data to come from SLD, and systematic error studies going on, the situation might change dramatically in the next year. Gluon splitting can now be ruled out by experiment as a source of excess of b events. A Z' can be invoked to explain both the R_b, R_c discrepancies and many others. More naturally, the MSSM can produce effects on R_b only, but then the direct measurement of R_b is somewhat contradicted by that of the hadronic width. In this case the best guess for an anomaly is $\delta R_b = +0.0026 \pm 0.0017$. This is in fact very consistent with the MSSM scenarios, most of which also predict new particles for LEP2. One way or another, the next coming months will be exciting.

Acknowledgements

It is a pleasure to congratulate the organisers of Moriond QCD for organizing this very fruitful and open discussion. My colleagues have done a beautiful and thorough job at looking for mistakes or loopholes in their own work. All controversial conclusions in this summary are my responsibility.

References

- [1] A. Blondel, A. Bazarzo, J. Snyder, F. Martinez-Vidal, H. Przysiezniak, J. Baudot, G. Calderini, J. Branson, P. Wells, P. Chiapetta, P. Chankowski for Moriond QCD 1996. Related talks were given by M. Hildreth, E. Etzion, N. Di Bartolomeo and S. Pokorsky in Moriond Electroweak 1996.
- [2] ALEPH Coll., Phys. Lett. B313 (1993) 535.
- [3] P. Chiapetta et al., hep-ph 96011306.
- [4] G. Altarelli et al., hep-ph 96011324.
- [5] This point was brought up in Moriond Electroweak 1996, analysed "on-line" by K. McFarland, and followed-up by an addendum to [4], to appear in Phys. Lett. B.
- [6] See bibliography in P. Chiapetta's article.
For an extensive review of such scenarios see: P. Bamert et al., hep-ph 9602438.
- [7] J. Nachtman and P.P. Rebecchi, Moriond Electroweak 1996.